Air-Sea Interactions of Natural Long-Lived Greenhouse Gases (CO_2, N_2O, CH_4) in a Changing Climate

3

Dorothee C.E. Bakker, Hermann W. Bange, Nicolas Gruber, Truls Johannessen, Rob C. Upstill-Goddard, Alberto V. Borges, Bruno Delille, Carolin R. Löscher, S. Wajih A. Naqvi, Abdirahman M. Omar, and J. Magdalena Santana-Casiano

Abstract

Understanding and quantifying ocean–atmosphere exchanges of the long-lived greenhouse gases carbon dioxide (CO_2), nitrous oxide (N_2O) and methane (CH_4) are important for understanding the global biogeochemical cycles of carbon and nitrogen in the context of ongoing global climate change. In this chapter we summarise our current state of knowledge regarding the oceanic distributions, formation and consumption pathways, and oceanic uptake and emissions of CO_2, N_2O and CH_4, with a particular emphasis on the upper ocean. We specifically consider the role of the ocean in regulating the tropospheric content of these important radiative gases in a world in which their tropospheric content is rapidly increasing and estimate the impact of global change on their present and future oceanic uptake and/or emission. Finally, we evaluate the various uncertainties associated with the most commonly used methods for estimating uptake and emission and identify future research needs.

3.1 Introduction

Carbon dioxide (CO_2), nitrous oxide (N_2O) and methane (CH_4) are long-lived atmospheric greenhouse gases, whose global budgets are substantially determined by the marine system. Understanding and accurately predicting the evolution of the marine CO_2 sink and the marine emissions of N_2O and CH_4 is of great importance for future climate change scenarios as used in studies for the Intergovernmental Panel on Climate Change (Denman et al. 2007).

The tropospheric dry mole fractions of these three greenhouse gases (Box 3.1) have been increasing since the industrial revolution, principally reflecting anthropogenic inputs, but also comparatively small fluctuations in the balance of natural sources and sinks. The tropospheric abundance of CO_2 has been regularly monitored since the late 1950s, and those of N_2O and CH_4 since the 1970s (http://agage.eas.gatech.edu/index.htm; http://www.esrl.noaa.gov/gmd) (Fig. 3.1). Table 3.1 summarises the tropospheric abundances, lifetimes, and radiative forcings of CO_2, N_2O and CH_4 for 2005

D.C.E. Bakker (✉)
e-mail: d.bakker@uea.ac.uk

H.W. Bange (✉)
e-mail: hbange@geomar.de

N. Gruber (✉)
e-mail: nicolas.gruber@env.ethz.ch

T. Johannessen (✉)
e-mail: truls.johannessen@gfi.uib.no

R.C. Upstill-Goddard (✉)
e-mail: rob.goddard@ncl.ac.uk

P.S. Liss and M.T. Johnson (eds.), *Ocean-Atmosphere Interactions of Gases and Particles*,
Springer Earth System Sciences, DOI 10.1007/978-3-642-25643-1_3,

Box 3.1

Atmospheric gases are quantified by their dry mole fraction, given in units of ppm or μmol mol^{-1} for CO$_2$ and in units of ppb or nmol mol^{-1} for N$_2$O and CH$_4$. In this chapter we report annual fluxes in Pg C year^{-1} for CO$_2$, in Tg C year^{-1} for CH$_4$ and in Tg N year^{-1} for N$_2$O. One Pg (Petagram) is equivalent to 10^{15} g and one Tg (Teragram) is equivalent to 10^{12} g. The troposphere is the lower part of the atmosphere and extends from the Earth's surface to the tropopause at 10–15 km height. In this chapter we are mainly concerned with the troposphere, unless specified otherwise.

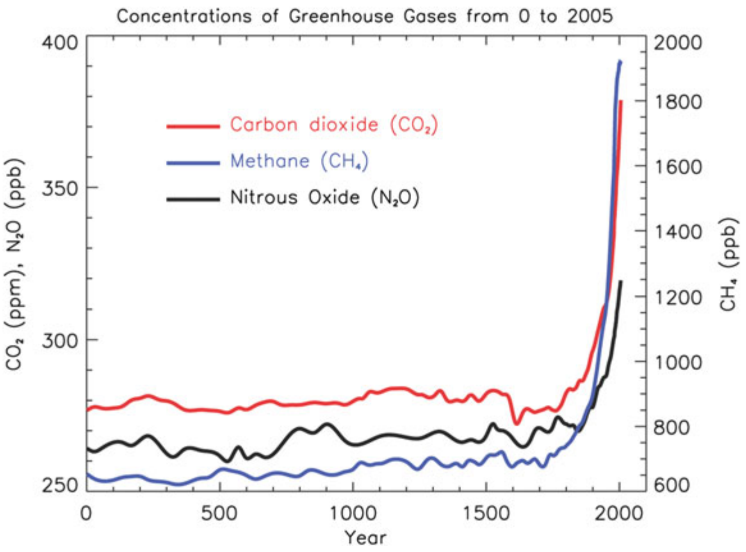

Fig. 3.1 Atmospheric concentrations of carbon dioxide, methane and nitrous oxide over the last 2,000 years (Reproduced from Forster et al. (2007) by permission of the IPCC)

Table 3.1 The tropospheric dry mole fractions, radiative forcings (RF) and lifetimes (adjustment time) of CO$_2$, N$_2$O and CH$_4$ (After Forster et al. 2007; WDCGG 2012)

Gas	Abundance in 2010	Abundance in 2005	RF in 2005 (W m^{-2})	Lifetime (years)
CO$_2$	389.0 ppm	379 ± 0.65 ppm	1.66	See below[a]
N$_2$O	323.2 ppb	319 ± 0.12 ppb	0.16	114
CH$_4$	1,808 ppb	1,774 ± 1.8 ppb	0.48	12

[a] No single adjustment time exists for CO$_2$ (Joos et al. 2001), as the rate of removal of CO$_2$ from the troposphere is determined by the removal rate of carbon from the surface ocean (Annexe I in IPCC 2007). An approximate value of 100 years may be given, while decay constants of 172.9 to 18.51 and 1.186 years have been used in models (Forster et al. 2007).

(Forster et al. 2007). An increase in the dry mole fractions (Box 3.1) of these long-lived greenhouse gases leads to tropospheric warming and stratospheric cooling, which may impact on chemical reaction rates and atmospheric dynamics (Wayne 2000). Other effects of changes in the dry mole fractions of these gases are listed in Table 3.2.

Global CO$_2$ emissions are currently increasing exponentially, primarily reflecting the accelerating development of large emerging economies such as China and India (Friedlingstein et al. 2010). If sustained, this recently rapid growth in tropospheric CO$_2$ may precipitate critical climate and other global environmental changes, possibly faster than previously identified (e.g. IPCC 2007).

Given its current tropospheric growth and the ongoing decline in chlorofluorocarbon (CFC) emissions, N$_2$O may soon replace CFCs as the fourth most important greenhouse gas after water vapour (H$_2$O), CO$_2$ and CH$_4$ (Forster et al. 2007). The major sink of N$_2$O is

Table 3.2 Air-sea exchange and impact of the long-lived greenhouse gases CO_2, N_2O and CH_4 in a changing climate, as discussed in this chapter. See Table 3.1 for the radiative forcings and atmospheric lifetimes

Gas	Role in atmospheric chemistry	Oceanic contribution to contemporary atmospheric budget	Impact of environmental change on air-sea gas exchange in the twenty-first century			
			Global warming	Ocean acidification	Open ocean deoxygenation	Coastal eutrophication and hypoxia
CO_2	Inert	Net ocean sink for about 30 % of CO_2 emissions from human activity partly mitigates climate change; the ocean ultimately controls atmospheric CO_2 content	The net ocean sink likely to decrease by 2100	Small effect on ocean CO_2 sink	Small effect	Coastal CO_2 sink likely to increase
N_2O	Largely inert in the troposphere; depletion of stratospheric O_3	Open ocean natural N_2O source, coastal regions (incl. rivers) anthropogenic N_2O source, equivalent to 20 % and 10 % of the global N_2O emissions	Increase of subsurface production	Unknown	Negligible or small increase in the open ocean N_2O source	Large increase in the coastal N_2O source
CH_4	Regulates tropospheric O_3 and OH radical; affects stratospheric O_3 chemistry; CO_2 source	Natural open ocean and coastal CH_4 sources equivalent to 10 % of the global, natural CH_4 sources; continental CH_4 seeps poorly known	Increased CH_4 release from CH_4 hydrates and increased CO_2 release upon oxidation of hydrate-derived CH_4	Unknown	Negligible or small increase in the open ocean CH_4 source	Negligible or small increase in coastal CH_4 source

Table 3.3 Sources and sinks of tropospheric CH_4. Ranges are derived from estimates for the period 1983–2004, as compiled by Denman et al. (2007)

	CH_4 sources and sinks (Tg C year^{-1})
Natural sources:	
Wetlands	75–173
Termites	15–22
Oceans, incl coastal regions	3–11
Hydrates	3–4
Geological sources	3–11
Wild animals	11
Wildfires	2–4
Total natural sources	**109–195**
Anthropogenic sources:	
Energy	56–58
Coal mining	23–36
Gas, oil, industry	36–68
Landfills and waste	26–52
Ruminants	57–142
Rice agriculture	23–84
Biomass burning	11–66
Vegetation	27
Total anthropogenic sources	**198–321**
Total sources:	**377–458**
Sinks:	
Tropospheric OH radical	321–383
Soils	20–26
Stratospheric loss	22–34
Total sinks	**386–436**

the stratosphere where it photochemically decomposes via reaction with O(^{1}D) (oxygen singlet D) to form nitric oxide (NO) radicals. The latter represent a major removal pathway for stratospheric ozone (O_3) (Crutzen 1970; Ravishankara et al. 2009). Indeed, N_2O is expected to become the dominant O_3 depleting compound during the twenty-first century (Ravishankara et al. 2009).

CH_4 is the most abundant organic species in the troposphere, where it influences oxidising capacity and regulates levels of O_3 and OH (hydroxyl free radical). Oxidation of CH_4 by OH to CO_2 and CO (carbon monoxide) is its major tropospheric sink (Table 3.3). In the stratosphere photo-oxidation of CH_4 is a major source of stratospheric H_2O, which influences both tropospheric warming and stratospheric cooling (Michelsen et al. 2000), and a small source of stratospheric CO_2. CH_4 plays a complex role in stratospheric O_3 chemistry (Wayne 2000). Additional stratospheric CO_2 arises from rapid CO oxidation. However, these two CO_2 sources are minor and as there are no recognised stratospheric sinks for CO_2 (Hall and Prather 1993); any variation in stratospheric CO_2 principally reflects the inflow of tropospheric air masses.

3.1.1 Atmospheric Greenhouse Gases from Ice Cores

Analysis of the composition of fossil air trapped in ice cores has extended the tropospheric histories of all three gases, to ~800,000 years before present (YBP) for CO_2 (Petit et al. 1999; EPICA community members 2004; Lüthi et al. 2008) and to ~650,000 YBP for N_2O and CH_4 (Spahni et al. 2005). These data show that during the last 650,000 years CO_2 has varied from ~170 ppm during glacials to ~280 ppm during interglacials, while during the preceeding 100,000 years the range was somewhat smaller. For comparison, tropospheric CO_2 increased from 280 ppm pre-industrially to 389 ppm in 2010 (Forster et al. 2007; WDCGG 2012). Changes in ocean circulation and biology and the feedbacks between them have been invoked to explain the glacial/interglacial fluctuations of tropospheric CO_2 but understanding the precise mechanistic details remains a substantial challenge (Jansen et al. 2007). Over the last 420,000 years, tropospheric CO_2 has tracked reconstructed changes in Antarctic temperature with a time lag of several hundred to a thousand years (Mudelsee 2001), implying that changes in the physical climate system such as temperature and the extent of glaciers have initiated changes in the global carbon cycle and tropospheric CO_2. The carbon cycle then has responded by amplifying these initial perturbations through positive carbon-climate feedbacks. Today the situation is fundamentally different in that the increasing greenhouse gas content drives changes in climate and environment.

Variation in stratospheric N_2O between 200 and 280 ppb during the past 650,000 years (Spahni et al. 2005) can be attributed to concurrent natural changes in both the terrestrial and the oceanic sources (Sowers et al. 2003; Flückiger et al. 2004). Since the pre-industrial era the mean tropospheric N_2O dry mole fraction has increased from 270 ± 7 to ~323 ppb. The current tropospheric N_2O growth rate of about 0.7 ppb year^{-1} can primarily be attributed to the continued increased use of nitrogen fertilisers (Forster et al. 2007; Montzka et al. 2011).

The tropospheric dry mole fraction of CH_4 has varied from ~400 ppb during glacials to ~700 ppb during interglacials. The current average tropospheric CH_4 dry mole fraction is ~1,808 ppb, reflecting large and growing anthropogenic CH_4 fluxes since the pre-industrial era (Table 3.3). Even so, tropospheric CH_4 growth is temporally quite variable. High annual growth rates of ~20 ppb year^{-1} during the 1970s were followed by growth rates of ~9–13 ppb year^{-1} through the 1980s, 0–13 ppb year^{-1} through most of the 1990s, almost zero growth during the late 1990s to early 2000s (Dlugokencky et al. 2003) and renewed growth rates of ~10 ppb year^{-1} during the late 2000s (Rigby et al. 2008). This complex behaviour reflects short-term source variability that has been variously ascribed to decreased fossil fuel output following the economic collapse of the former Soviet Union, volcanic activity, wetland and rice paddy emissions, biomass burning, changes in the global distributions of temperature and precipitation, and reduced microbial sources in the Northern Hemisphere (Denman et al. 2007; Dlugokencky et al. 2009; Aydin et al. 2011; Kai et al. 2011).

3.2 Surface Ocean Distribution and Air-Sea Exchange of CO_2

3.2.1 Global Tropospheric CO_2 Budget

In 2010 alone the tropospheric CO_2 increase was equivalent to 5.0 ± 0.2 Pg C (Box 3.1), principally due to the release of 9.1 ± 0.5 Pg C from fossil fuel burning and cement manufacture and 0.9 ± 0.7 Pg C from land use change (Fig. 3.2) (Global Carbon Project 2011; Peters et al. 2012). The ocean absorbs a substantial fraction of CO_2 emissions to the troposphere. From pre-industrial times to 1994 the oceans are estimated to have taken up 118 ± 19 Pg C from the troposphere, corresponding to roughly 50 % of fossil fuel CO_2 or about 30 % of the total anthropogenic emissions that include CO_2 emissions from land use change (Fig. 3.2; Table 3.2) (Sabine et al. 2004). Scientists are debating whether regional and global ocean CO_2 uptake has increased, remained constant or decreased in recent decades (Le Quéré et al. 2007, 2010; Schuster and Watson 2007; McKinley et al. 2011; Ballantyre et al. 2012).

A consequence of this ocean CO_2 uptake is a decrease in ocean pH, known as ocean acidification (Sect. 3.5.2) (Feely et al. 2004; Raven et al. 2005). If anthropogenic CO_2 emissions were to cease now, the oceans would eventually absorb 70–80 % of the anthropogenic CO_2 so far added to the troposphere, but this would take several hundred years (Archer et al. 1997; Watson and Orr 2003). Dissolution of calcium carbonate ($CaCO_3$) in deep ocean sediments and on land would further reduce tropospheric CO_2 to within 8 % of its pre-industrial level over thousands of years (Archer et al. 1997). Given the importance of the oceans in moderating human-induced climate change, quantifying net oceanic CO_2 uptake and estimating its long-term evolution are of critical importance. Although much progress has been made in quantifying CO_2 air-sea fluxes over the past decade, considerable uncertainties remain, in particular relating to inter-annual variability and long-term trends. The current state of knowledge is discussed here for the open ocean (Sect. 3.2.3) and for coastal seas (Sect. 3.2.4), with emphasis on the principal uncertainties (Sect. 3.6).

3.2.2 Processes Controlling CO_2 Dynamics in the Upper Water Column

The air-sea exchange fluxes of CO_2 show high spatial and temporal variability, reflecting a complex interplay between the biological and physical processes affecting surface water fCO_2 (Box 3.2) (Takahashi et al. 2002; Sarmiento and Gruber 2006). In addition, observations show surface water fCO_2 to rarely be in equilibrium with tropospheric fCO_2 (see below and Box 3.3). Key to understanding the behaviour of CO_2 with regard to equilibration is CO_2 chemistry, which we briefly review next. We also discuss the key processes controlling the CO_2 dynamics of the upper ocean.

Dissolved CO_2 in seawater chemically equilibrates with carbonic acid (H_2CO_3) and the bicarbonate (HCO_3^-) and carbonate (CO_3^{2-}) ions:

$$CO_2 + H_2O \leftrightarrow H_2CO_3 \tag{3.1}$$

$$H_2CO_3 \leftrightarrow H^+ + HCO_3^- \tag{3.2}$$

$$HCO_3^- \leftrightarrow H^+ + CO_3^{2-} \tag{3.3}$$

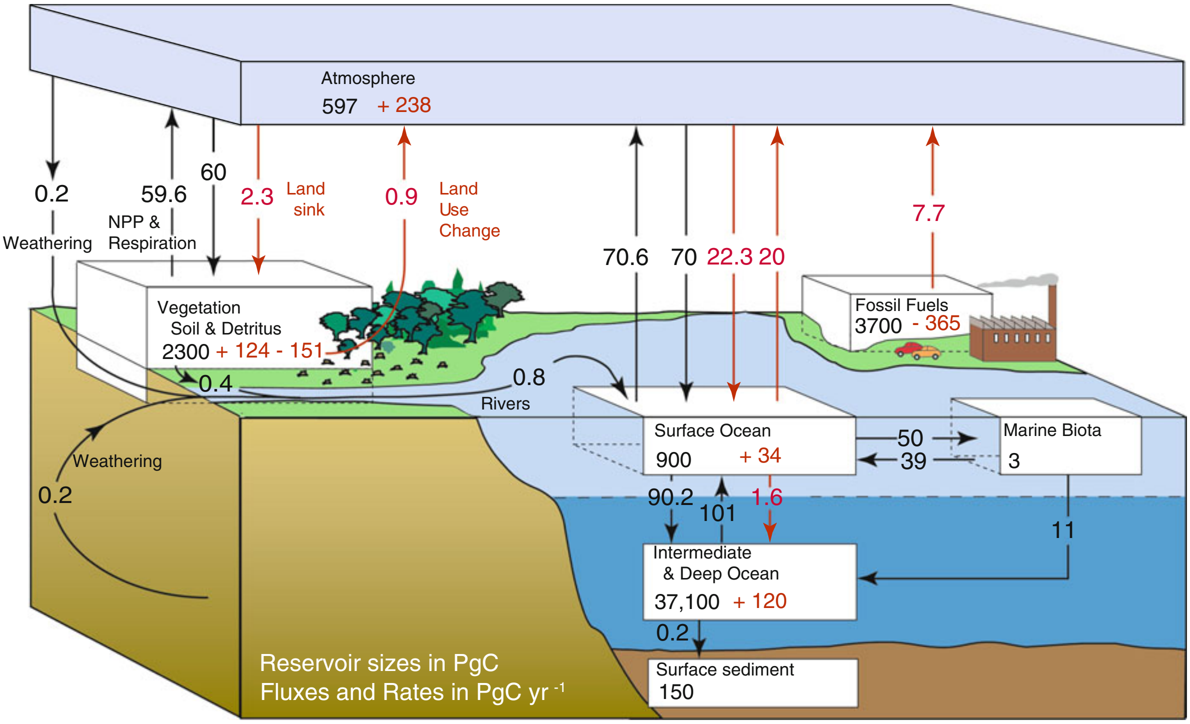

Fig. 3.2 The global carbon cycle with annual fluxes (in Pg C year^{-1}) for the years 2000–2009. Pre-industrial, natural fluxes are in *black* and anthropogenic fluxes are in *red*. Integrated fluxes and standing stocks are from 1850 to 2011. NPP is annual net terrestrial primary production. Cumulative changes are for end 2011 (The figure updates those in Sarmiento and Gruber (2002) and Denman et al. (2007). Figure courtesy of N Gruber)

Box 3.2

Whereas the amount of CO_2 dissolved in seawater is generally reported in terms of its partial pressure pCO_2 (unit: μatm or 0.101325 Pa) or fugacity fCO_2 (unit: μatm), N_2O and CH_4 are more commonly presented in concentration units (nM or nmol kg^{-1} seawater) or as percent (%) saturation. The latter is calculated from the ratio of the measured concentration to the theoretical equilibrium concentration, as determined by ambient water temperature, salinity and air pressure, and the atmospheric dry mole fraction corresponding to the time of last atmospheric contact. A surface saturation of 100 % indicates a water mass in equilibrium with overlying air, values below 100 % indicate undersaturation and values above 100 % indicate supersaturation. For all three gases, deviations from the air-sea equilibrium value are expressed as a negative or positive partial pressure difference (i.e. ΔpCO_2, ΔpN_2O, ΔpCH_4) or for N_2O and CH_4, as a negative or positive "concentration anomaly". In this chapter, positive values denote a partial pressure that is higher in the water than in the overlying air.

The fugacity of a gas is its partial pressure after correcting for any non-ideal behaviour by applying a fugacity coefficient γ (Weiss 1974). The equation for CO_2 is:

$$fCO_2 = \gamma \, pCO_2 \tag{3.4}$$

In practice the fugacity and partial pressure of CO_2 differ by only about 0.4 %. In this chaper we refer to fCO_2 throughout.

Box 3.3

Air-sea fluxes (F) can be quantified as the product of a gas transfer velocity (k), the gas solubility (K_0) and the difference in the gas fugacity (e.g. fCO_2) across the air-sea interface. For N_2O and CH_4 the difference in the partial pressure is usually applied.

$$F_{CO2} = k_{CO2} K_{0,CO2} \left(fCO_{2water} - fCO_{2air}\right) \tag{3.5}$$

$$F_X = k_X K_{0,X} \left(pX_{water} - pX_{air}\right) \left(\text{with } X = N_2O \text{ or } CH_4\right) \tag{3.6}$$

By convention, positive flux values indicate emission from the ocean and negative flux values indicate uptake by the ocean. For CO_2 these simplified equations neglect its possible chemical enhancement, although this effect is thought to be small (Wanninkhof 1992; Matthews 1999). They further assume that away from the air-sea interface both the lower troposphere and upper ocean are well mixed, so that bulk measurements within them can be used to define a gas concentration gradient at the interface. A final assumption is that the water temperature at the interface (the skin temperature) is the same as that of the well-mixed upper ocean (Robertson and Watson 1992; Van Scoy et al. 1995).

Atmospheric CO_2 needs to equilibrate with the large pool of dissolved inorganic carbon in seawater, resulting in an equilibration time-scale of the surface ocean for gas exchange of nearly 1 year (Broecker and Peng 1982), i.e. much longer than the time-scale typically associated with upper ocean perturbations (such as by the seasonal cycle). The equilibration time-scale for CH_4 and N_2O is about 10 times shorter than for CO_2 so that the deviations of these gases from equilibrium are generally smaller unless strong sources are present.

The gas transfer velocity (k) is a function of turbulence at the sea surface and is often parameterised as a function of wind speed, as discussed in detail in Chap. 2. Several parameterisations of k as a function of wind speed have been proposed (e.g. Liss and Merlivat 1986; Wanninkhof 1992; Wanninkhof and McGillis 1999; Nightingale et al. 2000; Ho et al. 2006; Sweeney et al. 2007; Prytherch et al. 2010). The uncertainty in k, which has been estimated at 30 % (Sweeney et al. 2007), adds further uncertainty to estimates of net gas uptake and/or emission determined from surface water measurements (Sect. 3.6).

On average surface seawater dissolved inorganic carbon (DIC) (alternatively referred to as total CO_2, ΣCO_2 and C_T) comprises about 90 % HCO_3^-, 9 % CO_3^{2-}, 1 % dissolved CO_2 and 0.001 % H_2CO_3. Thus, in order to equilibrate across the air-sea interface, CO_2 needs to equilibrate not only with the dissolved CO_2 pool, but with all chemical species making up DIC, explaining the long equilibration time scale. The dominant presence of HCO_3^- and CO_3^{2-} are also key to explaining the large uptake capacity of the ocean with regard to the anthropogenic perturbation of tropospheric CO_2, as it is the reaction of CO_3^{2-} with the dissolved CO_2 taken up to form two HCO_3^- ions that gives seawater its large capacity to take up CO_2 and that will enable the ocean to eventually take up nearly 80 % of total anthropogenic emissions. An important metric for this reaction is the oceanic buffer (or Revelle) factor, which is a measure of the degree to which this titration reaction occurs. The larger the concentration of the CO_3^{2-} ion, the higher this factor is, and thus the larger is the oceanic uptake capacity.

However, the current net rate of oceanic CO_2 uptake is overall set by its transport from the surface to the deep oceans (Fig. 3.2), leading to the observation that the current uptake fraction (about 30 %) is considerably smaller than the long-term potential (about 80 %).

The anthropogenic perturbation occurs on top of an intense but largely internal cycling of "natural" carbon, which is the primary driver of the high spatio-temporal variability of CO_2 in the surface ocean. This natural internal cycling is often conceptualised as a number of "pumps", namely the solubility pump, the soft tissue or organic carbon pump and the carbonate or hard tissue pump (Volk and Hoffert 1985; Heinze et al. 1991). The reason for the pump analogy is that the associated processes act as gradient makers in that they tend to reduce the surface concentration of DIC and enhance its concentration at depth, thereby acting against the tendency for these gradients to be eliminated by transport and mixing. The net effect of these pumps on the air-sea exchange of CO_2 is controlled by the interaction and relative importance of the downward pump component relative to upward mixing and transport (Gruber and Sarmiento 2002). Regions where the downward component dominates over upward transport are sinks for tropospheric CO_2, while regions where upward transport dominates are CO_2 sources. Given the need to consider both the downward and upward components, the concept of biogeochemical loops has been proposed (Gruber and Sarmiento 2002).

The solubility pump is maximal at high-latitudes during winter when cold surface water rich in DIC (due to higher CO_2 solubility at lower temperatures) sinks to depth, resulting in a net downward transport of DIC (Fig. 3.2) (Volk and Hoffert 1985; Heinze et al 1991). In contrast, the solubility pump acts in quasi reverse order, when colder waters rich in DIC are brought to the surface and warm, giving rise to reduced CO_2 solubility.

The soft tissue pump is initiated by the photosynthetic incorporation of CO_2 as phytoplankton cellular organic carbon. As this organic carbon travels up the food chain, a fraction of it is "lost" at each trophic step by respiration, excretion and the death of organisms (Kaiser et al. 2011). Bacteria and other microorganisms are critical to the recycling of carbon in the upper ocean (Fig. 3.2). Nevertheless, a significant fraction of the photosynthetically fixed carbon leaves the upper ocean as "export production" in the form of sinking organic particles, by vertical migration of zooplankton or as dissolved organic carbon (DOC) in sinking water (Volk and Hoffert 1985; Heinze et al. 1991; Sarmiento and Gruber 2006).

The carbonate or hard tissue pump involves the biological formation of calcium carbonate ($CaCO_3$) in near surface waters, its downward export primarily by sinking and its subsequent dissolution in deep water. The initial step is incorporation of the ${CO_3}^{2-}$ ion into the shells of calcifying organisms:

$$Ca^{2+} + {CO_3}^{2-} \leftrightarrow CaCO_3 \tag{3.7}$$

Equation 3.7 describes $CaCO_3$ precipitation at a physiological level; however, the uptake of ${CO_3}^{2-}$ leads to a chemical re-adjustment of DIC species with the overall equation:

$$Ca^{2+} + 2{HCO_3}^{-} \leftrightarrow CaCO_3 + CO_2 + H_2O \tag{3.8}$$

The precipitation of $CaCO_3$ leads to a shift from the ${HCO_3}^{-}$ pool to the CO_2 pool and a release of CO_2 to the surrounding water. The "released" CO_2 subsequently equilibrates with ${HCO_3}^{-}$, so that for each mole of $CaCO_3$ precipitated, less than one mole of CO_2 is "released". The fraction for average surface sea water is 0.6 (Frankignoulle et al. 1994). Consequently, where the ratio between net organic carbon production or net community production (NCP) and calcification is below 0.6, the waters are a CO_2 source and where this ratio exceeds 0.6, they are a CO_2 sink (Suzuki and Kawahata 2004).

In coral reefs NCP is close to zero (Gattuso et al. 1998). Hence the CO_2 "released" by $CaCO_3$ precipitation generally exceeds the CO_2 drawdown by NCP and coral reefs tend to act as CO_2 sources to the troposphere (Gattuso et al. 1993, 1997; Frankignoulle et al. 1996; Ohde and van Woesik 1999; Bates et al. 2001). In the pelagic realm, where the vast majority of calcification is carried out by the coccolithophore component of the phytoplankton (Buitenhuis et al. 1996; Harlay et al. 2010, 2011; Suykens et al. 2010), the average ratio of NCP to net $CaCO_3$ precipitation is between 11 and 16 (Sarmiento et al. 2002; Jin et al. 2006). The net consequence of biological production and the export of organic carbon and $CaCO_3$ from the pelagic realm is a tendency towards CO_2 uptake from the troposphere.

Mineral $CaCO_3$ in seawater occurs in two forms: calcite and the more soluble aragonite (Mucci 1983). For both, solubility increases with increased pressure (depth) and decreased temperature. The saturation state Ω describes whether sea-water is supersaturated ($\Omega > 1$) or undersaturated ($\Omega < 1$) with respect to the solubility product, K_{sp}, of either of these two $CaCO_3$ forms:

$$\Omega = [Ca^{2+}]\ [{CO_3}^{2-}]/K_{sp} \tag{3.9}$$

$$K_{sp} = [Ca^{2+}]_{sat}\,[{CO_3}^{2-}]_{sat} \tag{3.10}$$

At present nearly the entire upper ocean is supersaturated with regard to both calcite and aragonite, while most of the deep ocean is undersaturated. Organisms that form $CaCO_3$ shells and structures therefore do so largely in waters that are supersaturated, while the exported $CaCO_3$ eventually sinks into regions of undersaturation and dissolves.

A reduction in ocean pH due to anthropogenic activities (Feely et al. 2004; Orr et al. 2005; Raven et al. 2005) is one consequence of increased tropospheric CO_2 and its transfer to the ocean. While the term "ocean acidification" (OA) describes a decrease in ocean pH, this is not expected to fall below 7 (Kleypas et al. 2006). The uptake of CO_2 since pre-industrial times has led to a reduction in surface seawater pH of 0.1 units relative to the pre-industrial value of about 8.2 (Orr et al. 2005). This is equivalent to a 30 % increase in the hydrogen ion (H^+) concentration.

In situ pH measurements at the European Station for Time-series in the Ocean (ESTOC, 29°N 15°W) show a progressive reduction of pH and other changes in the carbonate chemistry of surface waters since 1995 (González-Dávila et al. 2010; Santana-Casiano and González-Dávila 2011). Figure 3.3 highlights a decrease in surface water pH_T (the pH corrected to a constant temperature of 25°C) of 0.0019 pH units $year^{-1}$ from 1995 to 2010, accompanied by increases in salinity normalised DIC (NC_T) and fCO_2. Similar trends in pH, DIC and fCO_2 have been observed at the Bermuda Atlantic Time-series Study, BATS (Gruber et al. 2002), and the Hawaii Ocean Time-Series site, HOT (Brix et al. 2004; Denman et al. 2007).

An important consequence of the net oceanic uptake of anthropogenic CO_2 from the troposphere is a decrease in the saturation states with regard to calcite and aragonite. This is due to the aforementioned titration of the ${CO_3}^{2-}$ ion by the CO_2 taken up, which leads to a fall in the ${CO_3}^{2-}$ concentration. These chemical changes are accompanied by an increase in the concentration of H^+ and CO_2 (Feely et al. 2004; Raven et al. 2005). The ESTOC time series demonstrates how the saturation states for calcite and aragonite have decreased at rates of 0.018 ± 0.006 units $year^{-1}$ and 0.012 ± 0.004 units $year^{-1}$, respectively, from 1995 to 2004 (Santana-Casiano and González-Dávila 2011).

Ocean acidification is suspected to lead to a reduction in calcification by calcifying organisms, such as coral reefs, coccolithophores, foraminifera, pteropods and shell fish (Sect. 3.5.2) (Raven et al. 2005). In addition, diminishing calcification would reduce net $CaCO_3$ transfer to the deep ocean (Feely et al. 2004; Denman et al. 2007).

3.2.3 Surface Ocean fCO_2 and Air-Sea CO_2 Fluxes in the Open Ocean

3.2.3.1 Surface Ocean fCO_2 Distribution

The seasonal cycle in surface water fCO_2 is relatively weak in tropical regions (14°S–14°N), which are strong CO_2 sources throughout the year (Takahashi et al. 2009) (Box 3.3). Surface water fCO_2 in temperate ocean regions (14–50°N and 14–50°S) has a strong seasonal cycle with high values in summer and low values in winter, as the seasonal effects of warming and cooling outweigh biological effects (Fig. 3.3) (Bates et al. 1996a; Dore et al. 2003; González-Dávila et al. 2003; Takahashi et al. 2009). The temperate Indian Ocean north of 14°N also has high fCO_2 in summer, but here seasonal upwelling in the southwest monsoon is the main driver (Takahashi et al. 2009). High latitude northern hemisphere waters have strong fCO_2 undersaturation in spring and summer as a result of biological CO_2 drawdown in the upper ocean (Takahashi et al. 2009). Biological activity equally creates a CO_2 sink in Southern Ocean waters from 50°S to 60°S during austral spring and summer (Takahashi et al. 2009). Seasonally ice covered waters south of ~60°S rapidly change from strong CO_2 supersaturation below sea ice to strong undersaturation upon ice melt, most likely driven by biological carbon uptake (Bakker et al. 2008).

Surface water fCO_2 data coverage has improved greatly over the past decade (Takahashi et al. 2009; Watson et al. 2009; Pfeil et al. 2013; Sabine et al. 2013). For example, a basin-wide network of fCO_2 measurements on Voluntary Observing Ships (VOS) and buoys has been operational in the North Atlantic Ocean since 2004, which allows the creation of basin-wide monthly fCO_2 maps, annual flux estimates and trend analyses (Schuster et al. 2009; Telszewski et al. 2009; Watson et al. 2009). Data coverage is similarly

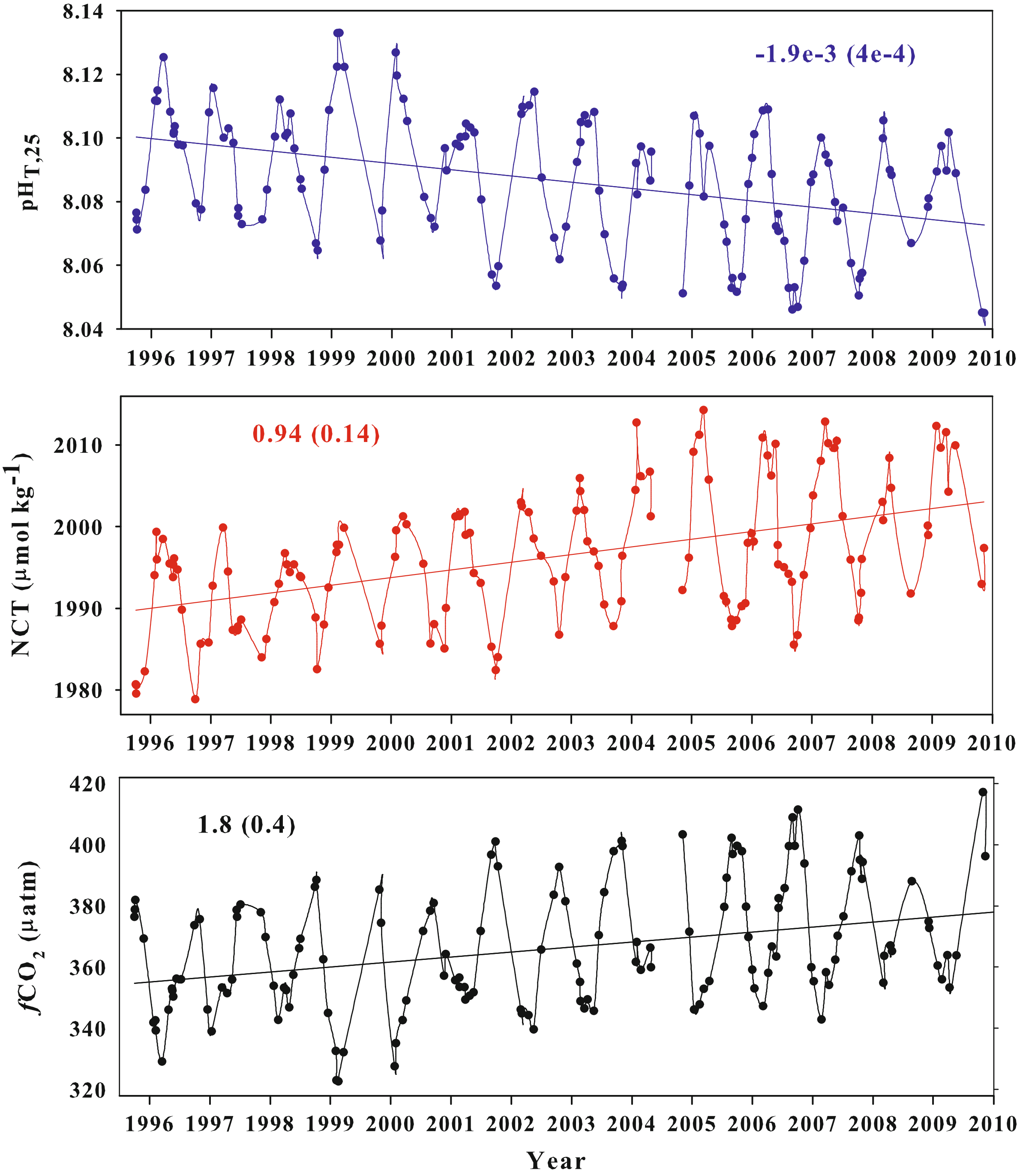

Fig. 3.3 Changes in total pH at 25 °C, salinity normalised dissolved inorganic carbon (NC_T) and fCO_2 from 1995 to 2010 at the European Station for Time-series in the Ocean (ESTOC, 29°N 15°W) for the full set of surface data (*upper* 10 m). The regression lines have slopes of -0.0019 ± 0.0004 pH units year^{-1} for pH$_{T,25}$, of 0.94 ± 0.14 μmol kg^{-1} year^{-1} for NC_T and of 1.8 ± 0.4 μatm year^{-1} for fCO_2. (Figure courtesy of M González-Dávila and JM Santana-Casiano)

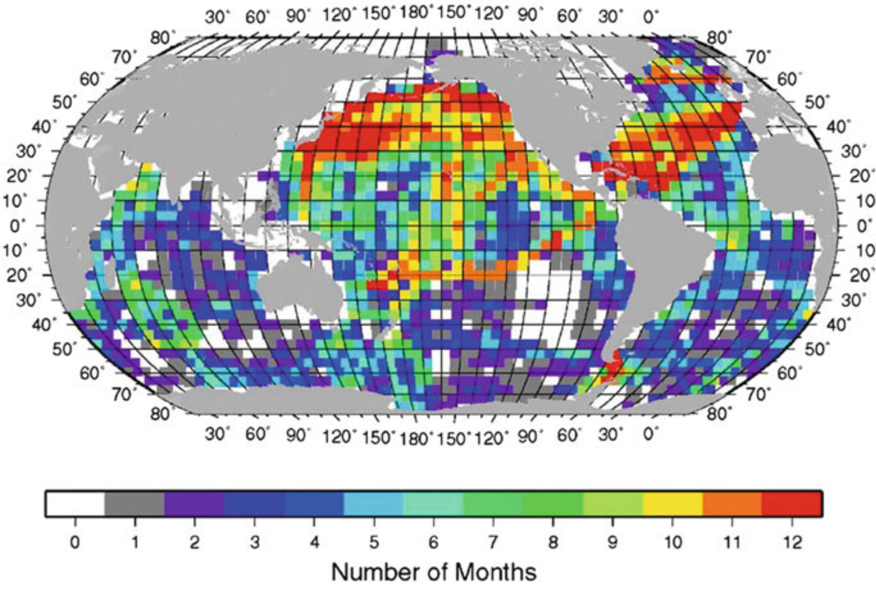

Fig. 3.4 Number of months in each 4° latitude by 5° longitude box with at least one surface water fCO_2 measurement between 1970 and 2007 (Reproduced from Takahashi et al. (2009) by permission of Elsevier)

high in the North Pacific (Feely et al. 2006; Ishii et al. 2009). Elsewhere data coverage has increased, but many regions remain data sparse, e.g. the Indian Ocean, the South Pacific Ocean, the South Atlantic Ocean and the Southern Ocean, notably in autumn and winter (Fig. 3.4) (Takahashi et al. 2009, 2011; Bakker et al. 2012; Pfeil et al. 2013; Sabine et al. 2013).

A variety of techniques have been applied to interpolate between surface ocean fCO_2 data, including a diffusion–advection based interpolation scheme (Takahashi et al. 1997, 2009), (multiple) linear regression (Boutin et al. 1999; Rangama et al. 2005; Olsen et al. 2008) and a neural network approach (Lefèvre et al. 2005; Telszewski et al. 2009). The principle of many of these methods is to correlate sparse fCO_2 data with more widely available parameters such as satellite-derived chlorophyll *a* concentrations, sea surface temperatures and mixed layer depths and then to use these correlations to predict fCO_2 where measurements are lacking.

The 'true' spatial distributions of surface water fCO_2 and air-sea CO_2 fluxes are unknown and the above methods only deliver approximations of them. Interestingly, however, Watson et al. (2009) derived similar air-sea CO_2 fluxes for the North Atlantic Ocean (10–65°N) using multiple linear regression and a neural network. For both the standard deviation of the annual mean fCO_2 was ~10 %. It was concluded that if the flux uncertainty arising from uncertainty in k is ignored, the overall air-sea CO_2 flux in this region is well constrained by fCO_2 observations and is thus relatively insensitive to the mapping technique used. Further development and testing of interpolation methods should be a priority.

3.2.3.2 Multi-Year Changes and Trends

Analysis of the decadal evolution of fCO_2 provides information on the evolution of the oceanic CO_2 sink. If the rate of increase of surface ocean fCO_2 matches the increase in tropospheric CO_2 the oceanic CO_2 sink is at steady state, but if it is higher, then the oceanic CO_2 sink is decreasing (Schuster et al. 2009). For example, Fig. 3.3 shows fCO_2 from 1995 to 2010 for the upper 10 m at ESTOC (29°N 15°W). Regression of the data reveals an increase in fCO_2 of 1.8 ± 0.4 µatm year^{-1}.

Globally, surface water fCO_2 increased at a mean rate of 1.5 µatm year^{-1} from 1970 to 2007, similar to the pace of the tropospheric CO_2 increase of 1.5 µatm year^{-1} from 1972 to 2005 (Takahashi et al. 2009). Relatively low rates of increase were found in the Equatorial Pacific Ocean (1.26 ± 0.55 µatm year^{-1}) and the North Pacific Ocean (1.28 ± 0.46 µatm year^{-1}), while fCO_2 increased more rapidly in the North Atlantic Ocean (1.80 ± 0.37 µatm year^{-1}) and between 50°S and 60°S (2.13 ± 0.64 µatm year^{-1}) (Takahashi et al. 2009). Similarly, surface water fCO_2 in the Southern Indian Ocean (south of 20°S) increased more rapidly (2.11 ± 0.07 µatm year^{-1}) than did tropospheric CO_2 (1.72 µatm year^{-1}) between 1991 and 2007 (Metzl 2009).

Regional and temporal differences in the rate of increase of surface water fCO_2 are not well understood but have been attributed to changes in seawater buffer capacity (Thomas et al. 2007), mixing and stratification (Schuster and Watson 2007), temperature (Corbière et al. 2007), biological activity (Lefèvre et al. 2004) and lateral and vertical water transport (Takahashi et al. 2009). The expanding database for fCO_2 highlights considerable year-to-year and multi-year variations in ocean carbon cycling.

Theory and biogeochemical models predict an increase in air-sea fCO_2 disequilibrium over time in high latitude regions. Here water from the interior ocean reaches the surface. This water has a relatively low DIC content, as it equilibrated with an atmospheric CO_2 mixing ratio below the present one, when the water last was at the surface. One might expect that the increase in surface water fCO_2 of these waters lags the increase in tropospheric CO_2 (Takahashi et al. 1997, 2002), given the long equilibration time for CO_2 of almost a year. Such an increase in the air-sea fCO_2 disequilibrium would be accompanied by an increase in the net oceanic CO_2 sink. However, the observation that surface water fCO_2 in some regions of the Southern Ocean is currently increasing more rapidly than tropospheric CO_2 (Metzl 2009; Takahashi et al. 2009) runs counter to these predictions. Air-sea CO_2 flux estimates derived from the inversion of tropospheric CO_2 data suggest that this may be a more wide-spread phenomenon in the Southern Ocean, extending to the entire region south of 45°S (Le Quéré et al. 2007). This hypothesis of a weakening relative sink strength in the Southern Ocean is supported by several ocean modelling studies (Wetzel et al. 2005; Le Quéré et al. 2007; Lovenduski et al. 2007) and is attributed to a trend of increasing Southern Ocean wind speeds, which enhance the upwelling of deeper waters with high concentrations of "natural" DIC (Lovenduski et al. 2008). The changing wind regime may be related to a strengthening of the Southern Annular Mode in response to increasing greenhouse gases and the depletion of stratospheric ozone (Lenton et al. 2009). These trends in Southern Ocean fCO_2, the strength of the oceanic CO_2 sink and the mechanisms responsible are currently topics of much scientific debate.

Recent studies provide evidence of multi-annual variation in surface water fCO_2 growth rates and CO_2 air-sea fluxes in other regions, notably the Pacific Ocean and the North Atlantic Ocean (Corbière et al. 2007; Schuster and Watson 2007; Ishii et al. 2009; Schuster et al. 2009; Watson et al. 2009). For example, the growth rates of surface water fCO_2 in the western Equatorial Pacific were different from 1985–1990 (0.3 ± 1.3 µatm year^{-1}) to 1990–1999 (2.2 ± 0.7 µatm year^{-1}) and 1999–2004 (−0.2 ± 1.0 µatm year^{-1}) (Ishii et al. 2009). Annual CO_2 uptake along a shipping route between the United Kingdom and the Caribbean strongly decreased from the early 1990s to 2002–2005 (Schuster and Watson 2007; Schuster et al. 2009). Annual air-sea CO_2 fluxes varied by more than a factor two for the period 2002–2007, with values rising and falling over several years (Fig. 3.5) (Watson et al. 2009). These gradual changes suggest multi-year or possibly decadal variation that might be linked to the North Atlantic Oscillation (Thomas et al. 2008).

3.2.3.3 Comparison of Air-Sea CO_2 Flux Estimates

Independent estimates of the global oceanic uptake of anthropogenic CO_2 for the 1990s and early 2000s range from 1.8 to 2.4 Pg C year^{-1} with model-based values often exceeding observation-based estimates (Gruber et al. 2009). An uptake of 1.8 ± 1.0 Pg C year^{-1} has been obtained by inversion of tropospheric CO_2 (Gurney et al. 2004; adjusted by Gruber et al. 2009), while a net ocean sink of 1.9 ± 0.7 Pg C year^{-1} has been estimated from a surface water CO_2 climatology (Takahashi et al. 2009; adjusted by Gruber et al. 2009). Ocean inversion of DIC has given an oceanic CO_2 sink of 2.2 ± 0.3 Pg C year^{-1}, (Gruber et al. 2009) and 2.4 ± 0.5 Pg C year^{-1} has been estimated using ocean biogeochemical models (Watson and Orr 2003). Other methods give a similar range of estimates (Joos et al. 1999; Gruber and Keeling 2001; Bender et al. 2005; Manning and Keeling 2006; Jacobson et al. 2007; Gruber et al. 2009).

Measurement and modelling techniques vary in whether they quantify anthropogenic CO_2 fluxes or net contemporary CO_2 fluxes and a correction needs to be made for the outgassing of carbon from rivers and for

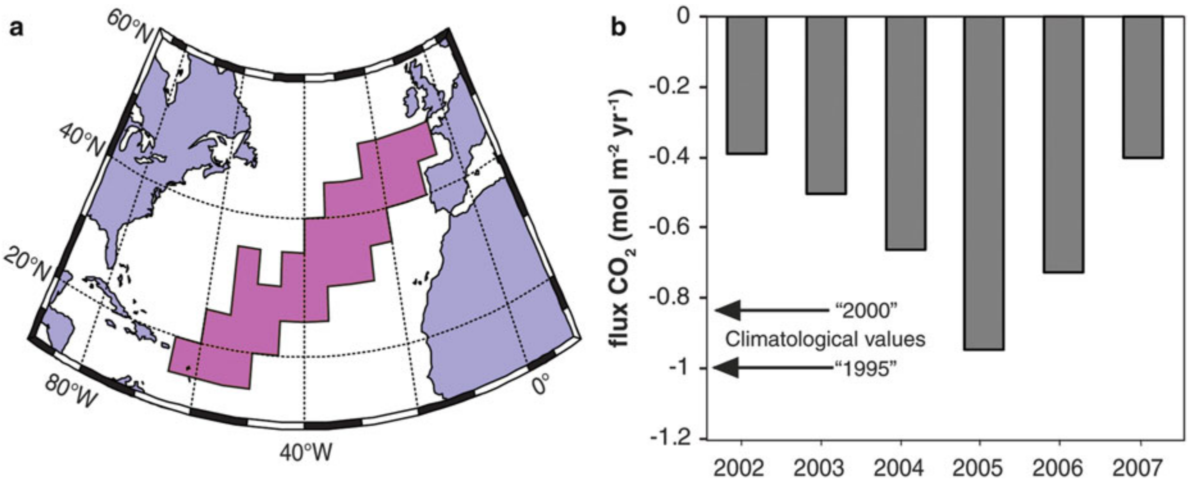

Fig. 3.5 Annual CO_2 uptake for the *pink shaded* ocean area between the UK and the Caribbean for 2002–2007. The size of climatological fluxes for the years 1995 and 2000 (Takahashi et al. 2002, 2009) is indicated on the *left axis* of the *right figure*. (Reproduced from Watson et al. (2009) by permission of Science)

other natural CO_2 fluxes when comparing such flux estimates (Gruber et al. 2009; Takahashi et al. 2009). The open ocean source of natural CO_2 arising from river inputs has been estimated as 0.5 ± 0.2 Pg C year^{-1} (Gruber et al. 2009, after Sarmiento and Sundquist 1992). However, this value could be too high by ~0.2 Pg C year^{-1} due to the substantial outgassing of river inputs during estuarine mixing (Sect. 3.2.4).

Figures 3.6 and 3.7 show the spatial distribution of net contemporary CO_2 fluxes as determined from a pCO_2-based climatology (Takahashi et al. 2009), ocean inversion (Gruber et al. 2009), atmospheric inversion (Baker et al. 2006) and ocean biogeochemistry models (Watson and Orr 2003). The fluxes from the four methods are in reasonable agreement for most ocean regions. The notable exception is the Southern Ocean (here south of 44°S), where marine biogeochemistry models predict a much larger CO_2 sink than the other methods, mainly as a result of a weak outgassing of natural CO_2 (Mikaloff Fletcher et al. 2007). A comparison of the ocean inverse results with the pCO_2 climatology shows that while both methods indicate a similar net contemporary CO_2 sink of 0.3 Pg C year^{-1} south of 44°S, the estimates disagree in the spatial distribution of the flux (Gruber et al. 2009). The climatology-derived flux estimates indicate a Southern Ocean sink between 44°S and 58°S and a small source south of 58°S (Takahashi et al. 2009), while the ocean inversion suggests a more uniform CO_2 sink south of 44°S (Gruber et al. 2009). It is worth noting that the recent addition of further surface water fCO_2 data in the Southern Ocean, and in particular in seasonally ice covered waters, has led to a revision of air-sea CO_2 flux estimates for 50–62°S (from −0.34 to −0.06 Pg C year^{-1}) and south of 62°S (from −0.04 to +0.01 Pg C year^{-1}) in successive climatologies (Takahashi et al. 2002, 2009).

The separation of contemporary air-sea CO_2 fluxes into natural CO_2 fluxes (here excluding river-induced fluxes), river borne fluxes and anthropogenic CO_2 fluxes, using an inversion of interior ocean inorganic carbon data, is shown in Fig. 3.7 (Gruber et al. 2009). Natural CO_2 fluxes in this study vary from CO_2 sources in the tropics and the Southern Ocean to CO_2 sinks in global temperate regions and the high latitude northern hemisphere (Gruber et al. 2009). On a global scale these natural fluxes (excluding river borne fluxes) cancel out. Anthropogenic CO_2 is taken up by all ocean regions, with the largest sinks in the tropics and the Southern Ocean.

3.2.3.4 Sea Ice

Sea ice influences marine DIC cycling and the air-sea exchange of CO_2 through physical processes such as brine rejection (e.g. Anderson et al. 2004; Omar et al. 2005; Rysgaard et al. 2011) and air-ice-sea exchange (e.g. Miller et al. 2011) (Chap. 2), in addition to

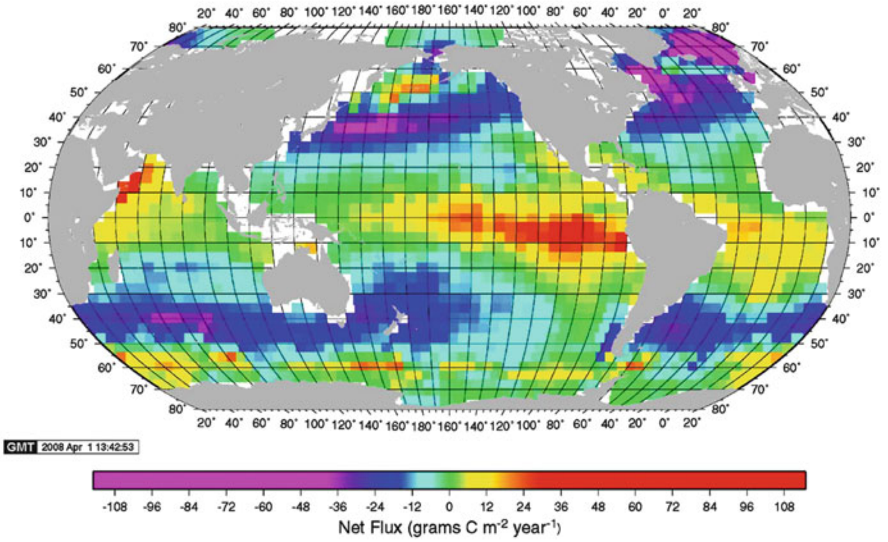

Fig. 3.6 Contemporary annual air-sea CO_2 fluxes for the year 2000 from a pCO_2 climatology (Reproduced from Takahashi et al. (2009) by permission of Elsevier)

biological and chemical processes (Delille et al. 2007; Bakker et al. 2008; Geibert et al. 2010). Although our understanding of the underlying processes is limited and quantitative estimates are scarce, the physical processes are thought to result in a net sink for tropospheric CO_2 during sea ice formation in the polar oceans. Recently, Rysgaard et al. (2011) estimated the net influx of CO_2 into the polar oceans at 33 Tg C year^{-1}, a flux resulting from the rejection of carbon from the ice crystal matrix during winter and subsequent formation of a surface layer of melt-water, undersaturated in CO_2 during summer. The sink would be much stronger (83 Tg C year^{-1}), if $CaCO_3$ crystals form in the sea ice. Omar et al. (2005) suggested a wintertime CO_2 sink of 5.2 g C m^{-2} associated with the formation of seasonal sea ice and brine rejection in the Arctic. With a seasonal sea ice extent of 14×10^6 km^2 (in 2005) this translated into a wintertime sink of 36 Tg C year^{-1}, which is on the higher end of estimates of 14 Tg C year^{-1} (no $CaCO_3$ precipitation) and 31 Tg C year^{-1} (with $CaCO_3$ precipitation) for the Arctic Ocean by Rysgaard et al. (2011). Sea ice related tropospheric CO_2 uptake was estimated as 19 Tg C year^{-1} for the Southern Ocean, which would increase to 52 Tg C year^{-1}, if $CaCO_3$ crystals form in the ice (Rysgaard et al. 2011). Oceanic CO_2 uptake during the seasonal cycle of sea ice growth and decay is thus equivalent to 17–42 % of net tropospheric CO_2 uptake in ice-free polar seas (Rysgaard et al. 2011).

3.2.3.5 Coastal to Open Ocean Carbon Exchanges

Exchanges of organic and inorganic carbon between coastal shelves and the deep ocean remain poorly quantified (Biscaye et al. 1988; Monaco et al. 1990; Biscaye and Anderson 1994; Wollast and Chou 2001), even though such exchange may be an important conduit for transferring tropospheric carbon to the interior ocean (Tsunogai et al. 1999; Thomas et al. 2004). For example an efficient 'continental shelf carbon pump', as proposed for the East China Sea and the North Sea, critically depends on the off-shelf transport of carbon-rich subsurface water (Tsunogai et al. 1999; Thomas et al. 2004) to below the permanent pycnocline of the deep ocean (Holt et al. 2008; Huthnance et al. 2009; Wakelin et al. 2012), but these carbon transports have not been verified in situ.

3.2.4 Air-Sea CO_2 Fluxes in Coastal Areas

3.2.4.1 Continental Shelves

Contemporary air-sea exchange fluxes of CO_2 in the coastal environment have been estimated by adjusting local flux data to the global scale using procedures of varying complexity (Box 3.4; Table 3.4). These range from extrapolating a single flux estimate from a continental shelf to the global scale, such as in the East China Sea (Tsunogai et al. 1999) or the North Sea

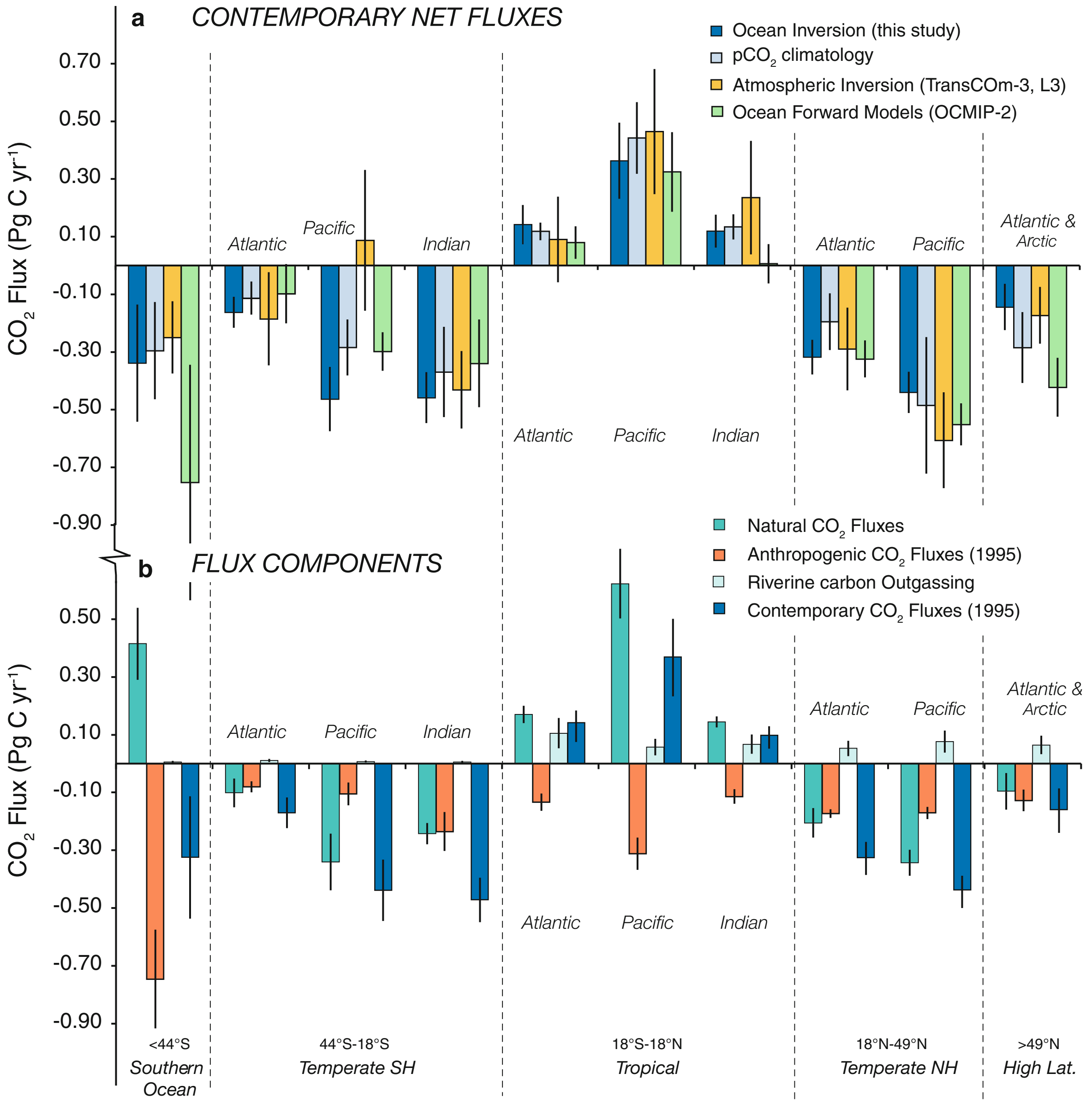

Fig. 3.7 Air-sea CO_2 fluxes for 10 regions per latitude range and per basin with positive fluxes for CO_2 leaving the ocean. (**a**) Net contemporary air-sea CO_2 fluxes from ocean inversion estimates (Gruber et al. 2009), a surface ocean pCO_2 climatology (Takahashi et al. 2009), mean estimates from 13 ocean biogeochemistry models (Watson and Orr 2003) and mean estimates from atmospheric inversion of CO_2 (Baker et al. 2006). Error bars for the ocean biogeochemistry model estimates are the unweighted standard deviation of the model outputs. The uncertainties in the atmospheric inversion estimates are based on the square of the errors within and between models. (**b**) Natural, anthropogenic, river-induced and contemporary air-sea CO_2 fluxes by ocean inversion. *Error bars* indicate the cross-model weighted standard deviation of the mean. Anthropogenic and contemporary fluxes are for the nominal year 1995. (Reproduced from Gruber et al. (2009) by permission of the American Geophysical Union)

(Thomas et al. 2004), to approaches that compiled flux values for several continental shelf systems with scaling by surface area. Areas have been grouped by latitudinal bands (Borges 2005; Borges et al. 2005), oceanic provinces (Cai et al. 2006) and surface areas derived from bathymetry (Chen and Borges 2009; Laruelle et al. 2010). The estimate of Laruelle et al. (2010) was based on a typological approach, whereby

Box 3.4

For the purpose of this work the coastal zone is defined to include near-shore systems, such as estuaries, and the continental shelf as far offshore as the 200 m depth contour (Walsh 1988; Gattuso et al. 1998; Liu et al. 2010). The continental margin consists of the coastal zone and the continental slope (from 200 to 2,000 m depth) (Liu et al. 2010). Inner estuaries are characterised by large salinity gradients, complex mixing and varying anthropogenic inputs. Laruelle et al. (2010) give a global inner estuarine area of ~1×10^6 km^2. Outer estuaries (estuarine plumes) have restricted salinity ranges and salinities typically below 34 (Frankignoulle et al. 1998). Estuarine plumes may extend tens of km offshore and may account for considerable estuarine mixing (Naudin et al. 1997). Barnes and Upstill-Goddard (2011) estimated that European outer estuaries account for more than 75 % of the total European estuarine area, but there is no comparable global estimate. Nonetheless, estuarine plumes are generally considered as part of the continental shelf and there is a concern that the characteristic distributions of CO_2, CH_4 and N_2O in such plumes may not be sufficiently sampled.

Table 3.4 CO_2 fluxes scaled globally for continental shelves and estuaries: n is the number of data points used in the up-scaling

CO_2 flux (Pg C $year^{-1}$)	CO_2 flux (mol m^{-2} $year^{-1}$)	Surface area (10^6 km^2)	n	Reference
Continental shelves globally				
−0.95	−2.90	27.0	1	Tsunogai et al. (1999)
−0.40	−1.33	25.2	1	Thomas et al. (2004)
−0.37	−1.17	25.8	15	Borges (2005)
−0.45	−1.44	25.8	17	Borges et al. (2005)
−0.22	−0.71	25.8	29	Cai et al. (2006)
−0.34	−0.92	30.0	58	Chen and Borges (2009)
−0.22	−0.71	24.7	37	Laruelle et al. (2010)
Estuaries globally				
+0.60	+36.5	1.40	13	Abril and Borges (2004)
+0.43	+38.2	0.94	16	Borges (2005)
+0.32	+28.6	0.94	16	Borges et al. (2005)
+0.36	+32.1	0.94	32	Chen and Borges (2009)
+0.27	+21.0	1.10	62	Laruelle et al. (2010)

continental shelves were defined as one of three types: enclosed, upwelling, and open. In these studies the Arctic Ocean was included in estimates for the coastal ocean, but other deep marginal seas were excluded.

The first global estimate of the continental shelf sink for CO_2, based on East China Sea data (Tsunogai et al. 1999) was 1.0 Pg C $year^{-1}$, whereas most recent estimates converge to a value ~0.3 Pg C $year^{-1}$ (Chen and Borges 2009; Laruelle et al. 2010; Cai 2011). While continental shelves cover less than 10 % of the total ocean surface area, their air-sea CO_2 flux density is about twice as large (Laruelle et al. 2010) as the global average for the open oceans based on the most recent CO_2 climatology (Takahashi et al. 2009). This is consistent with higher biogeochemical reaction rates on continental shelves; rates of net primary production and export production are twice as high as in the open ocean, for example (Wollast 1998). Even so, the zonal variability in air-sea CO_2 fluxes over continental shelves (Borges 2005; Borges et al. 2005; Laruelle et al. 2010) follows the patterns of the open ocean (Takahashi et al. 2009), with low latitude continental shelves being CO_2 sources and temperate and high latitude shelves being sinks for tropospheric CO_2. This suggests that the direction of air-sea CO_2 fluxes on continental shelves is to some extent dictated by a "background" signal of "incoming" open ocean waters, and that the intensity of the flux is further modulated (enhanced) by biogeochemical processes on the continental shelf.

Lee et al. (2011) recently evaluated the anthropogenic carbon inventory in four marginal seas (Arctic Ocean, Mediterranean Sea, Sea of Okhotsk, and East/Japan Sea). These authors conclude that each of these marginal seas stores proportionally more anthropogenic CO_2 than the global open ocean and they attribute this to a dynamic over-turning circulation in these marginal seas.

3.2.4.2 Near-Shore Systems

Near-shore systems such as estuaries are known to significantly modify the fluxes of organic carbon from land to sea (e.g. Smith and Hollibaugh 1993; Gattuso et al. 1998; Battin et al. 2008) and to also emit large quantities of N_2O and CH_4 (Sects. 3.3.5 and 3.4.5) (Barnes et al. 2006; Denman et al. 2007; Upstill-Goddard 2011). Estuaries are also characterised by a net annual emission of CO_2 to the troposphere with intense flux densities (Frankignoulle et al. 1998). Various estimates of the global emission of CO_2 to the troposphere from inner estuaries are based on scaling exercises (Table 3.4) (Abril and Borges 2004; Borges 2005; Borges et al. 2005; Chen and Borges 2009; Laruelle et al. 2010). All are based on the global surface area estimate of Woodwell et al. (1973) with the exception of Laruelle et al. (2010), which is based on the typology of estuaries from Dürr et al. (2011). The first estimate by Abril and Borges (2004) of the emission of CO_2 to the troposphere was 0.6 Pg C year^{-1} and the most recent estimates converge to ~0.3 Pg C year^{-1} (Laruelle et al. 2010; Cai 2011). The estimate of Laruelle et al. (2010) relies on an estuarine typology with four types (small deltas and small estuaries, tidal systems and embayments, lagoons, fjords and fjärds (sea inlets, which have been subject to glacial scouring, in a rocky area of low topography)). This is an important innovation relative to previous scaling attempts, since estuarine morphology and physical structure strongly modulate the exchange of CO_2 with the troposhere (Borges 2005; Koné et al. 2009; Borges and Abril 2011). Fjords and fjärds constitute the most abundant estuarine type (~43 %), although CO_2 flux data have been reported for only one system. This highlights the limitation of using scaling approaches that are too complex with regards to the available data, and the need to obtain further data in near-shore systems to improve estimates of air-sea exchange of CO_2.

In most macro-tidal estuaries the river input of DIC can only sustain a small fraction of the observed CO_2 emission (Borges et al. 2006), implying that the bulk of estuarine CO_2 emission is sustained by the degradation of allochthonous organic matter, in agreement with the net heterotrophic nature of these systems established from measurements of community metabolic rates (Odum and Hoskin 1958; Odum and Wilson 1962; Heip et al. 1995; Kemp et al. 1997; Gattuso et al. 1998; Gazeau et al. 2004; Hopkinson and Smith 2005). This implies that near-shore coastal environments are effective sites (or 'bypasses') for returning to the troposphere as CO_2, a fraction of the carbon passing from continents (through rivers) to the ocean. The removal of river borne organic carbon during estuarine transit can be roughly evaluated at ~60 % based on the above, given a global CO_2 emission of ~0.3 Pg C year^{-1} from near shore waters (Laruelle et al. 2010; Cai 2011) and known global organic carbon river inputs of ~0.4 Pg C year^{-1} (Schlünz and Schneider 2000). This is in general agreement with the analysis of organic carbon in estuaries (e.g. Abril et al. 2002). Such a bypass of carbon has important consequences for understanding and quantifying the global carbon cycle. For instance, the pre-industrial ocean is assumed to have been a CO_2 source driven by degradation of river borne organic carbon (Smith and Mackenzie 1987; Sarmiento and Sundquist 1992). In budget studies the contemporary ocean air-sea CO_2 flux is typically corrected for the pre-industrial air-sea CO_2 flux of 0.5 ± 0.2 Pg C year^{-1}, so as to derive the anthropogenic CO_2 flux (Sarmiento and Sundquist 1992; Gruber et al. 2009; Takahashi et al. 2009). However, if most of the degradation of river borne organic carbon occurs in near-shore coastal environments rather than in the open ocean, this correction may be overestimated by ~0.2 Pg C year^{-1}, corresponding to much of the estuarine CO_2 emissions of ~0.3 Pg C year^{-1} (Laruelle et al. 2010; Cai 2011).

3.2.4.3 Multi-Year Changes and Trends

Based on the decadal analysis of surface water fCO_2 in a very limited number of coastal regions, the coastal CO_2 sink could be increasing in some regions (Wong et al. 2010), while decreasing elsewhere (Thomas et al. 2007). Gypens et al. (2009) used a model reconstruction of the biogeochemistry of the Southern North Sea during the last 50 years to evaluate how the change of river nutrient loads has affected the annual exchange of CO_2 with the troposphere. These authors concluded that carbon sequestration in the southern North Sea increased from the 1950s to the mid 1980s due to an increase in primary production fuelled by eutrophication with an N to P (nitrogen to phosphorus) ratio close to Redfield of 16 to 1 (Redfield et al. 1963). In consequence, the system shifted from a source to a sink of tropospheric CO_2. During this period pH and calcite saturation increased, rather than decreased as one would have expected from ocean acidification alone (Borges and Gypens 2010). During a period of eutrophication reversal from the mid 1980s onwards, in which river borne nitrogen inputs continued to increase but phosphorus inputs were reduced, primary production in the southern North Sea decreased due to phosphorus limitation and the system shifted back to being a source of tropospheric CO_2. During this period, the carbonate chemistry changed faster than that expected from ocean acidification alone, i.e. ocean acidification was enhanced.

3.3 Marine Distribution and Air-Sea Exchange of N_2O

3.3.1 Global Tropospheric N_2O Budget

N_2O emissions from oceanic and coastal waters play a major role in the tropospheric N_2O budget (Table 3.5). According to the IPCC 4th Assessment Report (Denman et al. 2007) the oceans are a natural N_2O source of 3.8 Tg N year^{-1} (range 1.8–5.8 Tg year^{-1}), while coastal waters, estuaries, rivers and streams together are an anthropogenic N_2O source of 1.7 Tg N year^{-1} (range 0.5–2.9 Tg year^{-1}). These sources thus contribute 20 % and 10 % respectively, of total global N_2O emissions (Tables 3.2 and 3.5). Considerable uncertainties arise over these emission estimates for reasons that are discussed in Sects. 3.3.5 and 3.6. The quantification of oceanic N_2O emissions and the identification of the marine pathways of N_2O formation and consumption have received increased attention in recent decades (Bange 2008, 2010b).

Table 3.5 Anthropogenic and natural sources of N_2O to the troposphere with the range of estimates between brackets (Denman et al. 2007)

	N_2O source (Tg N year^{-1})
Anthropogenic sources	
Fossil fuel combustion and industrial processes	0.7 (0.2–1.8)
Agriculture	2.8 (1.7–4.8)
Biomass burning	0.7 (0.2–1.0)
Human excreta	0.2 (0.1–0.3)
Rivers, estuaries, coastal zones	1.7 (0.5–2.9)
Atmospheric deposition	0.6 (0.3–0.9)
Total anthropogenic sources	6.7
Natural sources	
Soils under natural vegetation	6.6 (3.3–9.0)
Oceans	3.8 (1.8–5.8)
Atmospheric chemistry	0.6 (0.3–1.2)
Total natural sources	11.0
Total sources	17.7

3.3.2 Nitrous Oxide Formation Processes

Oceanic N_2O is formed exclusively by prokaryotes (bacteria and archaea) via two major processes: nitrification (i.e. oxidation of ammonium, NH_4^+, to nitrate, NO_3^-) and denitrification (i.e. reduction of NO_3^- to N_2) (Fig. 3.8). Nitrification is the dominant N_2O formation process whereas denitrification contributes about 7–35 % to the overall N_2O budget of the oceans (Bange and Andreae 1999; Freing et al. 2012). The contributions to oceanic N_2O production from other microbial processes such as dissimilatory nitrate reduction to ammonia (DNRA) are largely unknown. In general, biological N_2O production strongly depends on the availability of dissolved oxygen (O_2). Under oxic conditions, as found in the majority of oceanic waters, N_2O formation occurs via nitrification. Suboxic to anoxic conditions, which occur in about 0.1–0.2 % of the ocean volume, favour the net formation of N_2O via denitrification (Box 3.5) (Codispoti 2010).

3.3.2.1 Denitrification

During denitrification N_2O occurs as an intermediate which can be both produced and consumed. The denitrification pathway consists of the four step reduction of NO_3^- to N_2 (Fig. 3.8), thus it constitutes a net loss of bioavailable (or “fixed”) nitrogen (N). Denitrification is catalysed by four independent metallo-enzymes (Zumft 1997). Both bacterial and archaeal denitrifiers (Philippot 2002; Cabello et al. 2004) are able to respire NO_3^- when O_2 becomes limiting. Denitrification may therefore be considered the ancestor of aerobic respiration (Cabello et al. 2004). The O_2 sensitivity of the enzymes involved in denitrification increases step by step along the reduction chain. The enzymes are induced sequentially and a complete denitrification process can only take place at O_2 concentrations below 2–10 μM (Fig. 3.9) (Codispoti et al. 2005). With the observed

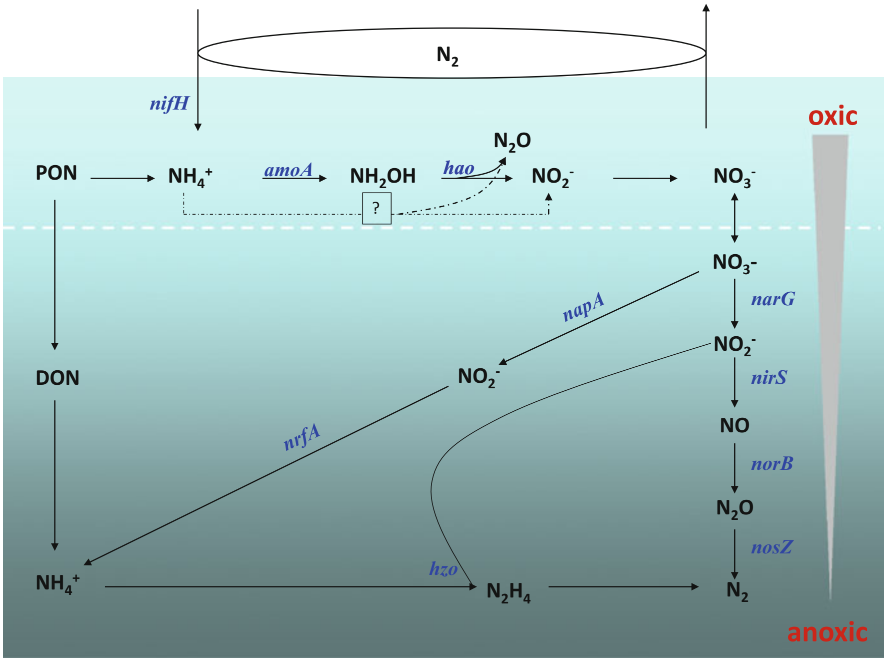

Fig. 3.8 The nitrogen cycle in the oceanic water column along a vertical oxygen gradient. Key functional genes are shown in *blue italic letters* for the transformations, the oxycline is indicated by a *horizontal, white dashed line*, and archaeal ammonia-oxidation is indicated by a *horizontal, thin, black dashed-dotted line*. (Modified from Francis et al. (2007))

Box 3.5

Dissolved oxygen concentrations play an important role in N_2O and CH_4 cycling. Here we define hypoxic or low oxygen conditions as an O_2 concentration below ~60 μM, suboxic conditions as an O_2 concentration below 5 μM (Deutsch et al. 2011) and anoxic conditions where O_2 is undetectable.

expansion of Oxygen Minimum Zones (OMZs) in the open ocean (Stramma et al. 2010) and the ongoing deoxygenation of highly productive eastern boundary upwelling areas (Codispoti 2010), net N_2O formation by denitrification may increase in the future (Sect. 3.5.3).

3.3.2.2 Nitrification

Under the oxic conditions present in more than 90 % of the ocean, N_2O is formed as a metabolic by-product during nitrification, the stepwise oxidation of NH_4^+ to nitrite (NO_2^-) by both ammonia-oxidising bacteria (AOB) and archaea (AOA). Bacteria form N_2O during the oxidation of NH_4^+ via hydroxylamine (NH_2OH) to NO_2^- (Fig. 3.8). Alternatively, N_2O can be formed during the reduction of NO_2^- via nitric oxide (NO) to N_2O, the so-called nitrifier-denitrification pathway (Cantera and Stein 2007). However, the enzymes involved in the nitrifier-denitrification pathway are different from those involved in classical denitrification (Sect. 3.3.2.1). The production of N_2O during nitrification increases with decreasing O_2 concentrations (Goreau et al. 1980; Codispoti et al. 1992). This implies that a significant in situ N_2O production in the upper mixed layer is unlikely, as this layer tends to be well oxygenated.

Until recently the formation of N_2O by nitrification was regarded as an exclusive property of AOB. This view has subsequently been revised in the light of recent work showing that AOA are the key organisms for oceanic nitrification (Wuchter et al. 2006, 2007) and that AOA are able to produce N_2O in large amounts (Santoro et al. 2011; Löscher et al. 2012). Experiments using AOA enriched cultures and pure cultures of *Nitrosopumilus maritimus*, as well as onboard incubation

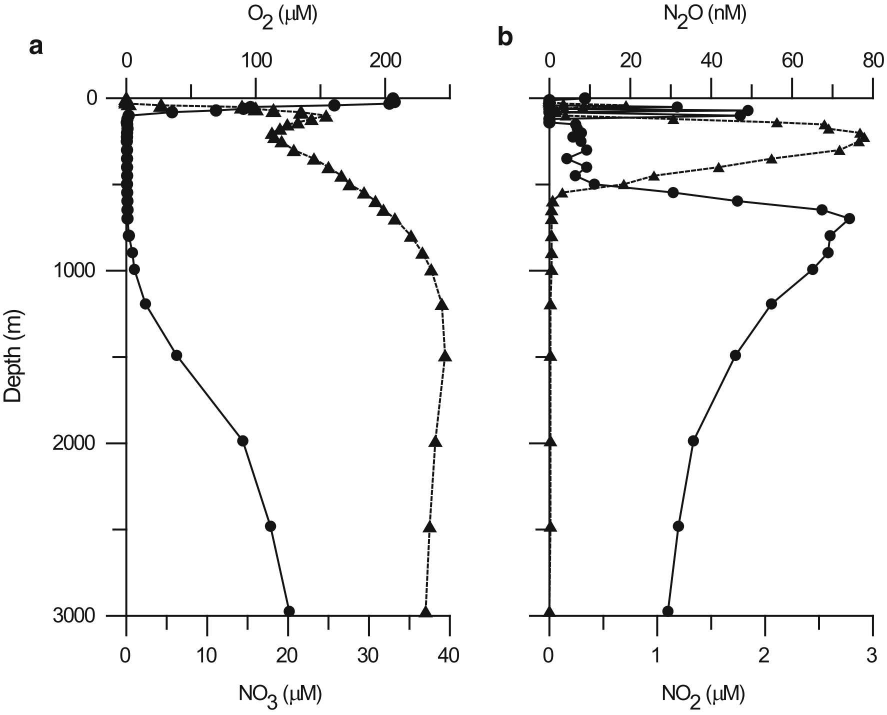

Fig. 3.9 Vertical profiles of (**a**) dissolved oxygen (*circles*) and nitrate (*triangles*), and (**b**) nitrite (*triangles*) and nitrous oxide (*circles*) at 19°N 67°E in the Arabian Sea. Note the pronounced minimum in nitrous oxide within the denitrifying zone, characterised by a minimum in nitrate and a maximum in nitrite. Maxima in nitrous oxide are found at the peripheries of this zone. (Reproduced from Naqvi (2008) by permission of Elsevier)

experiments with the archaea inhibitor GC7 (Jansson et al. 2000), demonstrated that AOA are the key organisms for N_2O production (Löscher et al. 2012). Nevertheless, the precise metabolic pathway remains unknown. The high affinity of archaea for NH_4^+ indicates their potential to outcompete AOB even under the nutrient depleted (oligotrophic) conditions (Martens-Habbena et al. 2009) which characterise large areas of the open (surface) ocean. It can thus be hypothesised that archaeal NH_4^+ oxidation is the major source of oceanic N_2O formation.

3.3.2.3 N_2O Formation by Dissimilatory Nitrate Reduction to Ammonium

Dissimilatory nitrate reduction to ammonium (DNRA) via NO_2^- is a known source of N_2O (Cole 1988), but was previously considered unimportant in the oceanic water column. However, it was recently found to significantly impact nitrogen cycling in OMZs (Lam et al. 2009) and so may be a more important source of N_2O than previously thought. A variety of bacteria (*Bacillus* sp., *Clostridium* sp., *Enterobacter* sp.) are able to carry out DNRA (Fazzolari et al. 1990a, b) and are widespread in the ocean and in other environments. N_2O is produced during the second stage of DNRA, the reduction of NO_2^- to NH_4^+ catalysed by NO_2^- reductase (Jackson et al. 1991). Nevertheless, information on the biochemical regulation of DNRA in oceanic environments remains sparse (Baggs and Philippot 2010).

3.3.3 Global Oceanic Distribution of Nitrous Oxide

Global maps of N_2O in the surface ocean have been computed by Nevison et al. (1995) (N95) and by Suntharalingam and Sarmiento (2000) (SS00) (Fig. 3.10). The N95 map is based on more than 60,000 measurements mainly made by the Scripps Institution of Oceanography between 1977 and 1993. Oceanic regions with no measurements were filled with a simple statistical routine. The SS00 map was derived from the same N_2O data set, but employed a multivariate adaptive regression spline method using mixed

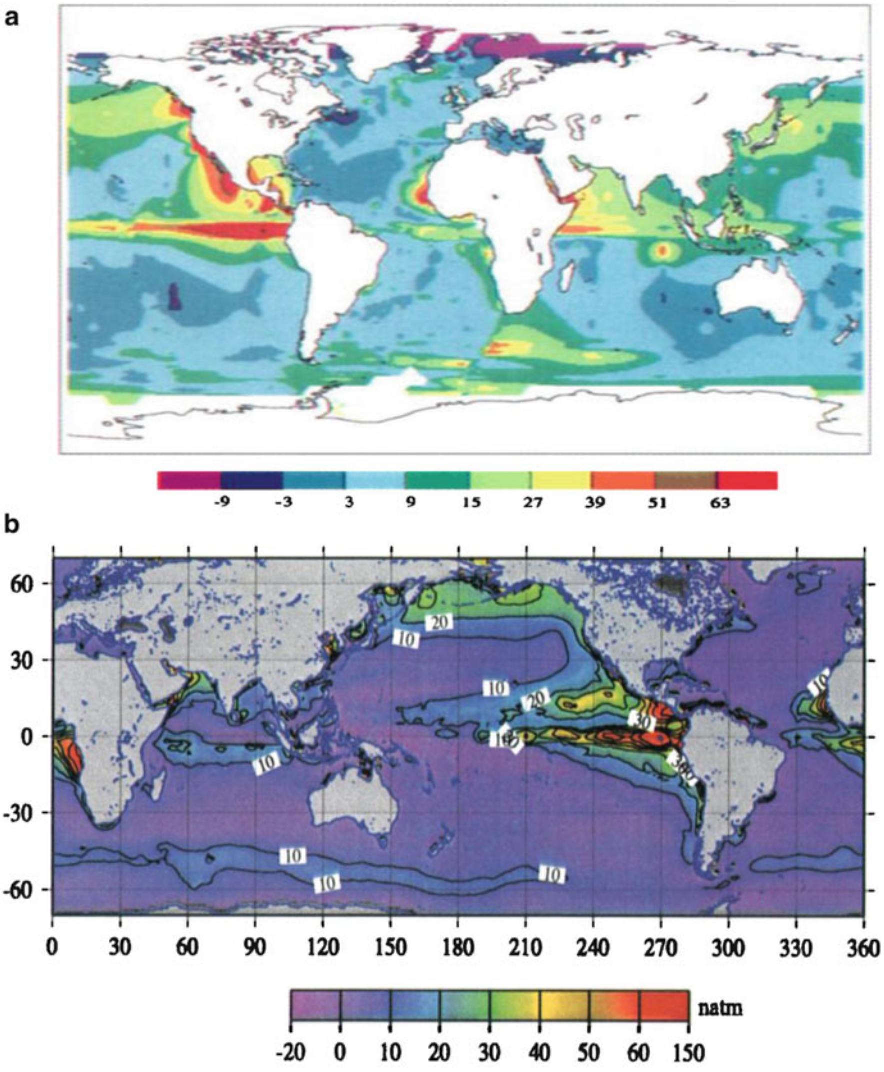

Fig. 3.10 Maps of ΔpN_2O (in natm) in the surface layer of the world's oceans: (**a**) map by Nevison et al. (1995) and (**b**) map by Suntharalingam and Sarmiento (2000). Note that the colour coding is non-linear and different for both maps. (Reproduced from Nevison et al. (1995) and Suntharalingam and Sarmiento (2000) by permission of the American Geophysical Union)

layer depth, O_2, sea surface temperature and upwelling rate as predictor variables. Differences in the two maps result mainly from the different computation methods but they share important common features: (i) enhanced N_2O anomalies (i.e. supersaturation of N_2O) in the equatorial upwelling regions of the eastern Pacific and Atlantic Oceans and in coastal upwelling regions such as along the west coasts of North and Central America, off Peru, off Northwest Africa and in the northwestern Indian Ocean (Arabian Sea); (ii) N_2O anomalies close to zero (i.e. near equilibrium) in the North and South Atlantic Ocean, the South Indian Ocean and the central gyres of the North and South Pacific Oceans. Both maps are biased by insufficient data coverage in some ocean regions (for example in the Indian and western Pacific Oceans). Since the studies of N95 and SS00 the number of available N_2O measurements has been steadily increasing. With this in mind the MEMENTO (MarinE MethanE and NiTrous Oxide) initiative was launched with the aim of collecting and archiving N_2O (and CH_4)

data sets and to provide surface N_2O (and CH_4) concentration fields for use in deriving emissions estimates (Bange et al. 2009) (Chap. 5).

Nevison et al. (1995) calculated a global mean N_2O surface saturation of 103.5 %, which indicates that the global ocean is a net source of N_2O to the troposphere. Apart from the spatial variability of N_2O surface concentrations described above, considerable seasonal variability has been observed in areas such as the Greenland and Weddell Seas. This seasonality can be caused by (i) rapid temperature shifts resulting in pronounced changes in solubility at a faster rate than N_2O exchange across the air-sea interface (e.g. in the Greenland Sea) and (ii) mixing of surface waters with N_2O enriched subsurface waters (e.g. in the Weddell Sea) (Nevison et al. 1995). While a biological source of N_2O in the well-oxygenated mixed layer seems unlikely, some studies suggested in situ mixed layer production based on a mismatch between the N_2O air-sea flux and the diapycnal flux into the mixed layer (Dore and Karl 1996; Morell et al. 2001). In a recent study of N_2O air-sea and diapycnal fluxes in the eastern tropical North Atlantic (including the upwelling off Mauritania, NW Africa) the mean air-sea flux, calculated using a common gas exchange approach, was about three to four times larger than the mean diapycnal flux into the mixed layer (Kock et al. 2012). Neither vertical advection nor biological production could explain this discrepancy. Kock et al. (2012) speculated that surfactants may dampen air-sea gas exchange of N_2O and other gases such as CO_2 (see for example Tsai and Liu 2003) in areas with a high biological productivity.

3.3.4 Coastal Distribution of Nitrous Oxide

During the last two decades coastal areas such as estuaries, upwelling regions, and mangrove ecosystems have received increased attention as sites of intense N_2O formation and release to the troposphere. Studies of the N_2O pathways in coastal regions have mostly been undertaken in European and North American coastal regions but the number of studies from other coastal regions (e.g. from Asia and South America) has recently been increasing. In general, strongly positive N_2O anomalies are found in nitrogen-rich estuaries (Zhang et al. 2010; Barnes and Upstill-Goddard 2011) and in coastal upwelling systems (Nevison et al. 2004). Coastal N_2O emissions contribute significantly to the overall oceanic emission (Table 3.6).

Nitrous oxide saturations in estuaries are highly variable and can reach values up to 6,500 % (Zhang et al. 2010; Barnes and Upstill-Goddard 2011). N_2O formation in estuaries heavily depends on the availability of NH_4^+ fuelling nitrification in the water column and/or sedimentary denitrification as major N_2O formation pathways (Bange 2006b; Barnes and Upstill-Goddard 2011). In nitrogen-rich estuarine systems, extremely high N_2O anomalies are usually only found in inner estuaries, whereas outer estuaries and adjacent shelf waters, which are not influenced by the river plumes, are close to equilibrium with the troposphere (Barnes and Upstill-Goddard 2011). In some European estuaries maximum N_2O concentrations are associated with the turbidity maximum zone at low salinities (Barnes and Upstill-Goddard 2011). The traditional view of a simple relationship between river inputs of dissolved inorganic nitrogen (the sum of NH_4^+ and NO_3^-) and estuarine N_2O formation has been challenged by recent findings that resuspended NH_4^+ and/or NH_4^+ derived from ammonification of particulate organic nitrogen in the turbidity maximum zone might dominate N_2O production (Barnes and Upstill-Goddard 2011). This implies that N_2O formation may not be related to river inputs of dissolved inorganic nitrogen in any simple way (Barnes and Upstill-Goddard 2011). High N_2O saturations in estuaries (and rivers) are also found at sites of sewage and industrial effluents.

The narrow bands of coastal upwelling systems such as those found in the northwestern Indian Ocean (Arabian Sea) and in the southeastern Pacific Ocean (off central Chile) have been identified as 'hot spots' of extremely high N_2O concentrations with N_2O saturations of up to 8,250 % and 2,426 %, respectively (Naqvi et al. 2005; Cornejo et al. 2007). The high N_2O saturations in coastal upwelling regions appear to be caused by the upwelling of N_2O enriched subsurface waters (Naqvi et al. 2005; Cornejo et al. 2007).

Some coastal upwelling areas show a rapid seasonal transition from oxic via suboxic to anoxic conditions and vice versa. In these systems, significant amounts of N_2O (up to several hundred nM) (Fig. 3.11) can accumulate temporarily during the short transition time, when the system is changing its oxygen regime. This phenomenon has been observed at different coastal time-series sites associated with coastal upwelling, such as off central

Table 3.6 N_2O emissions from marine waters

	Area (10^6 km^2)	N_2O emission (Tg N year^{-1})	Reference
Open ocean	–	1.8–5.8	Denman et al. (2007)
	313	0.6–1.1	Rhee et al. (2009)
Total open ocean	**348**[a]	**0.6–5.8**	
Coastal upwellings	1.75	0.05–0.2	Nevison et al. (2004)
	0.4[b]	0.0015–0.0035	Rhee et al. (2009)
Estuaries	1.4[c]	0.25	Kroeze et al. (2005)
Mangroves	0.2	0.1	Barnes et al. (2006)
Other coastal regions	10[d]	0.08 (± >25 %)	Nevison et al. (2004)
	48[b]	0.4–0.9	Rhee et al. (2009)
Total coastal regions (incl. upwelling, estuaries and mangroves)	**13.35**[e]	**0.4–1.45**	
Total ocean (open ocean and coastal regions)	**361**	**1.0–7.25**[f]	

[a] Estimated as the difference between the total ocean area (361 × 10^6 km^2) and the sum of the areas (in 10^6 km^2) of coastal upwelling (1.75), continental shelves with a depth <200 m (10), estuaries (1.4) and mangroves (0.2)
[b] Source not given
[c] As cited in Nevison et al. (2004)
[d] Continental shelves with a depth <200 m
[e] Estimated as the sum of the areas (in 10^6 km^2) of coastal upwelling (1.75), continental shelves with a depth <200 m (10), estuaries (1.4) and mangroves (0.2)
[f] Estimated as the sum of the regional minimum and maximum values, respectively

Chile and off West India, and in the western Baltic Sea (Naqvi et al. 2010). During the transition stages, the accumulation of N_2O does not occur in the anoxic zones, but at the oxic to anoxic boundaries. The exact cause of this extreme accumulation of N_2O is not well understood, although inhibition of the activity of N_2O reductase through frequent incursion of O_2 into the O_2-deficient layer has been proposed as one possible explanation. In anoxic zones, N_2O is usually found at very low or even undetectable concentrations.

Another intriguing feature is the much smaller N_2O accumulation at the upper boundary of the suboxic zone of enclosed anoxic basins (Black Sea, Baltic Proper) and some anthropogenically-formed anoxic zones (Tokyo Bay and Chesapeake Bay). In the hypoxic bottom waters of the East China Sea and the Gulf of Mexico, the observed N_2O build-up is modest. Overall, these results do not show comparable N_2O build-up in the anthropogenically-formed coastal hypoxic zones to those in naturally-formed, upwelling-related coastal suboxic zones (Naqvi et al. 2010). However, a large number of anthropogenically-formed anoxic zones remain to be investigated.

Mangrove ecosystems cover ~75 % of tropical coasts and are among the world's most productive ecosystems. Their open waters cover ~0.2 × 10^6 km^2, equivalent to ~20 % of the global estuarine area (Borges et al. 2003). The ecosystems of mangrove forests have a high potential of N_2O formation and release to the troposphere (Barnes et al. 2006). There seems to be no dominant formation process: N_2O in mangrove sediments from Puerto Rico was mainly produced by nitrification (Bauzá et al. 2002), whereas incubation experiments with mangrove soils from the east coast of Australia revealed denitrification to be the main N_2O formation pathway (Kreuzwieser et al. 2003). In a seasonal study of N_2O emissions from a pristine mangrove creek on South Andaman Island (Gulf of Bengal), Barnes et al. (2006) found that N_2O emissions were negatively correlated with tidal height, indicating that N_2O (and CH_4) is released from sediment pore waters during "tidal pumping", i.e. during cyclic decrease and increase of the hydrostatic pressure between low and high water (Fig. 3.12; Sect. 3.4.4).

3.3.5 Marine Emissions of Nitrous Oxide

The N_2O emission estimates in Tables 3.5 and 3.6 imply that coastal areas contribute significantly to total marine N_2O emissions, which is in line with previous emission estimates (Bange 2006a). The

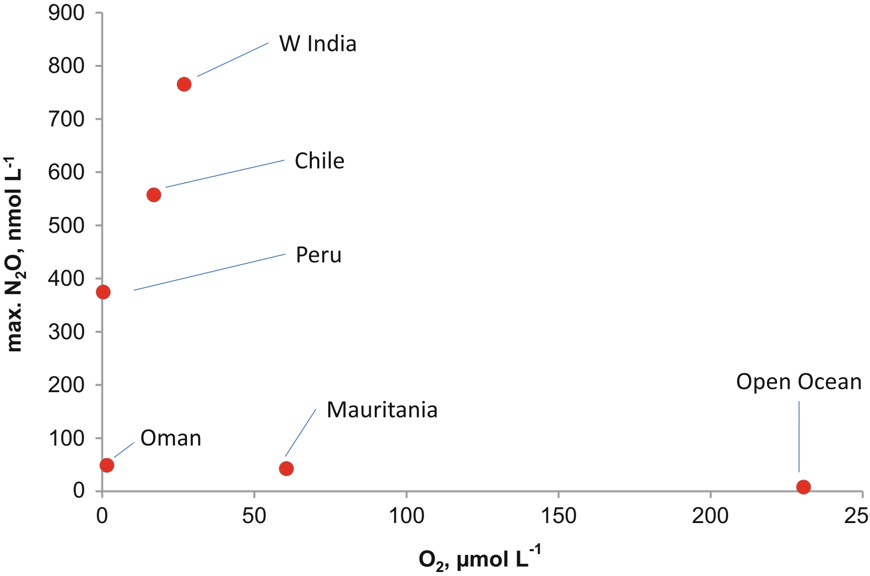

Fig. 3.11 Maximum N_2O concentrations and associated O_2 concentrations in coastal upwelling regions. A typical N_2O surface concentration in the tropical open ocean is also shown. (Data sources: W. India and Oman – S.W.A. Naqvi, pers. comm.; Mauritania – A. Kock and H.W. Bange, unpublished; Chile – Cornejo et al. (2006); Peru – C.R. Löscher and H.W. Bange, unpublished)

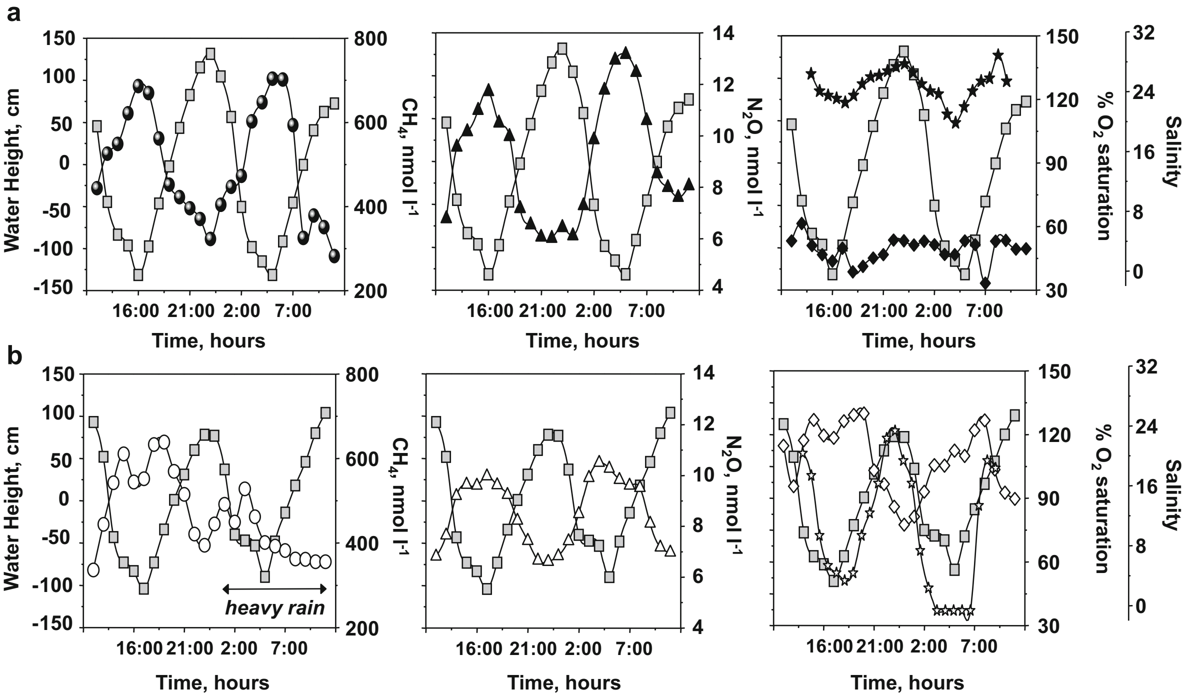

Fig. 3.12 Variation of CH_4 (*circles*), N_2O (*triangles*), tidal height (*squares*), O_2 saturation (*stars*) and salinity (*diamonds*) in a tropical mangrove creek (Wright Myo, Andaman Island) during (**a**) the dry season (January 2004) and (**b**) the wet season (July 2004) (Reproduced from Barnes et al. (2006) by permission of the American Geophysical Union)

emission estimates for coastal areas (upwelling regions, shelves, estuaries and mangroves) have a large uncertainty because of the small number of available measurements. In particular, natural coastal suboxic zones are strong N_2O sources to the troposphere. The total N_2O emission from these areas could be as high as 0.56 Tg N $year^{-1}$ (Naqvi et al. 2010), comparable to global emissions from estuaries (0.25 Tg N $year^{-1}$) and continental shelves (0.4–1.45 Tg N $year^{-1}$) (Table 3.6) (Seitzinger and Kroeze 1998). As is the case for open ocean emissions (see below), flux estimates from coastal areas need to consider seasonal variability (Wittke et al. 2010; Zhang et al. 2010; Barnes and Upstill-Goddard 2011).

The recent open ocean estimate by Rhee et al. (2009) is considerably lower than that of the widely used IPCC 4th Assessment Report (Table 3.6) (Denman et al. 2007). However, because the estimate by Rhee et al. (2009) is based on a single meridional transect in the Atlantic Ocean, it almost certainly includes an unquantified seasonal and regional bias.

Unfortunately, the seasonality of surface water N_2O concentrations over large regions of the ocean remains unknown because ship campaigns are limited in space and time and N_2O sensors are not yet available on gliders, floats or moorings. Neglecting the seasonality of surface N_2O concentrations introduces severe bias into the N_2O flux estimates. Freing (2009) demonstrated how both N_2O concentrations in surface water and N_2O fluxes in the North Atlantic Ocean (19–42°N) follow a seasonal cycle similar to that of fCO_2 (Fig. 3.13; Sect. 3.2.3). This seasonal cycle can be described by a harmonic function and is mainly controlled by temperature. The presence of such seasonal variation renders a mean flux, if calculated from a seasonally-biased dataset, a potentially poor estimate of the true annual net flux (Freing 2009). Integrating the harmonic function over a full annual cycle gives a better estimate of the net annual flux.

In ocean regions where the upper boundary of the OMZ is shallow, minor changes in the hydrographic or meteorological conditions can lead to entrainment of N_2O from the OMZ into the surface layer, thereby enhancing N_2O sea-to-air fluxes (Naik et al. 2008). As a result of high N_2O concentrations close to the sea surface, N_2O emissions in open-ocean regions with substantial N_2O accumulation at mid-depth (associated with O_2 depletion) (e.g. in the Eastern Tropical South Pacific and the Arabian Sea), are quite high. The N_2O emissions from these regions (0.8–1.35 Tg N $year^{-1}$) (Naqvi et al. 2010) make up a significant fraction of the overall N_2O emission from the oceans (Table 3.6).

3.4 Marine Distribution and Air-Sea Exchange of CH_4

3.4.1 Global Tropospheric CH_4 Budget

In contrast to the situation for CO_2 and N_2O, the marine system plays a relatively minor role in the global tropospheric CH_4 budget, representing a small net natural contribution (Tables 3.2 and 3.3). However, in common with other global CH_4 sources, marine-derived CH_4 has proven difficult to quantify with any great certainty (Table 3.3). Although detailed CH_4 surveys in specific ocean basins have been available since the 1970s, they are comparatively limited in number and many of the early measurements were derived in the absence of reliable solubility data (Reeburgh 2007). The global marine CH_4 dataset is thus rather limited in comparison to CO_2 or N_2O. Detailed maps of the global surface ocean distribution remain to be compiled, with the recent MEMENTO initiative (Bange et al. 2009) working towards this goal (Chap. 5).

3.4.2 Formation and Removal Processes for Methane

Methanogenesis is the final stage of organic matter decomposition and is a form of anaerobic respiration carried out exclusively by single celled archaea whose growth is severely O_2-limited. The terminal electron acceptor is therefore not O_2, but carbon from low molecular weight compounds. Carbon dioxide and acetic acid (CH_3COOH) are the most familiar:

$$CO_2 + 4H_2 \rightarrow CH_4 + 2H_2O \qquad (3.11)$$

$$CH_3COOH \rightarrow CH_4 + CO_2 \qquad (3.12)$$

Other low molecular weight compounds acting as methanogenic substrates include formic acid (HCOOH), methanol (CH_3OH), methylamine (CH_3NH_2), dimethylsulphide (CH_3SCH_3) and methanethiol (CH_3SH). Unsurprisingly, anoxic coastal marine sediments (Middelburg et al. 1996) and strongly O_2-deficient waters (Naqvi et al.

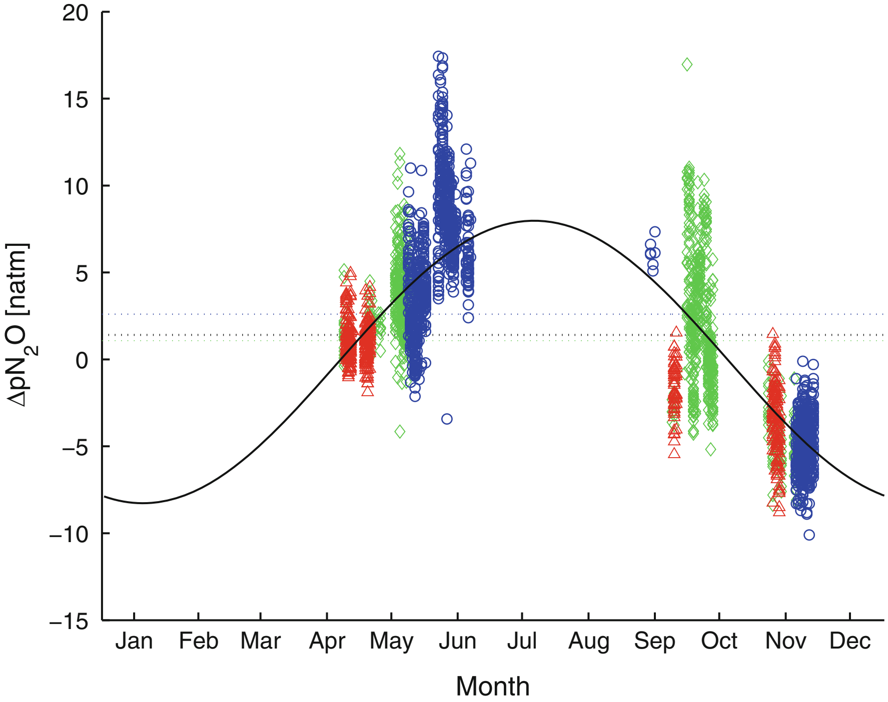

Fig. 3.13 ΔpN_2O (in natm) in the North Atlantic Ocean (19–42°N 10–66°W): Tropical (*red triangles*), western subtropical (*green diamonds*) and eastern subtropical (*blue circles*) regions. The *solid black line* denotes a fitted harmonic function. The *dotted lines* denote the respective annual mean for all data points (*black*, *middle line*), the western (*green*, *bottom line*) and the eastern (*blue*, *top line*) basin. (The figure is from Freing (2009))

2005) are major sites of methanogenesis. The ability of sulphate-reducing bacteria (SRB) to outcompete methanogens (Capone and Kiene 1988) means that CH_4 concentrations are generally low in near-surface sediment pore waters where sulphate reduction is active and that they are maximal below the depth where dissolved sulphate (SO_4^{2-}) becomes fully depleted (Blair and Aller 1995). This can be anywhere between several centimeters and several meters below the sediment surface. The role of SRB is an important consideration in estuaries, where water column SO_4^{2-} concentrations vary from micro- to milli-molar along the salinity gradient. In these situations the depth of SO_4^{2-} depletion increases and maximal CH_4 production generally decreases seaward. Methanogenesis rates have thus been shown to decrease by up to two orders of magnitude seaward (Abril and Borges 2004). In addition to SO_4^{2-} availability and associated SRB activity, rates of organic matter sedimentation and the availability of alternative electron acceptors also influence methanogenesis rates.

Despite inhibition of methanogenesis by both O_2 and SO_4^{2-} supply, CH_4 is typically supersaturated in the open ocean mixed layer (Sect. 3.4.3). Until recently the prevailing explanation for this so-called “marine CH_4 paradox” has been methanogenesis (Eqs. 3.11 and 3.12) within “anoxic microniches” inside zooplankton guts and suspended particles (Oremland 1979; De Angelis and Lee 1994). This notion is supported by an “oxic” methanogenic archaea isolated from coastal waters (Cynar and Yayanos 1991), the identification of methanogens in marine zooplankton guts and particles (Marty et al. 1997) and CH_4 release from sinking particles inferred from $\delta^{13}CH_4$ measurements (Sasakawa et al. 2008). Even though significant CH_4 release has been observed from mixed zooplankton-phytoplankton cultures (De Angelis and Lee 1994) and correlations of CH_4 with primary productivity indicators, such as chlorophyll *a*, have been found (Oudot et al. 2002), such correlations are weak (Upstill-Goddard et al. 1999; Holmes et al. 2000; Forster et al. 2009).

Recent investigations propose two alternative CH_4 production mechanisms, both implicating nutrient limitation in the control of mixed layer CH_4 formation. In the first hypothesis bacterioplankton successfully exploit phosphate-depleted waters, where nitrate is in excess, by deriving phosphorus from phosphonates such as methyl phosphonate (Karl et al. 2008). Methane is thus produced aerobically as a byproduct of methyl phosphonate decomposition. The second hypothesis proposes that certain microbes can catabolise dimethylsulphoniopropionate (DMSP) as a carbon source through methylotrophic methanogenesis in NO_3^- depleted waters, where phosphate (PO_4^{3-}) is plentiful (Damm et al. 2010). Based on the conversion of DMSP to hydrogen sulphide (H_2S) and CH_3SH by DMSP-utilising bacteria (Kiene et al. 2000) and a recent proposal for the intermediate formation of CH_3SH during CH_4 oxidation (Moran et al. 2008), Damm et al. (2010) proposed a thermodynamically plausible reverse reaction for the aerobic production of CH_4 from CH_3SH. The two mechanisms are entirely compatible and raise the intriguing possibility that deviations from the Redfield N:P ratio could be indirectly responsible for the marine CH_4 paradox through planktonic succession favouring species able to exploit alternative marine phosphorus and nitrogen stores.

Whatever the mechanisms responsible for upper ocean marine CH_4 production, emission of CH_4 to the troposphere is strongly moderated by aerobic and anaerobic microbial oxidation (Boetius et al. 2000). Aerobic CH_4 oxidation occurs in oxygenated water columns and oxic sediment pore waters:

$$CH_4 + 2O_2 \rightarrow CO_2 + 2H_2O \qquad (3.13)$$

Anaerobic oxidation of methane (AOM) occurs both in anoxic sediment pore waters and in anoxic water columns and is believed to involve consortia of archaea and SRB:

$$CH_4 + SO_4^{2-} \rightarrow HCO_3^- + HS^- + H_2O \qquad (3.14)$$

In sediment pore waters the SO_4^{2-}–CH_4 transition constrains upward CH_4 diffusion and leads to pore water CH_4 profiles having a concave-upward shape (Blair and Aller 1995).

3.4.3 Global Oceanic Distribution of Methane

Although CH_4 concentrations in the open ocean are generally rather low (a few nM), net mixed layer CH_4 production means that O_2-saturated near-surface waters are generally also supersaturated in CH_4, with typical values of 130–160 % and maxima near the base of the mixed layer (Oudot et al. 2002; Forster et al. 2009). Considerably higher mixed layer CH_4 supersaturation is, however, not uncommon. Figure 3.14 illustrates this for the upper 300 m of the water column on north–south Atlantic Ocean transects. In addition to upper ocean CH_4 production, lateral supply from continental margins (Sect. 3.4.4) has also been invoked to explain high mixed layer CH_4 concentrations (Reeburgh 2007).

Similar to N_2O, elevated CH_4 levels are also found in intermediate waters (~500–1,000 m depth) of the three major open ocean OMZs: the Eastern Tropical North and South Pacific and the Arabian Sea (Naqvi et al. 2010), and in the upwelling zones associated with these OMZs (Sect. 3.3.5). In these regions seasonal upwelling of nutrient-rich waters fuels primary productivity and enhances the downward flux of biogenic particles (Rixen et al. 1996), leading to O_2 consumption in the intermediate waters and subsequent methanogenesis.

Below the ocean mixed layer and away from the OMZ's, CH_4 concentrations progressively decrease through oxidation, such that CH_4 concentrations may approach undetectable levels in the deep ocean basins (Upstill-Goddard et al. 1999; Yoshida et al. 2011). Occasionally this deep water CH_4 signal impacts surface waters through oceanic upwelling, as is illustrated by the bottom panel of Fig. 3.14 where the effect of equatorial upwelling is evident as far north as ~15°N. Overall, on an annual basis the open ocean CH_4 budget is considered to be in steady-state with in situ production and vertical transport balancing CH_4 oxidation and emissions to the troposphere.

3.4.4 Coastal Distribution of Methane

3.4.4.1 Coastal Sediments

The total mass of CH_4 in shallow marine sediments remains unquantified but it is nevertheless thought to be substantial, with methanogenesis considered likely in at least 30 % of the global continental shelf area (Judd

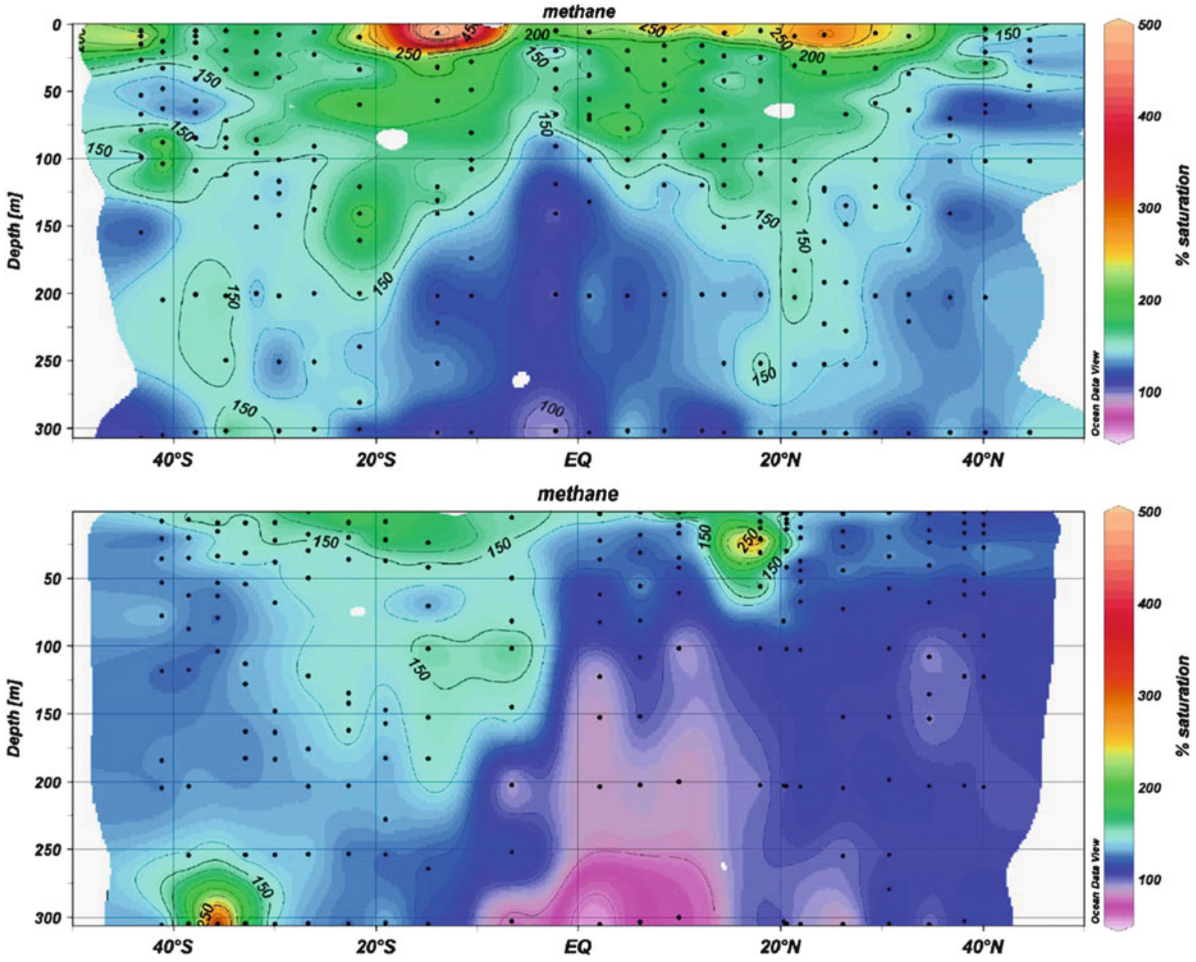

Fig. 3.14 CH_4 saturation in the upper 300 m of the Atlantic Ocean between 50°N and 52°S during 2003. *Top panel*: April–May; *bottom panel*: September–October. *Dots* represent water samples. (Reproduced from Forster et al. (2009) by permission of Elsevier)

and Hovland 2007), i.e. at least 7.4×10^6 km^2 (Laruelle et al. 2010). Although it is estimated that more than 90 % of the sediment CH_4 inventory may be consumed by AOM (Sect. 3.4.2) prior to sediment-water exchange (Dale et al. 2006), CH_4 emissions from individual sites can be very high per unit area (Middelburg et al. 1996; Abril and Iversen 2002) and can significantly impact the CH_4 signal in the overlying water. Figure 3.15 is an example from a UK estuary (Tyne) where the broad CH_4 maximum between salinities 5 and 20 may reflect inputs from anoxic intertidal mudflats in mid-estuary (Upstill-Goddard et al. 2000 and discussion below).

In some circumstances organic carbon burial may be sufficiently intense that the resulting rate of methanogenesis contributes to raising the total pore water gas concentration above the hydrostatic pressure in the sediment, with the result that gas bubbles are formed (Wever et al. 1998). It has been shown that bubbles start to form at CH_4 concentrations well below its solubility (~1 mM) and that these may contain ~40–100 % CH_4 (Chanton et al. 1989). This results in a rapid, episodic release of CH_4 enriched bubbles to the water column (ebullition) and potentially directly to the troposphere with minimal oxidation (Dimitrov 2002). CH_4 ebullition may typically exceed the diffusional sediment CH_4 flux by more than an order of magnitude (Ostrovsky 2003; Barnes et al. 2006; Nirmal Rajkumar et al. 2008). However, ebullition is notoriously difficult to quantify because spatial and temporal variability can confound attempts to accurately capture a representative sample. Perhaps

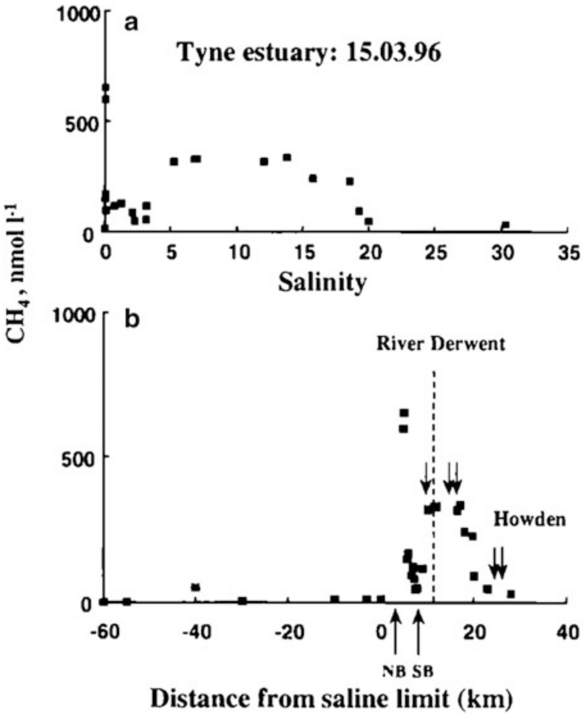

Fig. 3.15 Dissolved CH_4 in the Tyne estuary, UK. (**a**) CH_4 *versus* salinity; (**b**) CH_4 *versus* distance from the tidal limit (positive is downstream; negative is upstream). *Dotted line*: location of major tributary (Derwent); *arrows*: locations of additional freshwater discharges (Reproduced from Upstill-Goddard et al. (2000) by permission of the American Geophysical Union)

unsurprisingly, few studies have directly studied sediment CH_4 ebullition and hence the controlling processes have not been well quantified. Temperature is clearly important through solubility effects and its control of methanogenesis rates, as is water depth. In coastal waters ~3 m deep, minimal bubble dissolution was observed during migration to the air-sea surface (Martens and Klump 1980), but in deeper waters complete bubble dissolution may occur, before the bubbles reach the sea surface (Joyce and Jewell 2003). Contamination of CH_4-enriched bubbles by surfactants can also significantly reduce their rise velocities, thereby increasing the potential for dissolution (Leifer and Patro 2002). However, surfactants on the bubble surfaces will also decrease the rate of gas exchange between the bubbles and the water (e.g. Tsai and Liu 2003). Shakhova et al. (2010) reported bubbles of CH_4 entrapped in fast sea ice in the East Siberian Arctic Shelf, which they attributed to ebullition from underlying sediment. If sea ice acts to moderate the emission of CH_4 in this way, this has clear implications for Arctic CH_4 emissions as a consequence of sea ice retreat.

Vegetation strongly impacts the distribution and transport of CH_4 in coastal sediments. It has been proposed that plant-mediated CH_4 transport and CH_4 ebullition are mutually exclusive processes in tidal marshes (Van der Nat and Middelburg 1998, 2000). Vegetation impacts CH_4 concentrations in coastal sediments via the release of labile organic compounds that may stimulate methanogenesis. Vegetation also acts as a conduit for the transport of CH_4 to the troposphere and for transport of tropospheric O_2 to the rhizosphere favouring CH_4 oxidation, both transport pathways reducing CH_4 concentrations in near-surface sediments (Van der Nat and Middelburg 1998, 2000; Biswas et al. 2006). In addition, plants promote CH_4 oxidation at depth, where methanotrophs occur adjacent to or within macrophyte roots (Gerard and Chanton 1993; King 1994). Plant-mediated CH_4 transport is both passive via molecular diffusion and active via convective flow due to pressure gradients and is maximal during daylight hours in the growing season (Van der Nat et al. 1998; Van der Nat and Middleburg 2000). In two Tanzanian mangrove systems sediment-to-air CH_4 fluxes were enhanced up to fivefold in the presence of pneumatophores (above ground root systems) and it was estimated that transport via this pathway accounted for 38–64 % of the total sediment CH_4 source to air at low tide (Kristensen et al. 2008). In some situations both diffusive CH_4 exchange and ebullition can be enhanced by "tidal pumping" related to falling hydrostatic pressure (Sect. 3.3.4) (Barnes et al. 2006), with pressure changes of only a few percent having a large effect (Ostrovsky 2003). Figure 3.12 shows an inverse relation of CH_4 (and N_2O) concentrations with tidal height in a tropical mangrove creek. This indicates tidal pumping with CH_4-rich sediment pore waters seeping into the overlying creek waters at low tide, but remaining in the sediment as the hydrostatic pressure rises again. Barnes et al. (2006) suggested that tidal pumping is a major control of CH_4 and N_2O emissions from mangrove systems (Sect. 3.3.4).

Ancient microbial, thermogenic, and abiogenic CH_4 in coastal shelf sediments can become "geologically focussed", which may result in episodic CH_4 ebullition on a potentially large scale (Judd and Hovland 2007). The ephemeral nature of these "seep fluxes" is well illustrated by observations at a seep site in the outer Firth of Forth (North Sea). Dissolved CH_4 concentrations in the water column strongly increased towards the shallow seabed (~1,500 % CH_4 saturation at 90 m), but 1 year later the dissolved CH_4 concentration was only mildly supersaturated (Upstill-Goddard 2011). Shallow seeps clearly influence surface water CH_4 concentrations (Damm et al. 2005; Schmale et al. 2005). The North Sea has numerous well-documented "pock marks" (Dando et al. 1991); evidence for significant past CH_4 seepage.

3.4.4.2 Coastal Waters

Inland waters (lakes, reservoirs, streams, and rivers) can be substantial CH_4 sources to the coastal zone, although they are currently not well integrated in global greenhouse gas budgets (Table 3.3) (Bastviken et al. 2011). Most rivers studied to date are highly CH_4 supersaturated, including pristine, well-oxygenated regimes with minimal sediment cover or anthropogenic disturbance (Upstill-Goddard et al. 2000). Large CH_4 inputs from adjacent forest and/or agricultural soils have been suggested (Devol et al. 1990; Yavitt and Fahey 1991). The CH_4 concentration in river water is a complex function of catchment hydrology, vegetation cover, microbial activity, and re-aeration rates. Upstill-Goddard et al. (2000) found a general decrease in dissolved CH_4 with increasing river discharge. Their compilation of published CH_4 saturations in rivers worldwide revealed a typical range of ~1,000–40,000 %, with one extreme value for an organic-rich Amazon tributary exceeding 400,000 % (Upstill-Goddard et al. 2000). Data from 474 freshwater ecosystems point to a major CH_4 source in inland waters (Bastviken et al. 2011). Part of this contribution is almost certainly included in the source estimate for global wetlands (Table 3.3). The CH_4 source from inland waters should perhaps be formally specified as an important component in the global tropospheric CH_4 budget.

Most estuarine CH_4 data are for temperate systems. Methane saturations of up to 8,000 % have been reported for some shallow coastal embayments (Ferrón et al. 2007; Kitidis et al. 2007). A CH_4 saturation of up to 20,000 % may be typical of the mid- to upper-inner estuary (Upstill-Goddard et al. 2000; Abril and Iversen 2002; Middelburg et al. 2002). As much as 158,000 % CH_4 saturation has been reported in the Sado estuary, Portugal (Middelburg et al. 2002). The highest value recorded exceeds 3,000,000 % for the small, polluted subtropical Aydar estuary in SE India (Nirmal Rajkumar et al. 2008). This may be considered exceptional, resulting from a high organic carbon input in fresh domestic organic wastes and intense sediment methanogenesis. Indeed, methanogenesis rates were estimated to be close to maximal for the ambient temperature (Nirmal Rajkumar et al. 2008).

An important aspect of CH_4 cycling in many well-mixed macrotidal estuaries is strong tidal asymmetry with the velocity of the flood tide exceeding that of the ebb tide. This gives rise to the net transport of suspended particles upstream and retains river borne particles in a well defined turbidity maximum zone at low salinity (Uncles and Stephens 1993). High micro-organism numbers associated with the suspended particles (Plummer et al. 1987) and long particle lifetimes promote enhanced biogeochemical cycling in such regions and CH_4 concentrations can significantly exceed those in the input rivers (Fig. 3.15) (Upstill-Goddard et al. 2000). While this could result from active CH_4 release from the underlying sediments during particle resuspension (as discussed above), it could also reflect in situ water column production of CH_4 through attachment of methanogenic archaea to tidally suspended particles in the turbid, O_2–poor waters, analogous to the "anoxic microniche" hypothesis in the open ocean (Barnes and Upstill-Goddard 2011). By contrast, Abril et al. (2007) found significant CH_4 oxidation in laboratory sediment suspensions, although at higher turbidity than measured in situ by Upstill-Goddard et al. (2000). The conflicting results may reflect competition between methanogenesis and oxidation, implying complexity in the relationship between CH_4 concentrations and estuarine turbidity.

Mangrove ecosystems are significant contributors to the marine source of tropospheric CH_4 (Fig. 3.12; Table 3.7). Typically one half of mangrove net primary production is retained within the system (Dittmar et al. 2006; Bouillon et al. 2008) and this carbon is buried and/or recycled, resulting in significant CH_4 production in heterotrophic sediments and in the overlying water. The mangrove CH_4 source appears rather constant throughout the year, possibly as a result of small annual temperature excursions in mangrove systems that give minimal variability in methanogenesis rates (Barnes et al. 2006; Ramesh et al. 2007). CH_4 saturations in waters surrounding mangroves are spatially and temporally variable. Up to ~30,000 % saturation was observed in mangrove creek waters (Barnes et al. 2006), but regionally ~2,000–3,000 % might be more typical (Biswas et al. 2007).

Coastal shelf seas are almost always supersaturated in CH_4. Data for coastal shelf seas tend to be restricted to the temperate northern hemisphere with hardly any data available for coastal waters along much of the Russian Arctic, South America, East and West Africa and Antarctica. Bange (2006b) provides the most extensive regional data compilation to date, for a European shelf area estimated at ~3×10^6 km^2 or ~12 % of the global shelf sea area (Table 3.8). The variability between sites may partly reflect seasonal variation, but it is not straightforward to assess the extent of this seasonality due to a lack of seasonal measurements at individual locations.

Marine sediments are a major CH_4 source to coastal waters, in spite of the inhibition of methanogenesis by SRB and CH_4 oxidation by O_2 and SO_4^{2-}. Indeed, substantial accumulation of dissolved CH_4 in well-oxygenated bottom waters overlying organic-rich coastal sediments is well documented (Martens and Klump 1980). Order of magnitude higher concentrations have been observed in anoxic bottom waters overlying sediments with moderate organic carbon content in the Arabian Sea (Jayakumar et al. 2001). Production of CH_4 in sediments and its supply to bottom waters is primarily linked to biological productivity in the overlying waters, with hypoxia in the water exerting a secondary effect (Bange et al. 2010a). Most regions with high productivity are associated with coastal upwellings, the extent of which is set by Laruelle et al. (2010) at ~2.3×10^6 km^2. While this is only ~0.6 % of the total ocean area, these regions are "hot spots" of CH_4 emissions to the troposphere, with typical surface CH_4 saturations of ~150–250 % (Naqvi et al. 2005; Kock et al. 2008). Maximal water column CH_4 accumulation occurs in sulphidic deep waters within enclosed basins, such as the Black Sea and the Cariaco Basin, but this CH_4 is largely of geological origin (Kessler et al. 2005). By contrast, over the highly productive Namibian shelf, where sulphidic bottom water is also characteristic, the large CH_4 emission from underlying organic-rich sediments is a consequence of contemporary methanogenesis (Brüchert et al. 2009). In coastal zones, where the hypoxic conditions are caused by anthropogenic activities, the CH_4 distribution is highly variable. For example, maximum CH_4 concentrations in the Gulf of Mexico (Kelley 2003) are ~15 times higher than in the Changjiang Estuary and the East China Sea (Zhang et al. 2008).

3.4.4.3 Methane Hydrates

Methane hydrate is a quasi-stable solid, resembling ice, in which CH_4 molecules are trapped within the crystalline structure of water. Hydrate stability decreases with increasing temperature and decreasing pressure (Kvenvolden 1993). Hydrate occurs extensively in buried sediments and seabed outcrops along continental margins where water depths exceed 500 m (Beauchamp 2004) and along gravitationally unstable regions of the continental slope (Fig. 3.16). The distribution and extent of stable CH_4 hydrate can be predicted from in situ temperature and pressure, such that a theoretical gas hydrate stability zone (GHSZ) can be defined. Figure 3.17 is a schematic of the GHSZs in sediments at shallow and deep marine sites. The CH_4 source may be biogenic, volcanic, hydrothermal or thermogenic. Biogenic CH_4 from sediment methanogenesis tends to dominate (Sloan 2003).

Methane hydrates can be categorised into two broad types: structural and stratigraphic. The formation of structural hydrates involves migration of CH_4 along

Table 3.7 CH_4 emissions from marine waters

	Area (10^6 km^2)	CH_4 emission (Tg C year^{-1})	Reference
Open ocean	334	0.3	Bates et al. (1996b)
Coastal upwellings	2.3	0.02–0.15	Naqvi et al. (2005), Kock et al. (2008)
Continental shelves	24.7	0.38–7.3	EPA (2010)
Estuaries	1.0	0.08–2.3	Upstill-Goddard (2011)
Mangroves	0.2	1.7	Barnes et al. (2006)
Continental margin seeps	?	7.5–36	Hornafius et al. (1999)
			Kvenvolden and Rogers (2005)
Total	362.2	10–48	

Table 3.8 CH_4 saturations in European shelf surface waters (excluding estuaries). *SD* standard deviation (Modified from Bange (2006b))

Region	Date	CH_4 saturation (%) (range or SD)	Reference
Barents Sea	Aug 1991	120 (115–125)	Lammers et al. (1995)
Baltic Sea	1992[a]	254 (113–395)	Bange et al. (1994)
Southern N. Sea	Nov 1980	140	Conrad and Seiler (1988)
	Aug 1993	338 (118–701)	Upstill-Goddard et al. (2000)
German Bight	Sep 1991	126 ± 8	Bange et al. (1994)
Southern Bight	Mar 1989	113 (95–130)	Scranton and McShane (1991)
Central N. Sea	May 1994	215 (120–332)	Rehder et al. (1998)
UK East coast	1995–1999	129 (112–136)	Upstill-Goddard et al. (2000)
Bay of Biscay	Nov 1980	100	Conrad and Seiler (1988)
Adriatic Sea	Aug 1996	425 (420–450)[a]	Leip (1999)
E. Ionian Sea	Jul 1993	148 ± 22	Bange et al. (1996)
N. Aegean Sea	Jul 1993	231 ± 32	Bange et al. (1996)
NW Black Sea	Jul 1995	567	Amouroux et al. (2002)
Average		222 ± 142	

[a] Includes seasonal/interannual sampling

geological faults from deep sources and subsequent crystallisation on seawater contact (O'Connor et al. 2010). This can lead to accumulation of high CH_4 concentrations in domes or underneath impermeable sediments (Archer 2007). Structural CH_4 hydrates occur at relatively shallow depths and are typically "massive", i.e. they displace sediment to generate large hydrate chunks potentially filling tens of percent of the sediment volume (Tréhua et al. 2004). However, the majority of hydrate deposits are stratigraphic. These deposits are typically dilute, accounting for only a few percent of the sediment volume and are generally located some hundreds of metres below the sea floor. Gornitz and Fung (1994) further drew a distinction between marine hydrate synthesis in "passive" and "active" margins. Local sediment accumulation constrains hydrate formation in passive margins, whereas scavenging of organics deriving from adjacent areas leads to higher hydrate abundance in active margins. Hydrate formation is also sensitive to the O_2 concentration in the overlying water: a 40 μM decrease in the deep water O_2 concentration may enhance the CH_4 inventory twofold (Buffett and Archer 2004).

Knowledge of the true extent of marine CH_4 hydrate remains incomplete. Direct observations from well logs (e.g. Sloan and Koh 2008) are limited in number. Interpretations based on sea floor organic carbon derived from sea surface chlorophyll *a* can be unsuccessful (Gornitz and Fung 1994) and indirect hydrate detection via seismic profiling may prove similarly inconclusive (Sloan 2003). The perceived CH_4 hydrate inventory has been downscaled by 3–4 orders of magnitude since the 1970s due to improvements in hydrate understanding and detection. An early, widely adopted global estimate of ~10^4 Pg C in CH_4 hydrate, including a small contribution from terrestrial permafrost (Kvenvolden 1999), was more than twice the known

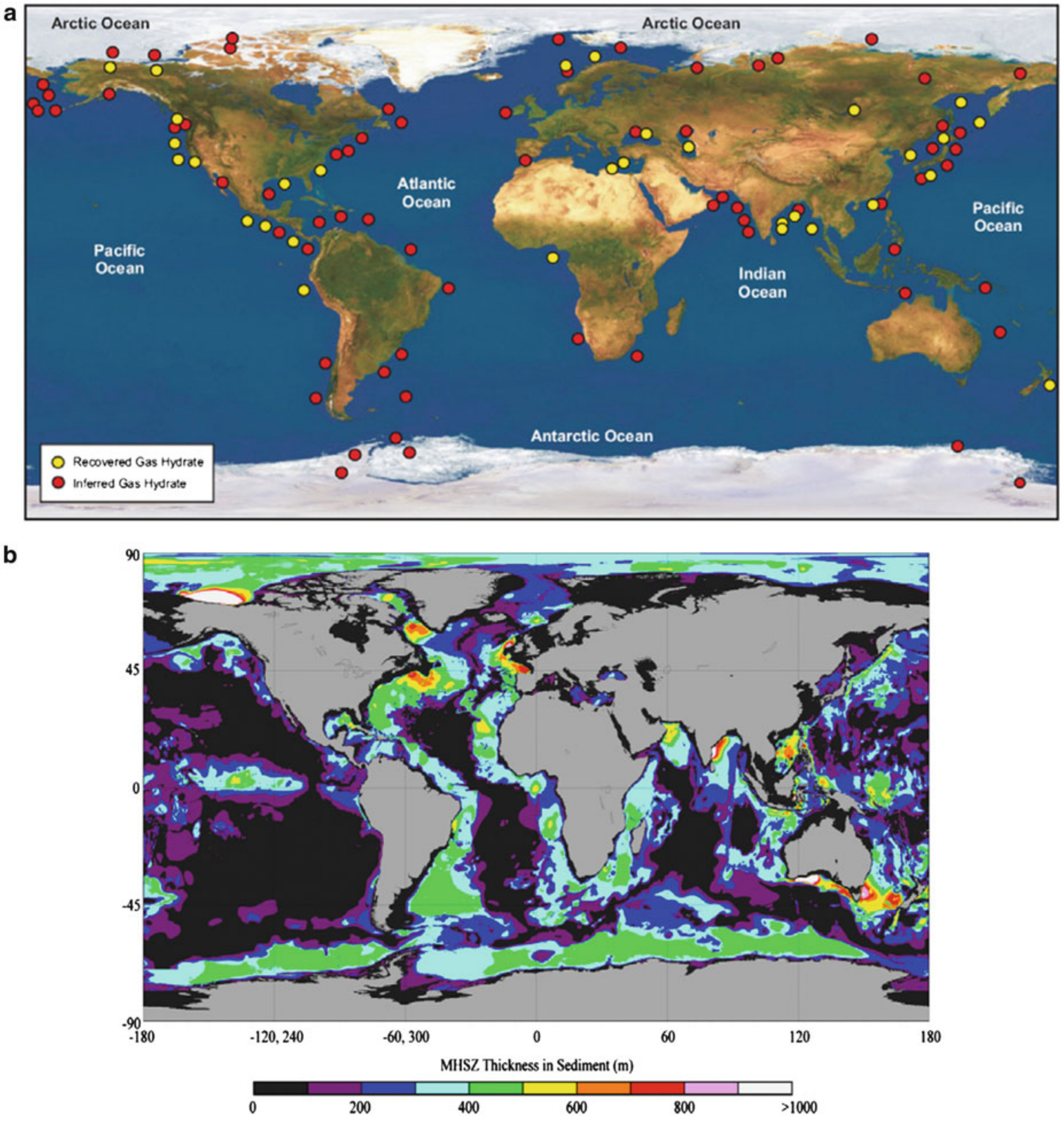

Fig. 3.16 (**a**) Distribution of known and inferred methane hydrate accumulations; (**b**) estimated thickness of the gas hydrate stability zone (GHSZ) in seafloor sediments (Reproduced from Krey et al. (2009) by permission of IOP publishing Ltd.)

fossil fuel carbon inventory. The most recent data synthesis gives a much lower estimate (170–1,000 Pg C) for marine CH_4 hydrate and a similar amount in associated free CH_4 bubbles (Archer 2007; Archer et al. 2009). O'Connor et al. (2010) set an order of magnitude uncertainty on these figures.

In excess of 250 CH_4 bubble plumes were recently observed over the GHSZ west of Spitsbergen, an area showing ~1 °C warming of bottom waters during the last 30 years (Westbrook et al. 2009). These bubble plumes were interpreted as upward migrating free gas formerly trapped below the GHSZ, implying a strong link between current warming and hydrate dissociation,

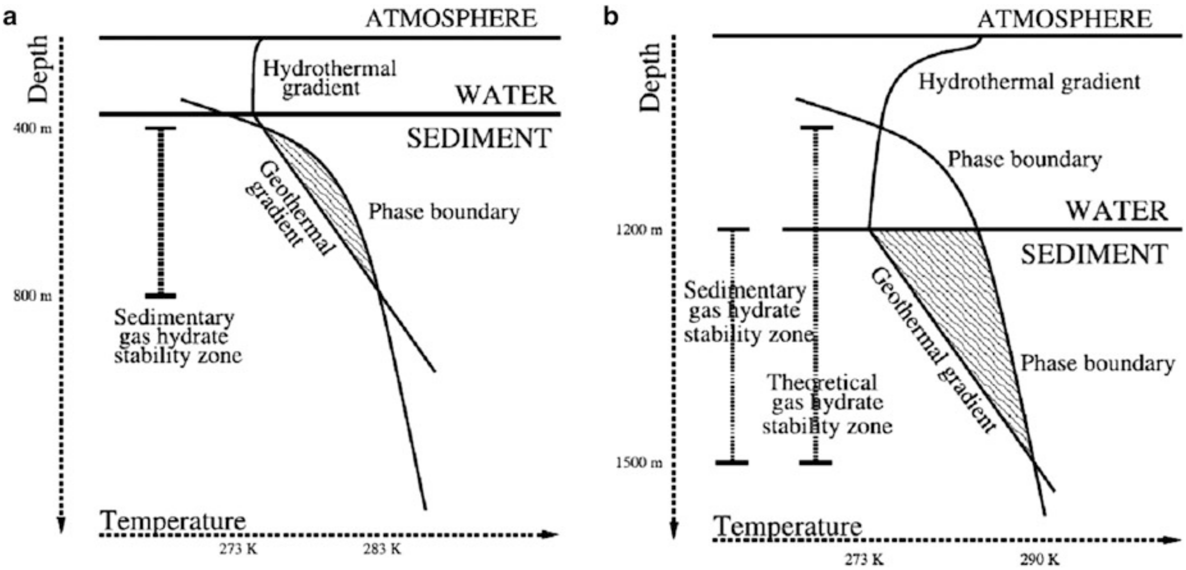

Fig. 3.17 The gas hydrate stability zone (GHSZ) associated with (**a**) shallow water and (**b**) deep water marine sediments. GHSZ volume is determined by the local geothermal gradient. Globally this is ~ 25–30 K km^{-1}, but it can show significant regional variability. (Adapted from O'Connor et al. (2010) by permission of the American Geophysical Union)

a conclusion later supported by modelling (Reagan and Moridis 2009). Lamarque (2008) calculated a potential CH_4 release at the sea floor of 420–1,605 Tg C $year^{-1}$ following hydrate destabilisation from a doubling of tropospheric CO_2. Adjusting for 1 % CH_4 leakage as observed at a large field site (Mau et al. 2007), this value was reduced to 4–16 Tg C $year^{-1}$. However these estimates do not take account of subsequent CH_4 oxidation in the water column, which can easily account for 90 % of the CH_4 released from the sea floor (Dale et al. 2006). Consequently, estimating the current tropospheric CH_4 flux from hydrate sources involves large uncertainty (Table 3.3).

3.4.5 Marine Emissions of Methane

Marine CH_4 emissions reflect the balance of rates of formation, removal and transport. Table 3.7 emphasises the dominance of coastal over open ocean waters in the marine CH_4 budget, reinforcing the conclusions of an early synthesis in which more than 75 % of marine CH_4 emissions were ascribed to coastal waters (Bange et al. 1994). The total CH_4 emission from open ocean areas, experiencing O_2 depletion in the water column, is rather small (0.3 Tg C $year^{-1}$) (Bates et al. 1996b). Similarly, in coastal zones where hypoxia is anthropogenically influenced, the available information suggests that these regions are currently only minor contributors to total coastal CH_4 emissions (less than 0.026 Tg C $year^{-1}$), although this estimate does not include a contribution from ebullition (Naqvi et al. 2010).

It is noteworthy that the low end of the range of total marine CH_4 emissions in Table 3.7 is at the high end of the range given in the IPCC 4th Assessment Report, as shown in Table 3.3 (Denman et al. 2007). The discrepancy can be largely accounted for by CH_4 emissions from continental margin seeps, which are not well characterised in the IPCC synthesis, but which could be the dominant contributor to the marine source of tropospheric CH_4. Such a large seep source is compatible with the notion of a "missing" fraction of fossil CH_4 (~56 ± 11 Tg C $year^{-1}$) deduced from tropospheric ^{14}C data (Crutzen 1991). The uncertainty in the seep estimate is compounded by the episodic nature of the seeps and by the migration of source regions on the sea floor (Kvenvolden and Rogers 2005). There is also large uncertainty in the spectrum of bubble sizes emitted and dissolution of the gas phase into seawater (Judd and Hovland 2007). Moreover, most current estimates of seep CH_4 emissions are indirect and involve large extrapolations. Overall, CH_4 emissions in seeps have a large uncertainty.

Estimating CH_4 emissions from estuaries and mangrove sites (Table 3.7) is compounded by uncertainties over ebullition rates. The importance of this mechanism is unique to CH_4 among reactive trace gases, as it results from intense methanogenesis in sediments. Importantly, although ebullition can account for more than 90 % of CH_4 emissions at some locations (Ostrovsky 2003; Barnes et al. 2006; Nirmal Rajkumar et al. 2008), it is excluded from routine air-sea emission estimates based on gas exchange relations applied to dissolved gas gradients (Upstill-Goddard 2006). In tidal estuaries and mangrove settings some fraction of the CH_4 emission occurs directly from sediments during emersion. While some progress has been made towards estimating the global surface area of estuarine water bodies (Dürr et al. 2011), no robust estimate is currently available for the global inter-tidal area. Borges and Abril (2011) made a crude estimate of estuarine inter-tidal areas and derived a global estuarine CH_4 emission ~5 Tg C $year^{-1}$, notably higher than the estimate of 0.1–2.3 Tg C $year^{-1}$ given in Upstill-Goddard (2011). Constraining marine CH_4 emissions more accurately clearly requires additional detailed studies.

3.5 Impact of Global Change

3.5.1 Future Changes in the Physics of the Oceanic Surface Layer

In order to assess the influence of global climate change on the air-sea exchange of long-lived greenhouse gases (Table 3.2), we need to separately discuss CO_2 from N_2O and CH_4, since the latter two gases have a fundamentally different global balance between the ocean and troposphere. In the case of CO_2, the ocean ultimately controls the tropospheric content of CO_2, with the CO_2 concentration in the surface layer being the immediate determinant of this ocean–atmosphere balance. This surface ocean concentration is controlled by physical, chemical, and biological processes that also create very important sources and sinks within the surface layer, causing the response of CO_2 to climate change to be complex. For N_2O and CH_4, the ocean acts as a net source of these gases to the troposphere, but their ultimate concentrations in the troposphere are on average controlled by other factors, such as their tropospheric lifetimes and terrestrial sources. Furthermore, excluding coastal regions, N_2O and CH_4 in marine waters are mostly produced away from the surface in the ocean's interior, so that the surface layer primarily acts as a conduit between the net ocean source and the net tropospheric sink.

3.5.1.1 Carbon Dioxide in the Open Ocean

For CO_2, it is furthermore of considerable help to distinguish clearly between the climate change processes acting upon the oceanic uptake of anthropogenic CO_2, and those that influence the cycling of natural carbon (Fig. 3.18). For the former, it is essentially sufficient to consider only CO_2 induced changes in the oceanic buffer capacity and in what way ocean circulation will change the net downward transport of anthropogenic CO_2. Changes in wind regimes are essentially irrelevant because air-sea exchange is not a rate limiting step for the oceanic uptake of anthropogenic CO_2 (Sarmiento et al. 1992). Changes in sea ice will locally impact the uptake of anthropogenic CO_2 significantly, but have a relatively small effect globally. Changes in temperature also have a negligible direct effect on the uptake of anthropogenic CO_2, since the buffer factor is essentially independent of temperature (Sarmiento and Gruber 2002).

Regarding the cycling of natural CO_2, changes in temperature are very important, as they directly impact CO_2 solubility in surface water. Changes in the ocean's biogeochemical loop are of fundamental importance. This loop (Sect. 3.2.2) consists of the downward (biological) component, often referred to as the biological pump, and an upward component driven by transport and mixing, which brings carbon-rich waters from the sub-surface ocean back to the surface (Gruber and Sarmiento 2002).

One of the most consistently predicted impacts of climate change on the ocean is an increase in upper ocean stratification (e.g. Bopp et al. 2002). This will largely result from continued oceanic uptake of excess heat from the troposphere that will warm the upper ocean more than the deep ocean (at least during a transient period of several hundred years). In addition, many high-latitude regions are predicted to become fresher in response to an acceleration of the hydrological cycle (Curry et al. 2003), increasing stratification there as well. In the lower latitudes, the enhanced evaporation will actually increase salinity, but this effect is much smaller than that of the higher temperature, so that the surface ocean is predicted to become

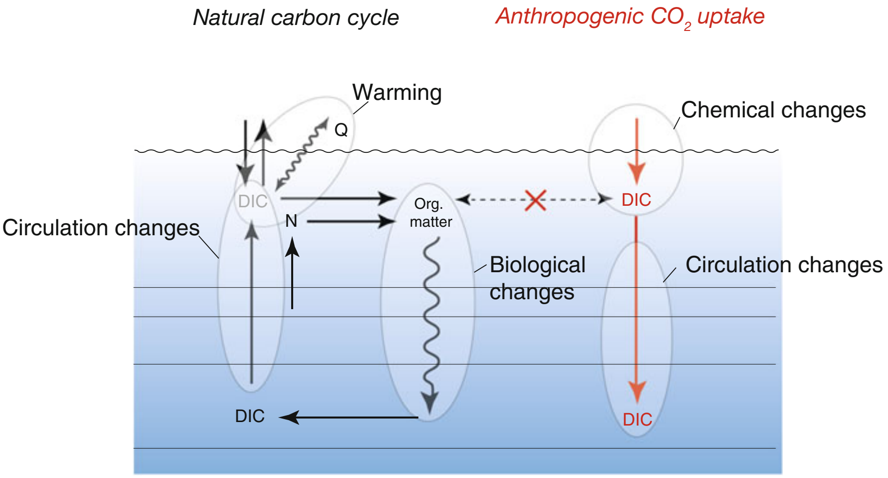

Fig. 3.18 Overview of the most important processes that affect the natural carbon cycle (*left*, *black*) and anthropogenic CO_2 uptake (*right*, *red*) in a changing world. At the center of the natural carbon cycle is the net formation of organic carbon by photosynthesis. Part of this organic matter is exported to depth, where it remineralises back to dissolved inorganic carbon (DIC). Circulation and mixing close this loop. Gas exchange through the air-sea interface connects this loop to the atmosphere. The magnitude of this exchange is governed by the balance of upward transport of DIC and downward transport of organic matter, as well as warming and cooling at the sea surface. The increase in atmospheric CO_2 has caused an additional flux across the air-sea interface, i.e. that of anthropogenic CO_2, leading to an anthropogenic increase in DIC (*red*). This DIC is then further transported to depth by mixing and transport. To first order, the anthropogenic CO_2 is not interacting with the natural carbon cycle, namely it does not affect the magnitude and pattern of the organic matter production and export (*red cross*). When looking closer, this is not entirely correct, as there is increasing evidence that the chemical changes associated with the uptake of anthropogenic CO_2 affect ocean biology. The *grey ellipses* indicate the processes that are most vulnerable to climate change, leading to a change in the net ocean–atmosphere balance of CO_2

more stably stratified nearly everywhere. Important exceptions might be coastal upwelling regions, and perhaps the Southern Ocean, where increased winds may cause enhanced upwelling, partially compensating for the increased stratification.

An increase in stratification and consequently in the surface-to-depth transport will have a strongly reducing impact on the uptake of anthropogenic CO_2. In contrast, increased stratification will produce a much more complex response of the ocean's natural carbon cycle. On the one hand, the circulation (upward) component of the biogeochemical loop will be reduced, but the net effect of this will depend on how ocean biology responds. If the net export of organic matter remains unchanged, the reduction in the upward transport will lead to a substantial increase in the rate of CO_2 uptake from the troposphere. This is because the soft-tissue part of the biological pump will continue to reduce surface CO_2 by fixing it into organic matter and exporting it to depth, while the re-supply by mixing from depth will be greatly reduced. Instead, the lost CO_2 will be replaced by uptake from the troposphere, constituting a negative feedback with regard to tropospheric CO_2. If the net export of organic matter increases, so will the uptake of CO_2 from the troposphere, but if it decreases then the net uptake of CO_2 from the troposphere will also decrease. The overall effect of expected changes in the biogeochemical loop on tropospheric CO_2 can be summarised by the efficiency of the soft-tissue pump, which describes the relative balance between the amount of (inorganic) carbon that is brought to the near-surface by mixing/transport and the amount of (organic) carbon that is exported to depth. It is currently expected that globally the efficiency of the soft-tissue pump will increase, such that the overall effect of the biogeochemical loop will be to enhance CO_2 uptake from the troposphere (Fig. 3.19). However, this conclusion critically depends on the biological response, which at present remains poorly understood.

At the same time, warming of the surface ocean will lead to a loss of CO_2 from the surface, constituting a clear positive feedback. The magnitude of this solubility-driven response is relatively well

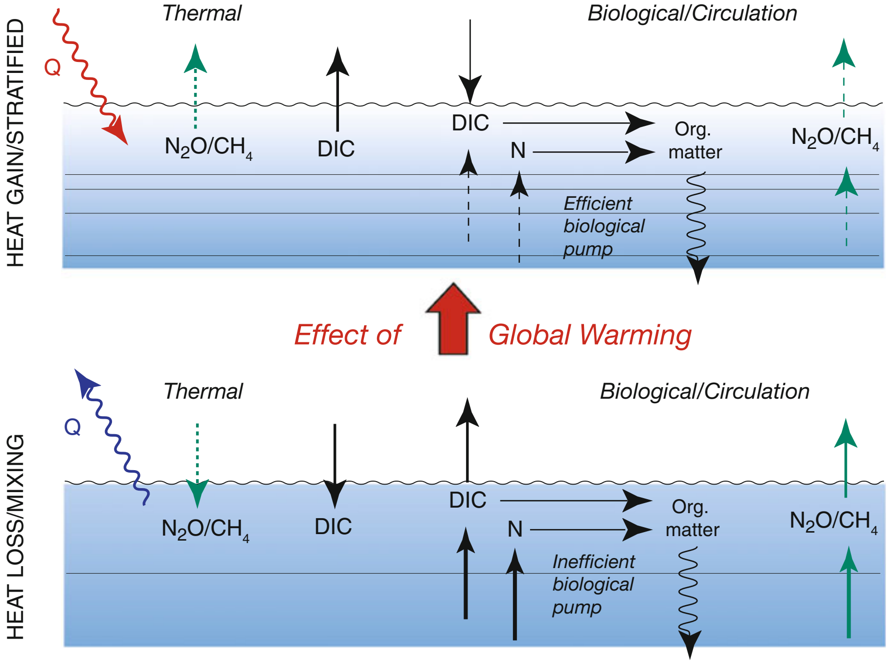

Fig. 3.19 Schematic diagram highlighting two typical situations and how they influence the exchange of natural CO_2, N_2O, and CH_4 across the air-sea interface. The *upper panel* shows a typical low-latitude situation characterised by a net heat gain from the atmosphere and stably stratified conditions. The *lower panel* represents a typical high latitude situation with a net loss of heat and weakly stratified conditions. Global warming will tend to make more regions of the global ocean behave like the *upper panel*

understood, and will largely depend on the magnitude of the ocean's future heat uptake. Changes in wind and sea ice extent will influence the net exchange of CO_2 across the air-sea interface as well. However this will be of secondary importance compared to the direct temperature and circulation effects, except in specific local regions where large changes in sea ice and/or winds might occur.

Based on an annual sea ice loss of 36,000 km^2 (mostly summer ice; Cavalieri et al. 2003), the air-sea CO_2 influx would increase by 2.0 ± 0.3 Tg C $year^{-1}$ for the Arctic Ocean (Bates et al. 2006). Bates et al. (2006) estimated that the Arctic Ocean sink for CO_2 increased from 24 to 66 Tg $year^{-1}$ over the past three decades due to sea ice retreat and that future sea ice melting will enhance this CO_2 uptake by 20 Tg $year^{-1}$ by 2012. Therefore, if one considers only the physical processes through which sea ice directly impacts air-sea CO_2 exchange, the decrease of summertime sea ice extent is expected to increase CO_2 uptake in the coming decades.

Summing up, the expected changes in surface temperature and upper ocean stratification will lead to a strong reduction of the uptake of anthropogenic CO_2, and a mixed response on the natural carbon side with a loss of carbon driven by solubility, and perhaps a gain from the biogeochemical loop (Table 3.9). The net balance is likely to be a decrease in the net uptake of CO_2 from the troposphere in response to climate change, with current models suggesting a reduction in the net ocean uptake of about -16 to -33 Pg $°C^{-1}$ warming until 2100 (Table 3.2) (Roy et al. 2011).

3.5.1.2 Carbon Dioxide in Coastal Seas

The potential feedbacks on increasing tropospheric CO_2 from changes in carbon flows in the coastal ocean could be disproportionately higher than in the open ocean. According to Borges (2011), the changes in carbon flows and related potential feedbacks in the coastal ocean could be driven by four main processes (Table 3.10): (i) changes in coastal physics (This section); (ii) changes in seawater carbonate chemistry (ocean acidification) (Sect. 3.5.2); (iii) changes in land use, waste water inputs and the use of agricultural fertilisers; (iv) changes in the hydrological cycle. These potential feedbacks remain largely unquantified

Table 3.9 Environmental influences on the future net ocean uptake of tropospheric CO_2. *BGC* biogeochemical

	Net ocean uptake	Magnitude	Understanding
Anthropogenic CO_2			
Chemical changes (buffer capacity)	Reduced	Large	High
Circulation/stratification changes	Reduced	Medium	Medium
Wind/sea ice changes	Increased/reduced	Small	Low
Natural CO_2			
Temperature changes	Reduced	Medium	Medium
Circulation changes affecting the BGC loop	Reduced	Medium	Low-medium
Biological changes affecting the BGC loop	Increased/reduced	Unknown	Very low
Wind/sea ice changes	Increased/reduced	Low	Low

due to a poor understanding of the underlying mechanisms, and/or a lack of data and models with which to evaluate them.

Feedbacks on increasing tropospheric CO_2 due to effects of carbon cycling in continental shelf seas related to changes in circulation or stratification could be important, but remain to be quantified (Table 3.10). The effect of changes of stratification on air-sea CO_2 fluxes are not straightforward to quantify since enhancement of stratification will depress primary production and export production due to the decrease of nutrient inputs, but at the same time will also decrease the vertical inputs of DIC and hence release of CO_2 to the troposphere. For example, on the Tasman shelf and in the adjacent open ocean the overall effect of enhanced stratification seems to be an enhancement of the CO_2 sink (Borges et al. 2008).

3.5.1.3 Nitrous Oxide and Methane

For N_2O and CH_4 the upper ocean acts mostly as a transport conduit from the ocean to the troposphere, where they are ultimately decomposed by chemical reactions. Changes in solubility are likely to exert a major effect on the exchange of these two gases in the open ocean, since their degree of supersaturation in the surface ocean is mostly determined by temperature and only to a smaller degree by the magnitude of the transport of supersaturated waters from below to the surface. Therefore, the increase in stratification induced by surface warming (and also by changes in salinity) is likely to lead to only a modest reduction in the ocean source strength of these two gases, provided that their rates of production remain about the same. Of course, if ocean warming and enhanced stratification lead to a strong loss of O_2, then N_2O and CH_4 production in the ocean might increase substantially, which could more than offset the reduction in the deep-to-surface transport induced by stratification (Table 3.2).

3.5.2 Ocean Acidification

3.5.2.1 Carbon Dioxide

Models predict that by the end of the twenty-first century the pH of seawater will decrease by another 0.3–0.4 units (Caldeira and Wickett 2003). This decrease will be accompanied by a reduction in the CO_3^{2-} concentration and in the saturation state for calcite and aragonite (Sect. 3.2.2). Surface waters in the Southern Ocean and the Subarctic Pacific Ocean are expected to become undersaturated with respect to aragonite by the year 2100 (Orr et al. 2005).

Ocean acidification will affect organic carbon production and calcification, but exactly how it will do this is uncertain and is a topic of ongoing research in ocean acidification programmes around the world. For example, ocean acidification may impact the shells of pelagic calcifiers by reducing the ability of organisms to calcify (Comeau et al. 2011) and by dissolving calcareous shells (Orr et al. 2005). However, a few studies have found an increase in calcification on ocean acidification (e.g. Iglesias-Rodriguez et al. 2008). In particular, coral reefs are highly susceptible to increases in temperature and CO_2 concentration (Kleypas et al. 1999). Coral reefs globally may have ceased to grow and started to dissolve by the time the atmospheric mole fraction of

Table 3.10 Global change forcing of carbon cycling in the coastal ocean and associated feedback from increasing tropospheric CO_2 to the year 2100 (Adapted from Borges 2011)

Global change forcings	Feedback	Changes in CO_2 sources and sinks (Pg C year^{-1})	Comment
Changes in coastal physics			
Enhanced stratification	– ?	?	1
Enhanced coastal upwelling	+ ?	?	2
Impact of expanding OMZ in coastal upwelling regions	+	?	3
Enhancement of air-sea CO_2 fluxes related to Arctic sea-ice retreat	–	0.002	4
Changes in land use, waste water inputs, agricultural fertilisers and changes in the hydrological cycle			
Increase of river organic carbon delivery to the Arctic Ocean	+	?	
Increase of river nutrients delivery to the Arctic Ocean	–	?	
Global increase in river nutrient and organic matter delivery	–	0.200	5
Global increase in nutrient atmospheric deposition	–	?	6
Expanding hypoxic and anoxic zones	+	?	3
Changes in seawater carbonate chemistry (ocean acidification)			
Decrease of benthic calcification			
Coral reefs	–	0.015–0.026	
Other benthic environments	–	0.025–0.046	
Decrease of pelagic calcification			
Coccolithophorids	–	0.013–0.019	
Other pelagic calcifiers	–	?	
Dissolution of metastable $CaCO_3$ in sediment porewaters	–	0.022	7
Enhancement of primary production and export production due to increasing [CO_2]	–	0.108–0.216	8

1 Negative feedback only reported in Tasman shelf (Borges et al. 2008) assuming pCO_2 behaviour during warm years is representative of response to global warming, if extrapolated globally would produce a negative feed-back of the order of ~0.1 PgC year^{-1}.
2 Assuming exact opposite response of model output (Plattner et al. 2004) with decreasing upwelling favourable winds
3 Assuming enhanced denitrification leading to decreased primary production
4 Feedback computed for the next decade and not until 2100 (Bates et al. 2006)
5 The enhancement of primary production by nutrient inputs balances the additional CO_2 production by organic matter inputs (Mackenzie et al. 2004).
6 Not taking into account enhancement of acidification of surface waters by sulphur atmospheric deposition (Doney et al. 2007)
7 Based on Andersson et al. (2003)
8 Based on a single mesocosm experiment with mixed diatom and coccolithophorid assemblage (Riebesell et al. 2007)

CO_2 reaches 560 ppm (Silverman et al. 2009). Ocean acidification may well increase primary production by some phytoplankton species (Rost and Riebesell 2004) and may change ratios of carbon to nitrogen uptake by phytoplankton and subsequent carbon export (Riebesell et al. 2007).

Ocean acidification will also impact marine biogeochemical processes. These include changes in the availability of essential trace metals like iron, which are modified in speciation by pH change (Santana-Casiano et al. 2006). A decrease in pH may affect the solubility of some minerals (Liu and Millero 2002) and also the distribution of chemical species, favouring the free dissolved forms of metals, and exerting significant physiological, ecological and toxicological effects on organisms.

On timescales of a few 100 years, a change in the hard tissue $CaCO_3$ pump is estimated to have a small impact on global CO_2 uptake by the oceans (Table 3.2) (Denman et al. 2007), although the effect could be very substantial on glacial to interglacial timescales (e.g. Archer et al. 2000; Matsumoto et al. 2002). The effects of ocean acidification have been estimated for coastal waters (Table 3.10). Overall, ocean acidification is likely to decrease pelagic and benthic calcification in coastal waters and to result in the dissolution of $CaCO_3$

in coastal sediments. These combined effects have been estimated to increase the uptake of tropospheric CO_2 by ~0.02 Pg C year^{-1}, an amount equivalent to ~10 % of the modern-day CO_2 sink in coastal seas (Tables 3.2 and 3.10). The increase in export production upon ocean acidification could also provide a significant negative feedback to increasing tropospheric CO_2, although the conclusions are based on a single perturbation experiment (Table 3.10) (Riebesell et al. 2007).

Denman et al. (2007) concluded that the combined effects of climate change and ocean acidification on the biological carbon pump are not clear and could either increase or decrease the uptake of tropospheric CO_2. What is more clear is that ocean acidification will likely result in the dissolution of $CaCO_3$ sediments in the interior ocean on a time scale of 40 kyear, thus creating a negative feedback on the increase in tropospheric CO_2.

3.5.2.2 Nitrous Oxide and Methane

One other important consequence of ocean acidification is a shift of the NH_3/NH_4^+ equilibrium towards NH_4^+ (e.g. Bange 2008). Beman et al. (2011) recently showed that nitrification rates decreased significantly when the pH was lowered to values expected to occur in the future ocean. One explanation for the pH sensitivity of nitrification rates is that the ammonia mono-oxygenase enzyme uses NH_3 and not NH_4^+ as substrate in the first step of the nitrification sequence. On the basis of these results Beman et al. (2011) suggested that future oceanic N_2O production via nitrification might decrease by up to 44 %, although Freing et al. (2012) contend that this scenario could be an over simplification. Nitrification is part of organic matter remineralisation (i.e. oxidation of organic matter with O_2 to CO_2) and it leads to decreases in both pH and O_2 (Sect. 3.3.2). In general decreasing O_2 concentrations lead to increasing N_2O production during nitrification, such that there seems to be only a minor effect of decreasing pH on N_2O production via nitrification as part of the organic matter remineralisation process. Laboratory experiments to verify the effect of ocean acidification on N_2O production in the ocean are yet to be carried out (Table 3.2). Similarly, the potential effect of ocean acidification on oceanic CH_4 production remains to be investigated (Table 3.2).

3.5.3 Deoxygenation and Suboxia in the Open Ocean

One of the most important effects of global change on the oceans will be the deoxygenation of seawater arising from surface water warming and increased stratification of the upper ocean. These processes will lead to a decrease in O_2 solubility and its supply to subsurface waters, respectively (Keeling et al. 2010). There is compelling evidence to show that this may already be happening (Joos et al. 2003; Stramma et al. 2008; Keeling et al. 2010; Helm et al. 2011). The model-predicted decrease in the oceanic O_2 inventory ranges from 1 % to 7 % by the year 2100 (Keeling et al. 2010). The effects of such a decrease are expected to be greatest in the oceanic OMZs. For example, while a 1 °C warming of the upper ocean, which would lower the O_2 solubility by ~5 μM, may lead to an increase in the volume of hypoxic waters by 10 %, the volume of suboxic waters may increase by a factor of 3 (Deutsch et al. 2011). The ongoing expansion and intensification of the OMZs (Stramma et al. 2008) is expected to profoundly impact the biogeochemical cycling of redox-sensitive elements, especially nitrogen, and will, in conjunction with ocean acidification, adversely affect marine life (Brewer and Peltzer 2009). This may also involve modification of the oceanic source terms for climatically important gases that are sensitive to O_2 concentrations, such as N_2O and CH_4 (Sects. 3.3.2 and 3.4.2).

N_2O formation by nitrification is enhanced when O_2 concentrations are lowered (Sect. 3.3.2). Stramma et al. (2008) showed that intermediate ocean waters (300–700 m water depth) have been losing O_2 at rates ranging from 0.09 ± 0.21 μmol kg^{-1} year^{-1} in the eastern equatorial Indian Ocean to 0.34 ± 0.13 μmol kg^{-1} year^{-1} in the eastern tropical Atlantic Ocean during the last 50 years. Assuming a mean $\Delta[N_2O]$/AOU (apparent oxygen utilisation) ratio of 10^{-4} (Walter et al. 2006), Bange et al. (2010) computed a maximum additional N_2O contribution from deoxygenation of 6 % above the mean N_2O background concentration in the intermediate waters of the tropical North Atlantic Ocean. It therefore seems reasonable to conclude that ongoing open ocean deoxygenation will have a minor effect on oceanic N_2O production and emissions (Table 3.2).

The total CH_4 emission from open ocean areas experiencing O_2 depletion in the water column is quite small (0.3 Tg C $year^{-1}$) (Table 3.7) (Bates et al. 1996b) and is unlikely to increase significantly due to the future expansion of open ocean OMZs (Table 3.2) (Naqvi et al. 2010).

3.5.4 Coastal Euthrophication and Hypoxia

Human activities related to the production of food and energy are causing the release of large quantities of nutrients, such as nitrogen and phosphorus, to the environment, a substantial fraction of which gets transported to coastal waters (Seitzinger et al. 2002; Smith et al. 2003). By 2100 changes in biological activity due to the increased nutrient delivery in rivers might cause a negative feedback on increasing tropospheric CO_2 similar in magnitude to the present-day CO_2 sink in coastal seas (0.2 Pg C $year^{-1}$) (Tables 3.2 and 3.10).

Stimulation of primary productivity and the degradation of photosynthesised organic matter due to nutrient over-enrichment (eutrophication) often results in dissolved O_2 depletion in the bottom waters of seasonally stratified shelf waters. Thus, over 400 hypoxic zones have developed in coastal areas all over the world in the last few decades (Diaz and Rosenberg 2008). Due to their severely detrimental ecological effects, such as the exclusion of higher animals, these hypoxic zones are often popularly referred to as “dead zones”. Although these “dead zones” differ from the naturally-formed O_2-deficient zones that occur on the continental shelves in eastern-boundary upwelling regions, there is now evidence that the latter are also intensifying as a result of anthropogenic nutrient loading and/or changes in circulation (Naqvi et al. 2000; Chan et al. 2008).

The expansion and intensification of O_2 deficiency in coastal areas is expected to affect the future cycling of N_2O and CH_4 in these regions. Currently, anthropogenic “dead zones” make a relatively insignificant (less than 0.043 Tg N $year^{-1}$) contribution to the total marine source of tropospheric N_2O (Naqvi et al. 2010). Nevertheless, it is likely that the comparatively large N_2O emissions from natural hypoxic zones include an anthropogenically-enhanced component. Taken together with the sensitivity of N_2O cycling in aquatic systems to minor changes in already low O_2 concentrations, this implies that further expansion and intensification of coastal hypoxia may significantly impact the global tropospheric N_2O budget (Table 3.2).

From the limited information available on CH_4 emissions from “dead zones”, it would appear that these regions do not contribute much (less than 0.026 Tg C $year^{-1}$) to the total marine source of tropospheric CH_4 (Naqvi et al. 2010), although it should be noted that this estimate does not include bubble ebullition. Given the lack of evidence for a primary control of bottom water hypoxia on sedimentary CH_4 production it would appear that future intensification and/or expansion of coastal hypoxia is unlikely to significantly increase total marine emissions of CH_4 to the troposphere (Table 3.2).

3.5.5 Changes in Methane Hydrates

There is substantial debate over the role of CH_4 hydrates in potential future climate change (O’Connor et al. 2010). What is clear is that the currently estimated CH_4 hydrate inventory (Sect. 3.4.4) is sufficiently large that the release of even a modest fraction to the troposphere over a 12-year period, the tropospheric lifetime of CH_4 (Table 3.1), could enhance greenhouse forcing by an amount equivalent to increasing the tropospheric CO_2 concentration by a factor larger than 10 (Archer 2007). The global CH_4 hydrate reservoir thus has the potential to promote substantial global warming (Table 3.2).

One region in which the effects of CH_4 hydrate destabilisation are likely to be most clearly manifested is the Arctic Ocean; a marine ecosystem that is highly susceptible to global change (Doney et al. 2012). Romanovski et al. (2005) modelled the extent and temporal evolution of submarine permafrost on the shelves of the Laptev Sea and East Siberian Sea and deduced that the entire Arctic shelf is underlain by relic permafrost stable enough to support CH_4 hydrate. Much of this Arctic CH_4 hydrate is comparatively shallow structural hydrate (Sect. 3.4.4) and the gas hydrate stability zone is ~200 m below the sea surface over much of the region. If dislodged from the sediment, for example during a submarine landslide (Brewer et al. 2002; Paull et al. 2003) or by erosion, large amounts of hydrate could potentially survive largely intact during ascent to the ocean surface. Contemporary hydrate melting is indeed apparent along the Siberian margin, due to rapid coastline recession that is exposing sub-sea floor deposits to overlying seawater at rates of ~10–15 km year^{-1}. The hydrate melting collapses further land into the sea, increasing the exposure of hydrates and leading to further melting, a process which is thought to have occurred continually over the past 7,500 years, resulting in ~100–500 km recession of the coastline (Hubberten and Romanovski 2001). As such these CH_4 releases are not abrupt, but rather tend to modestly increase the CH_4 background over time. For example, contemporary dissolved CH_4 saturations on the East-Siberian and Laptev Sea shelves are ~2,500 % in surface waters and in excess of 4,000 % in bottom waters, consistent with such seabed release (Shakhova and Semiletov 2007; Shakhova et al. 2007). Similarly, surface waters over the North Slope of Alaska are highly supersaturated in CH_4 (Kvenvolden 1999) and the release of hydrate-derived CH_4 has been clearly observed in the Beaufort Sea (Paull et al. 2008).

Notwithstanding such evidence for the ongoing release of hydrate-derived CH_4, Archer and Buffett (2005) and Archer (2007) argue that any significant climate induced hydrate melting response is likely to be on the time scale of millennia or longer, because the vast majority of CH_4 hydrate is of the stratigraphic type (Sect. 3.4.4) and is sufficiently insulated from the sediment surface by many hundreds of metres of overlying sediment. They also argue that any hydrate melting will occur below the gas hydrate stability zone, forming CH_4 bubbles whose fate is uncertain. Possibilities include their retention in the sediment, upward escape through the stability zone, or the initiation of submarine landslides through sediment column destabilisation. Although such a landslide would potentially cause abrupt CH_4 release, it is estimated that a landslide the size of the Storegga slide off Norway would typically release CH_4 sufficient only to affect climate on a scale comparable to a large volcanic eruption for ~10 years (Archer 2007).

Estimates of the rate at which melting hydrates are likely to increase the tropospheric CH_4 inventory over the timescale of decades (Table 3.2) are much less well constrained than changes in other CH_4 sources such as peat decomposition in thawing permafrost, fossil fuels and agriculture, although the potential rates may be comparable (Archer 2007). Major uncertainties exist over the rate and extent of CH_4 escape to the overlying water and troposphere, which is related to sediment stability and permeability and the ability of the gas hydrate stability zone to trap CH_4 bubbles (Archer 2007). On geologic timescales, due to the relative tropospheric lifetimes of CH_4 and CO_2 (Table 3.1), the largest climate impact will likely be from CO_2 deriving from CH_4 oxidation (Schmidt and Shindell 2003; Archer and Buffett 2005; Archer 2007). Following the cessation of hydrate CH_4 release, the enhanced CO_2 concentration will persist, while tropospheric CH_4 will recover relatively rapidly to a lower steady state (Schmidt and Shindell 2003). Significant oxidation of hydrate-derived CH_4 to CO_2 in the oceans would reduce the climate impact over several decades, but on timescales of millennia or more the climate impact might be significant, because of equilibration of this oceanic CO_2 with the troposphere over several hundred years. Indeed, there may well be positive climate feedback linking tropospheric CO_2, deep ocean temperature and CO_2 production from hydrate-derived CH_4 (Archer and Buffett 2005). These authors propose that in a worst case scenario, on the timescale of millennia to hundreds of millennia, the total global CH_4 hydrate source of tropospheric CO_2 could equal that from fossil fuels.

3.6 Key Uncertainties in the Air-Sea Transfer of CO_2, N_2O and CH_4

3.6.1 Outgassing of Riverine Carbon Inputs

The error bars on carbon inputs by rivers and estuarine outgassing create considerable uncertainty when attempting to convert from net contemporary fluxes to anthropogenic fluxes (Gruber et al. 2009; Takahashi et al. 2009). If the outgassing of river borne CO_2 by the open ocean has indeed been overestimated by ~0.2 Pg C year^{-1} as argued in Sect. 3.2.4, the anthropogenic CO_2 sink derived from CO_2 climatologies (e.g. Takahashi et al. 2009) would have been over-estimated by the same amount.

3.6.2 Heterogeneity in Coastal Systems

Obtaining meaningful air-sea gas transfer estimates for CO_2, CH_4 and N_2O in coastal systems is a substantial challenge and the ranges in Tables 3.4, 3.5 and 3.7 have large inherent uncertainties. These uncertainties reflect the heterogeneity and biogeochemical complexity of coastal systems and include: (i) gross scaling errors arising from the degree to which study sites are representative globally of each "compartment"; (ii) bias in the CO_2, N_2O and CH_4 values reflecting incomplete spatial and temporal data resolution; (iii) uncertainties in gas exchange rates arising from selected gas transfer relations and representative wind speeds (Chap. 2) (Upstill-Goddard 2006; Wanninkhof et al. 2009). Minimising gross scaling errors largely relies on the availability of accurate area determinations. General problems of defining the extent of oceanic upwellings are well documented (Nevison et al. 2004; Naqvi et al. 2005), as are the difficulties of defining representative estuarine areas (Barnes and Upstill-Goddard 2011). Minimising measurement bias has a clear seasonal aspect; production and consumption of CO_2, N_2O and CH_4 are biologically driven and as such have strong temperature dependence. Seasonality also affects the intensity of upwelling and river runoff, which affects nutrient and carbon supply. Unfortunately, most sampling campaigns take place during summer. There is also a regional aspect; most coastal regions outside the northern hemisphere are either undersampled or are not sampled at all.

Given the likelihood that coastal regions will play an important role in future trace gas budgets due to increased economic and population pressures, additional studies of CO_2, N_2O and CH_4 fluxes from key coastal regions will be required. Sampling campaigns should be spatially and temporally focused and ideally coordinated internationally. In particular CH_4 emissions by ebullition and from seeps and inland waters need more to be more accurately quantified.

3.6.3 Sea Ice

The role of sea ice in air-sea gas exchange remains poorly understood (Chap. 2). Until recently sea ice was regarded as a lid that effectively precluded air-sea gas exchange, as evidenced by under ice concentrations of dissolved gases (CFCs, O_2, CO_2) far from equilibrium with their tropospheric contents (Gordon et al. 1984; Weiss et al. 1992; Klatt et al. 2002; Bakker et al. 2008). However, recent evidence now points to significant gas exchange between sea ice and the troposphere (Delille et al. 2007; Geilfus et al. 2012), highlighting a need for more detailed research in this area.

3.6.4 Parameterising Air-Sea Gas Transfer

The choice of turbulence-driven air-sea gas exchange relations may introduce significant bias (Chap. 2), especially where bottom-driven turbulence is a major contributor to gas exchange in shallow systems (Upstill-Goddard 2006, 2011). In addition, wind speeds in coastal systems have short spatio-temporal variability and often the appropriate wind speed distributions required for gas exchange relations are not available. Similarly, current speeds and water depths required for non-wind speed driven gas exchange relations may also be lacking (Upstill-Goddard 2006).

3.6.5 Data Collection, Data Quality and Data Synthesis

The detailed study of interannual and decadal variations and trends in regional surface water fCO_2 and air-sea CO_2 fluxes has only recently become possible. Our future understanding of these trends and of the underlying mechanisms responsible is expected to improve due to more extensive data coverage and as longer observational records become available. Future long term data collection and data synthesis will require the development of instrumentation that is more reliable and accurate while being less labour intensive. In addition the rigorous standardisation of data collection and quality control procedures will be essential. Such technical developments will require substantial and sustained funding (Borges et al. 2010; Byrne et al. 2010; Feely et al. 2010; Gruber et al. 2010; Monteiro et al. 2010).

Encouragingly, the marine CO_2 community is already making good progress towards coordinated data collection and synthesis. Notable is the agreed use of certified reference materials for the analysis of DIC and total alkalinity and traceable calibration gases for fCO_2 analysis (DOE 1994; Dickson et al. 2007). There is also agreement on recommendations for reporting fCO_2 measurements (IOCCP 2004). The International Ocean Carbon Coordination Project (IOCCP) plays the key role in coordinating the marine carbon community and in ensuring the implementation of international agreements. By contrast, the status of marine N_2O and CH_4 research is far less mature in this regard. The N_2O and CH_4 communities have yet to progress towards discussing the adoption of either internationally agreed analytical standards or recommended analytical protocols.

Recent synthesis products for ocean carbon enable the intercomparison of model-data, the analysis of variation and trends in CO_2 air-sea fluxes, and the processes driving these. A vast and expanding global surface water fCO_2 database is now available for assessing CO_2 air-sea climatologies (Takahashi et al. 1997, 2002, 2009) and since 2011 the Surface Ocean CO_2 Atlas (SOCAT; www.socat.info) enables public access to a large CO_2 data archive for the global oceans and coastal seas (Bakker et al. 2012; Pfeil et al. 2013; Sabine et al. 2013) (Chap. 5). Other data synthesis efforts are also underway, notably MEMENTO for surface ocean N_2O and CH_4 concentrations (Chap. 5) and syntheses of carbon in the ocean interior: GLODAP (Global Ocean Data Analysis Project), CARINA (CARbon IN the Atlantic Ocean), PACIFICA (PACIFic ocean Interior Carbon) and GLODAP-2 (Key et al. 2004; Bange et al. 2009; Tanhua et al. 2010; Suzuki et al. 2013). Such data synthesis efforts, along with modelling and data-model intercomparisons (Gruber et al. 2009) are critical to improving our current understanding of the exchanges of CO_2, N_2O and CH_4 between the troposphere, coastal seas, the surface open ocean and the ocean interior.

3.7 Conclusions and Outlook

3.7.1 Carbon Dioxide

In general, the enhanced rate of change in tropospheric CO_2 observed today (Global Carbon Project 2011) will have a strong impact on future climate and environmental change. Presently it appears that neither the oceans nor terrestrial systems will absorb CO_2 as efficiently in the future as they do today. In addition, ocean acidification will become, and probably is already, an issue for ecosystems in the ocean. Both the climate and environmental effects and feedbacks make it very difficult to firmly predict future changes in ocean sources and sinks for CO_2. From time-series we can clearly identify the rate of change in CO_2 uptake and in ocean acidification. From surface water CO_2 measurements on Voluntary Observing Ships we can make CO_2 air-sea flux maps and assess temporal and spatial variation in the oceanic uptake of CO_2. Finally, repeat hydrography elucidates the storage of carbon in the interior ocean. More important will be to predict the effect of changes in processes controlling oceanic uptake and release of carbon, notably of changes in ocean circulation, the magnitude of the biological pumps and carbon storage. This will require a comprehensive measuring system for future observations and improved modelling tools. Today, there is a clear lack of the observations required to reduce the uncertainties in air-sea CO_2 exchange and to predict its future behaviour. This in turn is very important for predicting the occurrence of levels of ocean acidification that are harmful to ecosystems. The latter also requires results from biological perturbation experiments under varying CO_2 scenarios. The future vision is:

- The design of a comprehensive network of VOS, repeat hydrographic sections and time-series. Optimalisation might be obtained through modelling, statistical analysis and experience, based upon the existing network;
- The development of automated ocean stations. Cable-based systems might be applied along coastal areas, and moored systems and buoys in open ocean situations. Remotely controlled floats and other moving platforms, such as gliders, would provide additional process information;
- The development of data storage, data reduction, data synthesis, data assimilation and visualisation techniques, as well as continuation, automation and expansion of ongoing data synthesis efforts;
- The development of models that can be validated by data;

(Borges et al. 2010; Byrne et al. 2010; Feely et al. 2010; Gruber et al. 2010; Monteiro et al. 2010).

3.7.2 Nitrous Oxide and Methane

While our knowledge of the oceanic distribution, the formation pathways and the oceanic emissions of N_2O and CH_4 has increased considerably during the last four decades, we are far from having a comprehensive picture. Major questions and technical challenges remain to be solved:

- Reliable and fast, high-precision N_2O and CH_4 sensors for use at open ocean and coastal time-series stations and on ships of opportunity should be developed in order to expand the spatial and temporal coverage of oceanic N_2O and CH_4 measurements. Recently developed OA-ICOS (Off-Axis Integrated Cavity Output Spectrometer) instruments coupled to a continuously working equilibration device are a promising technology for use on VOS lines (Gülzow et al. 2011).
- We still only have a rudimentary understanding of N_2O and CH_4 cycling in coastal areas. We need to know more about seasonality in the major formation, consumption and transport pathways and the driving forces behind these. In this context, the ongoing dramatic increase in the number of coastal "dead zones" is a critical consideration because ongoing coastal eutrophication may well modify greatly, current emissions of N_2O and CH_4 from coastal areas.

References

Abril G, Borges AV (2004) Carbon dioxide and methane emissions from estuaries. In: Tremblay A, Varfalvy L, Roehm C, Garneau M (eds) Greenhouse gas emissions: fluxes and processes, hydroelectric reservoirs and natural environments. Springer, Berlin, pp 187–207

Abril G, Iversen N (2002) Methane dynamics in a shallow, non-tidal estuary (Randers Fjord, Denmark). Mar Ecol Prog Ser 230:171–181

Abril G, Nogueira E, Hetcheber H, Cabeçadas G, Lemaire E, Brogueira MJ (2002) Behaviour of organic carbon in nine contrasting European estuaries. Estuar Coast Shelf Sci 54:241–262

Abril G, Commarieu MV, Guerin F (2007) Enhanced methane oxidation in an estuarine turbidity maximum. Limnol Oceanogr 52:470–475

Amouroux D, Roberts G, Rapsomanikis S, Andreae MO (2002) Biogenic gas (CH_4, N_2O, DMS) emission to the atmosphere from near-shore and shelf waters of the north-western Black Sea. Estuar Coast Shelf Sci 54:575–587

Anderson LG, Falck E, Jones EP, Jutterström S, Swift J (2004) Enhanced uptake of atmospheric CO_2 during freezing of seawater: a field study in Storfjorden, Svalbard. J Geophys Res 109, C06004. doi:10.1029/2003JC002120

Andersson AJ, Mackenzie FT, Ver LM (2003) Solution of shallow-water carbonates: an insignificant buffer against rising atmospheric CO_2. Geology 31:513–516

Archer D (2007) Methane hydrate stability and anthropogenic climate change. Biogeosciences 4:521–544. doi:10.5194/bg-4-521-2007

Archer D, Buffett B (2005) Time-dependent response of the global ocean clathrate reservoir to climatic and anthropogenic forcing. Geochem Geophys Geosyst 6, Q03002. doi:10.1029/2004GC000854

Archer D, Kheshgi H, Maier-Reimer E (1997) Multiple timescales for neutralization of fossil fuel CO_2. Geophys Res Lett 24:405–408

Archer D, Winguth A, Lea D, Mahowald N (2000) What casued the glacial/interglacial atmospheric pCO_2 cycles? Rev Geophys 38(2):159–189

Archer D, Buffett B, Brovkin V (2009) Ocean methane hydrates as a slow tipping point in the global carbon cycle. Proc Natl Acad Sci USA 106(49):20596–20601

Aydin M, Verhulst KR, Saltzman ES, Battle MO, Montzka SA, Blake DR, Tang Q, Prather MJ (2011) Recent decreases in fossil-fuel emissions of ethane and methane derived from firn air. Nature 476:198–201. doi:10.1038/nature10352

Baggs E, Philippot L (2010) Microbial terrestrial pathways to nitrous oxide. In: Smith K (ed) Nitrous oxide and climate change. Earthscan, London, pp 36–62

Baker DF, Law RM, Gurney KR, Rayner P, Peylin P, Denning AS, Bousquet P, Bruhwiler L, Chen Y-H, Ciais P, Fung IY, Heimann M, John J, Maki T, Maksyutov S, Masarie K, Prather M, Pak B, Taguchi S, Zhu Z (2006) TransCom 3 inversion intercomparison: impact of the transport model errors on the interannual variability of regional CO_2 fluxes, 1988–2003. Global Biogeochem Cycle 20, GB1002. doi:10.1029/2004GB002439

Bakker DCE, Hoppema M, Schröder M, Geibert W, De Baar HJW (2008) A rapid transition from ice covered CO_2–rich waters to a biologically mediated CO_2 sink in the eastern Weddell Gyre. Biogeosciences 5:1373–1386. doi:10.5194/bg-5-1373-2008

Bakker DCE, Pfeil B, Olsen A, Sabine CL, Metzl N, Hankin S, Koyuk H, Kozyr A, Malczyk J, Manke A, Telszewski M (2012) Global data products help assess changes to the ocean carbon sink. Eos Trans Am Geophys Union 93(12):125–126. doi:10.1029/2012EO120001

Ballantyre AP, Alden CB, Miller JB, Tans PP, White JWC (2012) Increase in observed net carbon dioxide uptake by land and oceans during the past 50 years. Nature 488:70–73. doi:10.1038/nature11299

Bange HW (2006a) New directions: the importance of the oceanic nitrous oxide emissions. Atmos Environ 40:198–199

Bange HW (2006b) Nitrous oxide and methane in European coastal waters. Estuar Coast Shelf Sci 70:361–374

Bange HW (2008) Gaseous nitrogen compounds (NO, N_2O, N_2, NH_3) in the ocean. In: Capone DG, Bronk DA, Mulholland MR, Carpenter EJ (eds) Nitrogen in the marine environment, 2nd edn. Elsevier, Amsterdam, pp 51–94

Bange HW, Andreae MO (1999) Nitrous oxide in the deep waters of the world's oceans. Global Biogeochem Cycle 13(4):1127–1135

Bange HW, Bartell UH, Rapsomanikis S, Andreae MO (1994) Methane in the Baltic and North Seas and a reassessment of the marine emissions of methane. Global Biogeochem Cycle 8:465–480

Bange HW, Rapsomanikis S, Andreae MO (1996) The Aegean Sea as a source of atmospheric nitrous oxide and methane. Mar Chem 53:41–49

Bange HW, Bell TG, Cornejo M, Freing A, Uher G, Upstill-Goddard RC, Zhang G (2009) MEMENTO: a proposal to develop a database of marine nitrous oxide and methane measurements. Environ Chem 6:195–197

Bange HW, Bergmann K, Hansen HP, Kock A, Koppe R, Malien F, Ostrau C (2010a) Dissolved methane during hypoxic events at the Boknis Eck time series station (Eckernförde Bay, SW Baltic Sea). Biogeosciences 7:1279–1284

Bange HW, Freing A, Kock A, Löscher C (2010b) Marine pathways to nitrous oxide. In: Smith K (ed) Nitrous oxide and climate change. Earthscan, London, pp 36–62

Barnes J, Upstill-Goddard RC (2011) N_2O seasonal distribution and air-sea exchange in UK estuaries: implications for tropospheric N_2O source from European coastal waters. J Geophys Res 116, G01006. doi:10.1029/2009JG001156

Barnes J, Ramesh R, Purvaja R, Nirmal Rajkumar A, Senthil Kumar B, Krithika K, Ravichandran K, Uher G, Upstill-Goddard RC (2006) Tidal dynamics and rainfall control N_2O and CH_4 emissions from a pristine mangrove creek. Geophys Res Lett 33, L15405. doi:10.1029/2006GL026829

Bastviken D, Tranvik LJ, Downing JA, Crill PM, Enrich-Prast A (2011) Freshwater methane emissions offset the continental carbon sink. Science 331:50

Bates NR, Michaels AF, Knap AH (1996a) Seasonal and interannual variability of oceanic carbon dioxide species at the U.S. JGOFS Bermuda Atlantic Time-series Study (BATS) site. Deep-Sea Res Part II 43(2–3):347–383

Bates TS, Kelly KC, Johnson JE, Gammon RH (1996b) A reevaluation of the open ocean source of methane to the atmosphere. J Geophys Res 101:6953–6961

Bates NR, Samuels L, Merlivat L (2001) Biogeochemical and physical factors influencing seawater fCO_2 and air-sea CO_2 exchange on the Bermuda coral reef. Limnol Oceanogr 46(4):833–846

Bates NR, Moran SB, Hansell DA, Mathis JT (2006) An increasing CO_2 sink in the Arctic Ocean due to sea-ice loss. Geophys Res Lett 33, L23609. doi:10.1029/2006GL027028

Battin TJ, Kaplan LA, Findlay S, Hopkinson CS, Marti E, Packman AI, Newbold JD, Sabater F (2008) Biophysical controls on organic carbon fluxes in fluvial networks. Nat Geosci 1:95–100

Bauzá JF, Morrell JM, Corredor JE (2002) Biogeochemistry of nitrous oxide production in the Red Mangrove (*Rhizophora mangle*) forest sediments. Estuar Coast Shelf Sci 55:697–704

Beauchamp B (2004) Natural gas hydrates: myths, facts and issues. C R Geosci 336:751–765. doi:10.1016/j.crte.2004.04.003

Beman JM, Chow C-E, King AL, Feng Y, Fuhrman JA, Andersson A, Bates NR, Popp BN, Hutchins DA (2011) Global declines in oceanic nitrification rates as a consequence of ocean acidification. Proc Natl Acad Sci USA 108 (1):208–213. doi:101073/pnas.1011053108

Bender ML, Ho DT, Hendricks MB, Mika R, Battle MO, Tans PP, Conway TJ, Sturtevant B, Cassar N (2005) Atmospheric O_2/N_2 changes, 1993–2002: implications for the partitioning of fossil fuel CO_2 sequestration. Global Biogeochem Cycle 19, GB4017. doi:10.1029/2004GB002410

Biscaye PE, Anderson R (1994) Particle fluxes on the slope of the southern Mid-Atlantic Bight: SEEP-II. Deep-Sea Res Part II 41:459–469

Biscaye PE, Anderson R, Deck BL (1988) Fluxes of particles and constituents to the Eastern United States continental slope and rise: SEEP-I. Cont Shelf Res 8:888–904

Biswas H, Mukhopadhayay SK, De TK, Sen S, Jana TK (2006) Methane emission from the wetland rice fields in Sagar Island, NE coast of Bay of Bengal, India. Int J Agric Res 1(1):78–86

Biswas H, Mukhopadhyay SK, Sen S, Jana TK (2007) Spatial and temporal patterns of methane dynamics in the tropical mangrove dominated estuary, NE coast of Bay of Bengal, India. J Mar Syst 68:55–64

Blair NE, Aller RC (1995) Anaerobic methane oxidation on the Amazon shelf. Geochim Cosmochim Acta 59:3707–3715

Boetius A, Ravenschlag K, Schubert CJ, Rickert D, Widdel F, Gieseke A, Amann R, Jørgensen BB, Witte U, Pfannkuche O (2000) A marine microbial consortium apparently mediating anaerobic oxidation of methane. Nature 407:623–626

Bopp L, Le Quéré C, Heimann M, Manning AC (2002) Climate-induced oceanic oxygen fluxes: implications for the contemporary carbon budget. Global Biogeochem Cycle 16(2):1022. doi:10.1029/2011GB001445

Borges AV (2005) Do we have enough pieces of the jigsaw to integrate CO_2 fluxes in the Coastal Ocean? Estuaries 28(1):3–27

Borges AV (2011) Present day carbon dioxide fluxes in the coastal ocean and possible feedbacks under global change. In: Duarte PM, Santana-Casiano JM (eds) Oceans and the atmospheric carbon content. Springer, Berlin, pp 47–77

Borges AV, Abril G (2011) Carbon dioxide and methane dynamics in estuaries. In: Wolanski E, McLusky DS (eds) Treatise on estuarine and coastal science, vol 5, Biogeochemistry. Elsevier, Amsterdam, pp 119–161. doi:10.1016/B978-0-12-374711-2.00504-0

Borges AV, Gypens N (2010) Carbonate chemistry in the coastal zone responds more strongly to eutrophication than to ocean acidification. Limnol Oceanogr 55:346–353

Borges AV, Djenidi S, Lacroix G, Théate J, Delille B, Frankignoulle M (2003) Atmospheric CO_2 flux from mangrove surrounding waters. Geophys Res Lett 30(11):1558. doi:10.1029/2003GL017143

Borges AV, Delille B, Frankignoulle M (2005) Budgeting sinks and sources of CO_2 in the coastal ocean: diversity of ecosystems counts. Geophys Res Lett 32, L14601. doi:10.1029/2005GL023053

Borges AV, Schiettecatte L-S, Abril G, Delille B, Gazeau F (2006) Carbon dioxide in European coastal waters. Estuar Coast Shelf Sci 70(3):375–387

Borges AV, Tilbrook B, Metzl N, Lenton A, Delille B (2008) Inter-annual variability of the carbon dioxide oceanic sink south of Tasmania. Biogeosciences 5:141–155

Borges AV, Alin SR, Chavez FP, Vlahos P, Johnson KS, Holt JT, Balch WM, Bates N, Brainard R, Cai W-J, Chen CTA, Currie K, Dai M, Degrandpré M, Delille B, Dickson A, Evans W, Feely RA, Friederich GE, Gong G-C, Hales B, Hardman-Mountford N, Hendee J, Hernandez-Ayon JM, Hood M, Huertas E, Hydes D, Ianson D, Krasakopoulou E, Litt E, Luchetta A, Mathis J, McGillis WR, Murata A, Newton J, Ólafsson J, Omar A, Perez FF, Sabine C, Salisbury

JE, Salm R, Sarma VVSS, Schneider B, Sigler M, Thomas H, Turk D, Vandemark D, Wanninkhof R, Ward B (2010) A global sea surface carbon observing system: inorganic and organic carbon dynamics in coastal oceans. In: Hall J, Harrison DE, Stammer D (eds) Proceedings of OceanObs'09: sustained ocean observations and information for society, vol 2, Venice, Italy, 21–25 Sept 2009, ESA publication WPP-306. doi:10.5270/OceanObs09.cwp.07

Bouillon S, Middelburg JJ, Dehairs F, Borges AV, Abril G, Flindt MR, Ulomi S, Kristensen E (2008) Importance of intertidal sediment processes and pore water exchange on the water column biogeochemistry in a pristine mangrove creek (Ras Dege, Tanzania). Biogeosciences 4:311–322

Boutin J, Etcheto J, Dandonneau Y, Bakker DCE, Feely RA, Inoue HY, Ishii M, Ling RD, Nightingale PD, Metzl N, Wanninkhof R (1999) Satellite sea surface temperature: a powerful tool for interpreting in situ pCO_2 measurements in the equatorial Pacific Ocean. Tellus 51B:490–508

Brewer PG, Peltzer ET (2009) Limits to marine life. Science 324:347–348

Brewer PG, Paull C, Peltzer ET, Ussler W, Rehder G, Friederich G (2002) Measurement of the fate of gas hydrates during transit through the ocean water column. Geophys Res Lett 29:38. doi:10.1029/2002GL014727

Brix H, Gruber N, Keeling CD (2004) Interannual variability of the upper ocean carbon cycle at station ALOHA near Hawaii. Global Biogeochem Cycle 18, GB4019. doi:10.1029/2004GB002245

Broecker WS, Peng T-H (1982) Tracers in the sea. Eldigio Press, Lamont-Doherty Geological Observatory, Columbia University, Palisades

Brüchert V, Currie B, Peard KR (2009) Hydrogen sulphide and methane emissions on the central Namibian shelf. Prog Oceanogr 83:169–179

Buffett B, Archer D (2004) Global inventory of methane clathrate: sensitivity to changes in the deep ocean. Earth Planet Sci Lett 227:185–199. doi:10.1016/j.epsl.2004.09.005

Buitenhuis E, Van Bleijswijk J, Bakker DCE, Veldhuis MJW (1996) Trends in inorganic and organic carbon in a bloom of *Emiliania huxleyi* in the North Sea. Mar Ecol Prog Ser 143:271–282

Byrne RH, DeGrandpre MD, Short RT, Martz TR, Merlivat L, McNeil C, Sayles FL, Bell R, Fietzek P (2010) Sensors and systems for in situ observations of marine carbon dioxide system variables. In: Hall J, Harrison DE, Stammer D (eds) Proceedings of OceanObs'09: sustained ocean observations and information for society, vol 2, Venice, Italy, 21–25 Sept 2009, ESA publication WPP-306. doi:10.5270/OceanObs09.cwp.13

Cabello P, Roldán MD, Moreno-Vivián C (2004) Nitrate reduction and the nitrogen cycle in archaea. Microbiology 150 (11):3527–3546

Cai W-J (2011) Estuarine and coastal ocean carbon paradox: CO_2 sinks or sites of terrestrial carbon incineration? Annu Rev Mar Sci 3:123–145

Cai W-J, Dai MH, Wang YC (2006) Air-sea exchange of carbon dioxide in ocean margins: a province-based synthesis. Geophys Res Lett 33, L12603. doi:10.1029/2006GL026219

Caldeira K, Wickett ME (2003) Anthropogenic carbon and ocean pH. Nature 425:365

Cantera JJL, Stein LY (2007) Role of nitrite reductase in the ammonia-oxidizing pathway of *Nitrosomonas europaea*. Arch Microbiol 188(4):349–354

Capone DG, Kiene RP (1988) Comparison of microbial dynamics in marine and freshwater sediments: contrasts in anaerobic carbon catabolism. Limnol Oceanogr 33(4 part 2):725–749

Cavalieri DJ, Parkinson CL, Vinnikov KY (2003) 30-Year satellite record reveals contrasting Arctic and Antarctic decadal sea ice variability. Geophys Res Lett 30(18):1970. doi:10.1029/2003GL018031

Chan F, Barth JA, Lubchenco J, Kirincich A, Weeks H, Peterson WT, Menge BA (2008) Emergence of anoxia in the California current large marine ecosystem. Science 319:920–920

Chanton JP, Martens CS, Kelley CA (1989) Gas transport from methane-saturated, tidal freshwater and wetland sediments. Limnol Oceanogr 34(5):807–819

Chen CTA, Borges AV (2009) Reconciling opposing views on carbon cycling in the coastal ocean: continental shelves as sinks and near-shore ecosystems as sources of atmospheric CO_2. Deep-Sea Res Part II 56(8–10):578–590

Codispoti LA (2010) Interesting times for marine N_2O. Science 327:1339–1340

Codispoti LA, Elkins JW, Friederich GE, Packard TT, Sakamoto CM, Yoshinari T (1992) On the nitrous oxide flux from productive regions that contain low oxygen waters. In: Desai BN (ed) Oceanography of the Indian ocean. Oxford-IBH, New Delhi, pp 271–284

Codispoti LA, Flagg C, Kelly V (2005) Hydrographic conditions during the 2002 SBI process experiments. Deep-Sea Res Part II 52(24–26):3199–3226

Cole JA (1988) Assimilatory and dissimilatory reduction of nitrate to ammonia. Symp Soc Gen Microbiol 42:281–329

Comeau S, Gattuso JP, Nisumaa AM, Orr J (2011) Impact of aragonite saturation state changes on migratory pteropods. Proc Royal Soc B Biol Sci. doi:10.1098/rspb.2011.0910

Conrad R, Seiler W (1988) Methane and hydrogen in seawater (Atlantic Ocean). Deep-Sea Res 35:1903–1917

Corbière A, Metzl N, Reverdin G, Brunet C, Takahashi T (2007) Interannual and decadal variability of the oceanic carbon sink in the North Atlantic subpolar gyre. Tellus 59B:168–178

Cornejo M, Farías L, Paulmier A (2006) Temporal variability in N_2O water content and its air-sea exchange in an upwelling area off central Chile (36°S). Mar Chem 101:85–94

Cornejo M, Farías L, Gallegos M (2007) Seasonal cycle of N2O vertical distribution and air-sea fluxes over the continental shelf waters off central Chile (36°S). Prog Oceanogr 75:383–395

Crutzen PJ (1970) The influence of nitrogen oxides on the atmospheric ozone content. Q J R Meteorol Soc 96:320–325

Crutzen PJ (1991) Methane's sinks and sources. Nature 350:380–381

Curry R, Dickson R, Yashayaev I (2003) A change in the freshwater balance of the Atlantic Ocean over the past four decades. Nature 426:826–829

Cynar FJ, Yayanos AA (1991) Enrichment and characterization of a methanogenic bacterium from the oxic upper layer of the ocean. Curr Microbiol 23:89–96

Dale AW, Regnier P, Van Cappellen P (2006) Bioenergetic controls on anaerobic oxidation of methane (AOM) in coastal marine sediments: a theoretical analysis. Am J Sci 306:246–294. doi:10.2475/ajs.306.4.246

Damm E, Mackensen A, Budéus G, Faber E, Hanfland C (2005) Pathways of methane in seawater: plume spreading in an Arctic shelf environment (SW Spitsbergen). Cont Shelf Res 25:1453–1472

Damm E, Helmke E, Thoms S, Schauer U, Nöthig E, Bakker K, Kiene R (2010) Methane production in aerobic oligotrophic surface water in the central Arctic Ocean. Biogeosciences 7:1099–1108

Dando PR, Austen MC, Burke RA, Kendall MA, Kennicutt MC, Judd AG, Moore DC, Ohara SCM, Schmaljohann R, Southward AJ (1991) Ecology of a North-Sea pockmark with an active methane seep. Mar Ecol Prog Ser 70:49–63

De Angelis MA, Lee C (1994) Methane production during zooplankton grazing on marine phytoplankton. Limnol Oceanogr 39:1298–1308

Delille B, Jourdain B, Borges AV, Tison J-L, Delille D (2007) Biogas (CO_2, O_2, dimethylsulfide) dynamics in spring Antarctic fast ice. Limnol Oceanogr 52(4):1367–1379

Denman KL, Brasseur G, Chidthaisong A, Ciais P, Cox PM, Dickinson RE, Hauglustaine D, Heinze C, Holland E, Jacob D, Lohman U, Ramachandran S, Da Silva Dias PL, Wofsy SC, Zhang X (2007) Couplings between changes in the climate system and biogeochemistry. In: Solomon S, Qin D, Manning M, Chen Z, Marquis M, Averyt KB, Tignor M, Miller HL (eds) Climate change 2007: The physical science basis. contribution of working group i to the fourth assessment report of the intergovernmental panel on climate change. Cambridge University Press, Cambridge/New York, pp 499–587

Deutsch C, Brix H, Ito T, Frenzel H, Thompson L (2011) Climate-forced variability of ocean hypoxia. Science 333:336–339

Devol AH, Richey JE, Forsburg BR, Martinelli LA (1990) Seasonal dynamics in methane emissions from the Amazon river floodplain. J Geophys Res 95:16417–16426

Diaz RJ, Rosenberg R (2008) Spreading dead zones and consequences for marine ecosystems. Science 321:926–929

Dickson AG, Sabine CL, Christian JR (eds) (2007) Guide to best practices for ocean CO_2 measurements, vol 3, PICES special publication. North Pacific Marine Science Organization, Sidney, BC, Canada

Dimitrov L (2002) Contribution to atmospheric methane by natural seepages on the Bulgarian continental shelf. Cont Shelf Res 22:2429–2442

Dittmar T, Hertkorn N, Kattner G, Lara RJ (2006) Mangroves, a major source of dissolved organic carbon to the oceans. Global Biogeochem Cycle 20, GB1012. doi:10.1029/2005GB002570

Dlugokencky EJ, Houweling S, Bruhwiler L, Masarie KA, Lang PM, Miller JB, Tans PP (2003) Atmospheric methane levels off: temporary pause or a new steady-state? Geophys Res Lett 30(19):1992. doi:10.1029/2003GL018126

Dlugokencky EJ, Bruhwiler L, White JWC, Emmons LK, Novelli PC, Montzka SA, Masarie KA, Lang PM, Crotwell AM, Miller JB, Gatti LV (2009) Observational constraints on recent increases in the atmospheric CH_4 burden. Geophys Res Lett 36, L18803. doi:10.1029/2009GL039780

DOE (1994) In: Dickson AG, Goyet C (eds) Handbook of methods for the analysis of the various parameters of the carbon system in sea water; version 2. ORNL/CDIAC-74, Carbon Dioxide Information Analysis Center, Oak Ridge National Laboratory, US Department of Energy, Oak Ridge, Tennessee, USA

Doney SC, Mahowald N, Lima I, Feely RA, Mackenzie FT, Lamarque J-F, Rasch PJ (2007) Impact of anthropogenic atmospheric nitrogen and sulfur deposition on ocean acidification and the inorganic carbon system. Proc Natl Acad Sci USA 104(37):14580–14585

Doney SC, Ruckelshaus M, Duffy JE, Barry JP, Chan F, English CA, Galindo HM, Grebmeier JM, Hollowed AB, Knowlton N, Polovina J, Rabalais NN, Sydeman WJ, Talley LD (2012) Climate change impacts on marine ecosystems. Annu Rev Mar Sci 4:11–37. doi:10.1146/annurev-marine-041911-111611

Dore JE, Karl DM (1996) Nitrification in the euphotic zone as a source for nitrite, nitrate, and nitrous oxide at station ALOHA. Limnol Oceanogr 41:1619–1628

Dore JE, Lukas R, Sadler DW, Karl DM (2003) Climate-driven changes to the atmospheric CO_2 sink in the subtropical North Pacific Ocean. Nature 424:754–757

Dürr HH, Laruelle GG, Van Kempen CM, Slomp CP, Meybeck M, Middelkoop H (2011) Worldwide typology of nearshore coastal systems: defining the estuarine filter of river inputs to the oceans. Estuar Coasts 34:441–458

EPA (2010) Methane and nitrous oxide emissions from natural sources. 430-R-10-001. Office of Atmospheric Programs (6207J), United States Environmental Protection Agency, Washington, DC

EPICA Community Members (2004) Eight glacial cycles from an Antarctic ice core. Nature 429:623–628

Fazzolari E, Mariotti A, Germon JC (1990a) Nitrate reduction to ammonia – a dissimilatory process in *Enterobacter-Amnigenus*. Can J Microbiol 36(11):779–785

Fazzolari E, Mariotti A, Germon JC (1990b) Dissimilatory ammonia production vs. denitrification in vitro and in inoculated agricultural soil samples. Can J Microbiol 36(11):786–793

Feely RA, Sabine CL, Lee K, Berelson W, Kleypas J, Fabry VJ, Millero FJ (2004) Impact of anthropogenic CO_2 on the $CaCO_3$ system in the oceans. Science 305:362–366

Feely RA, Takahashi T, Wanninkhof R, McPhaden MJ, Cosca CE, Sutherland SC, Carr M-E (2006) Decadal variability of the air-sea CO_2 fluxes in the equatorial Pacific Ocean. J Geophys Res 111, C08S90. doi:10.1029/2005JC003129

Feely RA, Fabry VJ, Dickson AG, Gattuso J-P, Bijma J, Riebesell U, Doney S, Turley C, Saino T, Lee K, Anthony K, Kleypas J (2010) An international observational network for ocean acidification. In: Hall J, Harrison DE, Stammer D (eds) Proceedings of OceanObs'09: sustained ocean observations and information for society, vol 2, Venice, Italy, 21–25 Sept 2009, ESA publication WPP-306. doi:10.5270/OceanObs09.cwp.29

Ferrón S, Ortega T, Gómez-Parra A, Forja JM (2007) Seasonal study of dissolved CH_4, CO_2 and N_2O in a shallow tidal system of the bay of Cádiz (SW Spain). J Mar Syst 66:244–257. doi:10.1016/j.jmarsys.2006.03.021

Flückiger J, Blunier T, Stauffer B, Chappellaz J, Spahni R, Kawamura K, Schwander J, Stocker TF, Dahl-Jensen D (2004) N_2O and CH_4 variations during the last glacial epoch: insight into global processes. Global Biogeochem Cycle 18, GB1020. doi:10.1029/2003GB002122

Forster P, Ramaswamy V, Artaxo P, Berntsen T, Betts R, Fahey DW, Haywood J, Lean J, Lowe DC, Myhre G, Nganga J, Prinn R, Rage G, Schulz M, Van Dorland R (2007) Changes in atmospheric constituents and in radiative forcing.

In: Solomon S, Qin D, Manning M, Chen Z, Marquis M, Averyt KB, Tignor M, Miller HL (eds) Climate change 2007: the physical science basis. Contribution of working group I to the fourth assessment report of the intergovermental panel on climate change. Cambridge University Press, Cambridge/New York. pp 130–234

Forster G, Upstill-Goddard RC, Gist N, Robinson C, Uher G, Woodward EMS (2009) Nitrous oxide and methane in the Atlantic Ocean between 50°N and 52°S: latitudinal distribution and sea-to-air flux. Deep-Sea Res Part II 56:964–976. doi:10.1016/j.dsr2.2008

Francis CA, Beman JM, Kuypers MM (2007) New processes and players in the nitrogen cycle: the microbial ecology of anaerobic and archaeal ammonia oxidation. ISME J 1(1):19–27

Frankignoulle M, Canon C, Gattuso J-P (1994) Marine calcification as a source of carbon dioxide: positive feedback of increasing CO_2. Limnol Oceanogr 39(2):458–462

Frankignoulle M, Gattuso J-P, Biondo R, Bourge I, Copin-Montégut G, Pichon M (1996) Carbon fluxes in coral reefs 2. Eulerian study of inorganic carbon dynamics and measurement of air-sea CO_2 exchanges. Mar Ecol Prog Ser 145:123–132

Frankignoulle M, Abril G, Borges A, Bourge I, Canon C, Delille B, Libert E, Théate MJ (1998) Carbon dioxide emission from European estuaries. Science 282:434–436. doi:10.1126/science.282.5388.434

Freing A (2009) Production and emissions of oceanic nitrous oxide. Ph.D. thesis. University of Kiel, Kiel

Freing A, Wallace DWR, Bange HW (2012) Global oceanic production of nitrous oxide (N_2O). Philos Trans R Soc B 367:1245–1255

Friedlingstein P, Houghton RA, Marland G, Hacker J, Boden TA, Conway TJ, Canadell JC, Raupach MR, Ciais P, Le Quéré C (2010) Update on CO_2 emissions. Nat Geosci 3:811–812. doi:10-1038/ngeo1022

Gattuso J-P, Pichon M, Delesalle B, Frankignoulle M (1993) Community metabolism and air-sea CO_2 fluxes in a coral reef ecosystem (Moorea, French Polynesia). Mar Ecol Prog Ser 96:259–267

Gattuso J-P, Payri CE, Pichon M, Delesalle B, Frankignoulle M (1997) Primary production, calcification, and air-sea CO_2 fluxes of a macroalgal-dominated coral reef community (Moorea, French Polynesia). J Phycol 33(5):729–738

Gattuso J-P, Frankignoulle M, Wollast R (1998) Carbon and carbonate metabolism in coastal aquatic ecosystems. Annu Rev Ecol Syst 29:405–433

Gazeau F, Smith SV, Gentili B, Frankignoulle M, Gattuso J-P (2004) The European coastal zone: characterization and first assessment of ecosystem metabolism. Estuar Coast Shelf Sci 60(4):673–694

Geibert W, Assmy P, Bakker DCE, Hanfland C, Hoppema M, Pichevin L, Schröder M, Schwarz JN, Stimac I, Usbeck U, Webb A (2010) High productivity in an ice melting hotspot at the eastern boundary of the Weddell Gyre. Global Biogeochem Cycle 24, GB3007. doi:10.1029/2009GB003657

Geilfus N-X, Carnat G, Papakyriakou T, Tison J-L, Else B, Thomas H, Shadwick E, Delille B (2012) Dynamics of pCO_2 and related air-ice CO_2 fluxes in the Arctic coastal zone (Amundsen Gulf, Beaufort Sea). J Geophys Res 117, C00G10. doi:10.1029/2011JC007117

Gerard G, Chanton J (1993) Quantification of methane oxidation in the rhizosphere of emergent aquatic macrophytes: defining upper limits. Biogeochemistry 23:79–97

Global Carbon Project (2011) Carbon budget and trends 2010. www.globalcarbonproject.org/carbonbudget. Accessed 13 Jan 2012

González-Dávila M, Santana-Casiano JM, Rueda MJ, Llinás O, González-Dávila E-F (2003) Seasonal and interannual variability of sea-surface carbon dioxide species at the European Station for Time Series in the Ocean at the Canary Islands (ESTOC) between 1996 and 2000. Global Biogeochem Cycle 17(3):1076. doi:10.1029/2002GB001993

González-Dávila M, Santana-Casiano JM, Rueda MJ, Llinás O (2010) The water column distribution of carbonate system variables at the ESTOC site from 1995 to 2004. Biogeosciences 7:3067–3081

Gordon AL, Huber BA (1990) Southern Ocean winter mixed layer. J Geophys Res 95:11655–11672

Goreau TJ, Kaplan WA, Wofsy SC, McElroy MB, Valois FW, Watson SW (1980) Production of NO_2^- and N_2O by nitrifying bacteria at reduced concentrations of oxygen. Appl Environ Microbiol 40:526–532

Gornitz V, Fung I (1994) Potential distribution of methane hydrates in the world's oceans. Global Biogeochem Cycle 8(3):335–347. doi:10.1029/94GB00766

Gruber N, Keeling CD (2001) An improved estimate of the isotopic air-sea disequilibrium of CO_2: implications for the oceanic uptake of anthropogenic CO_2. Geophys Res Lett 28 (3):555–558. doi:10.1029/2000GL011853

Gruber N, Sarmiento JL (2002) Large-scale biogeochemical/physical interactions in elemental cycles. In: Robinson AR, McCarthy JJ, Rothschild BJ (eds) The sea, vol 12. Wiley, New York, pp 337–399

Gruber N, Keeling CD, Bates NR (2002) Interannual variability in the North Atlantic Ocean carbon sink. Science 298:2374–2378

Gruber N, Gloor M, Mikaloff Fletcher SE, Doney SC, Dutkiewicz S, Follows MJ, Gerber M, Jacobson AR, Joos F, Lindsay K, Menemenlis D, Mouchet A, Müller SA, Takahashi T (2009) Oceanic sources, sinks, and transport of atmospheric CO_2. Global Biogeochem Cycle 23, GB1005. doi:10.1029/2008GB003349

Gruber N, Körtzinger A, Borges A, Claustre H, Doney SC, Feely RA, Hood M, Ishii M, Kozyr A, Monteiro P, Nojiri Y, Sabine CL, Schuster U, Wallace DWR, Wanninkhof R (2010) Plenary Paper: Toward an integrated observing system for ocean carbon and biogeochemistry at a time of change. In: Hall J, Harrison DE, Stammer D (eds) Proceedings of OceanObs'09: sustained ocean observations and information for society, vol 1, Venice, Italy, 21–25 Sept 2009, ESA publication WPP-306. doi:10.5270/OceanObs09. p 18

Gülzow W, Rehder G, Schneider B, Schneider von Deimling J, Sadkowiak B (2011) A new method for continuous measurement of methane and carbon dioxide in surface waters using off-axis integrated cavity output spectroscopy (ICOS): an example from the Baltic Sea. Limnol Oceanogr Methods 9:168–174

Gurney KR, Law RM, Denning AS, Rayner PJ, Pak BC, Baker D, Bousquet P, Bruhwiler L, Chen Y-H, Ciais P, Fung IY, Heimann M, John J, Maki T, Maksyutov S, Peylin P, Prather M, Taguchi S (2004) Transcom 3 inversion intercomparison: model mean results for the estimation of seasonal carbon sources and sinks. Global Biogeochem Cycle 18, GB1010. doi:10.1029/2003GB002111

Gypens N, Borges AV, Lancelot C (2009) Effect of eutrophication on air-sea CO_2 fluxes in the coastal Southern North Sea: a model study of the past 50 years. Global Change Biol 15(4):1040–1056

Hall TM, Prather MJ (1993) Simulations of the trend and annual cycle in stratospheric CO_2. J Geophys Res 98:10573–10581. doi:10.1029/93JD00325

Harlay J, Borges AV, Van Der Zee C, Delille B, Godoi RHM, Schiettecatte L-S, Roevros N, Aerts K, Lapernat P-E, Rebreanu L, Groom S, Daro M-H, Van Grieken R, Chou L (2010) Biogeochemical study of a coccolithophorid bloom in the northern Bay of Biscay (NE Atlantic Ocean) in June 2004. Prog Oceanogr 80:317–336. doi:10.1016/j.pocean.2010.04.029

Harlay J, Chou L, De Bodt C, Van Oostende N, Piontek J, Suykens K, Engel A, Sabbe K, Groom S, Delille B, Borges AV (2011) Biogeochemistry and carbon mass balance of a coccolithophore bloom in the northern Bay of Biscay (June 2006). Deep-Sea Res Part I 58:111–127

Heinze C, Maier-Reimer E, Winn K (1991) Glacial pCO_2 reduction by the world ocean: experiments with the Hamburg carbon cycle model. Paleoceanography 6(4):395–430

Heip C, Goosen NK, Herman PMJ, Kromkamp J, Middelburg JJ, Soetaert K (1995) Production and consumption of biological particles in temperate tidal estuaries. Oceanogr Mar Biol: Annu Rev 33:1–149

Helm KP, Bindoff NL, Church JA (2011) Observed decreases in oxygen content of the global ocean. Geophys Res Lett 38, L23602. doi:10.1029/2011GL049513

Ho DT, Law CS, Smith MJ, Schlosser P, Harvey M, Hill P (2006) Measurements of air-sea gas exchange at high wind speeds in the Southern Ocean: implications for global parameterizations. Geophys Res Lett 33, L16611. doi:10.1029/2006GL026817

Holmes ME, Sansone FJ, Rust TM, Popp BN (2000) Methane production, consumption, and air-sea exchange in the open ocean: an evaluation based on carbon isotopic ratios. Global Biogeochem Cycle 14:1–10

Holt J, Wakelin S, Huthnance J (2008) Down-welling circulation of the northwest European continental shelf: a driving mechanism for the continental shelf carbon pump. Geophys Res Lett 36, L14602. doi:10.1029/2009GL038997

Hopkinson CSJ, Smith EM (2005) Estuarine respiration: an overview of benthic, pelagic and whole system respiration. In: Del Giorgio PA, Williams PJL (eds) Respiration in aquatic ecosystems. Oxford University Press, Oxford

Hornafius JS, Quigley DC, Luyendyk BP (1999) The world's most spectacular marine hydrocarbons seeps (Coal Oil Point, Santa Barbara Channel, California): quantification of emissions. J Geophys Res 104(C9):20703–20711

Hubberten H-W, Romanovski NN (2001) Terrestrial and offshore permafrost evolution of the Laptev Sea region during the last Pleistocene-Holocene glacial-eustatic cycle. In: Paepe R, Melnikov V (eds) Permafrost response on economic development, environmental security and natural resources. Proc-NATO-ARW, Novosibirsk, 1998. Kluwer, Dordrecht, pp 43–60

Huthnance JM, Holt JT, Wakelin SL (2009) Deep ocean exchange with west-European shelf seas. Ocean Sci 5:621–634

Iglesias-Rodriguez M, Halloran PR, Rickaby REM, Hall IR, Colmenero-Hidalgo E, Gittins JR, Green DRH, Tyrrell T, Gibbs SJ, Von Dassow P, Rehm E, Armbrust EV, Boessenkool KP (2008) Phytoplankton calcification in a High-CO_2 World. Science 320(5874):336–340. doi:10.1126/science.1154122

IOCCP (2004) Ocean surface pCO_2, data integration and database development workshop, National Institute for Environmental Studies, Tsukuba, Japan, 14–17 Jan 2004. IOCCP (International Ocean Carbon Coordination Project) report 2. www.ioccp.org

IPCC (2007) In: Solomon S, Qin D, Manning M, Chen Z, Marquis M, Averyt KB, Tignor M, Miller HL (eds) Climate change 2007: the physical science basis. Contribution of working group I to the fourth assessment report of the intergovernmental panel on climate change. Cambridge University Press, Cambridge/New York

Ishii M, Inoue HY, Midorikawa T, Saito S, Tokieda T, Sasano D, Nakadate A, Nemoto K, Metzl N, Wong CS, Feely RA (2009) Spatial variability and decadal trend of the oceanic CO_2 in the western equatorial Pacific warm/fresh water. Deep-Sea Res Part II 56(8–10):591–606

Jackson MA, Tiedje JM, Averill BA (1991) Evidence for a no-rebound mechanism for production of N_2O from nitrite by the copper-containing nitrite reductase from *Achromobacter-Cycloclastes*. FEBS Lett 29(1):41–44

Jacobson AR, Mikaloff Fletcher SE, Gruber N, Sarmiento JL, Gloor M (2007) A joint atmosphere–ocean inversion for surface fluxes of carbon dioxide: 1. Methods and global-scale fluxes. Global Biogeochem Cycle 21, GB1019. doi:10.1029/2005GB002556

Jansen E, Overpeck J, Briffa KR, Duplessy J-C, Joos F, Masson-Delmotte V, Olago D, Otto-Bliesner B, Peltier WR, Rahmstorf S, Ramesh R, Raynaud D, Rind D, Solomina O, Villalba R, Zhang D (2007) Paleoclimate. In: Solomon S, Qin D, Manning M, Chen Z, Marquis M, Averyt KB, Tignor M, Miller HL (eds) Climate change 2007: the physical science basis. Contribution of working group I to the fourth assessment report of the intergovermental panel on climate change. Cambridge University Press, Cambridge/New York, pp 434–497

Jansson BPM, Malandrin L, Johannson HE (2000) Cell cycle arrest in Archaea by the hypusination inhibitor N1-Guanyl-1,7-Diaminoheptane. J Bacteriol 182:1158–1161. doi:10.1128/JB.182.4.1158-1161

Jayakumar DA, Naqvi SWA, Narvekar PV, George MD (2001) Methane in coastal and offshore waters of the Arabian Sea. Mar Chem 74:1–13

Jin X, Gruber N, Dunne JP, Sarmiento JL, Armstrong RA (2006) Diagnosing the contribution of phytoplankton functional groups to the production and export of particulate organic carbon, $CaCO_3$, and opal from global nutrient and alkalinity distributions. Global Biogeochem Cycle 20, GB2015. doi:10.1029/2005GB002532

Joos F, Meyer R, Bruno M, Leuenberger M (1999) The variability in the carbon sinks as reconstructed for the last 1000 years. Geophys Res Lett 26:1437–1441

Joos F, Prentice IC, Sitch S, Meyer R, Hooss G, Plattner G-K, Gerber S, Hasselmann K (2001) Global warming feedbacks on terrestrial carbon uptake under the Intergovernmental Panel on Climate Change (IPCC) emission scenarios. Global Biogeochem Cycle 15(4):891–907

Joos F, Plattner G-K, Stocker TF, Körtzinger A, Wallace DWR (2003) Trends in marine dissolved oxygen: implications for ocean circulation changes and the carbon budget. Eos Trans Am Geophys Union 84(21):197. doi:10.1029/2003EO210001

Joyce J, Jewell PW (2003) Physical controls on methane ebullition from reservoirs and lakes. Environ Eng Geosci 9:167–178

Judd A, Hovland M (2007) Seabed fluid flow. Impact on geology, biology and the marine environment. Cambridge University Press, Cambridge, UK

Kai FM, Tyler SC, Randerson JT, Blake DR (2011) Reduced methane growth rate explained by decreased northern hemisphere microbial sources. Nature 476:194–197. doi:10.1038/nature10259

Kaiser M, Attrill M, Jennings S, Thomas DN, Barnes D, Brierley A, Hiddink JG, Kaartokallio H, Polunin NVC, Raffaelli D (2011) Marine ecology: processes, systems and impacts, 2nd edn. Oxford University Press, Oxford

Karl DM, Beversdorf L, Björkman KM, Church MJ, Martinez A, Delong EF (2008) Aerobic production of methane in the sea. Nat Geosci 1:473–478

Keeling RF, Körtzinger A, Gruber N (2010) Ocean deoxygenation in a warming world. Annu Rev Mar Sci 2:199–229

Kelley C (2003) Methane oxidation potential in the water column of two diverse coastal marine sites. Biogeochemistry 65:105–120

Kemp WM, Smith EM, Marvin-DiPasquale M, Boynton WR (1997) Organic carbon-balance and net ecosystem metabolism in Chesapeake Bay. Mar Ecol Prog Ser 150:229–248

Kessler JD, Reeburgh WS, Southon J, Varela R (2005) Fossil methane source dominates Cariaco Basin water column methane geochemistry. Geophys Res Lett 32, L12609. doi:10.1029/2005GL022984

Key RM, Kozyr A, Sabine CL, Lee K, Wanninkhof R, Bullister J, Feely RA, Millero F, Mordy C, Peng T-H (2004) A global ocean carbon climatology: results from GLODAP. Global Biogeochem Cycle 18, GB4031

Kiene RP, Linn LJ, Bruton JA (2000) New and important roles for DMSP in marine microbial communities. J Sea Res 43:209–224

King GM (1994) Ecophysiological characteristics of obligate methanotrophic bacteria and methane oxidation in situ. In: Murrell JC, Kelly DP (eds) Microbial growth on C1 compounds. Intercept Press, Andover, pp 303–313

Kitidis V, Tizzard L, Uher G, Judd A, Upstill-Goddard RC, Head IM, Gray ND, Taylor G, Durán R, Diez R, Iglesias J, García-Gil S (2007) The biogeochemical cycling of methane in Ria de Vigo, NW Spain: sediment processing and sea–air exchange. J Mar Syst 66:258–271

Klatt O, Roether W, Hoppema M, Bulsiewicz K, Fleischmann U, Rodehacke C, Fahrbach E, Weiss RF, Bullister JL (2002) Repeated CFC sections at the Greenwich Meridian in the Weddell Sea. J Geophys Res 107:3030. doi:10.1029/2000JC000731

Kleypas JA, Buddemeier RW, Archer D, Gattuso J-P, Langdon C, Opdyke BN (1999) Geochemical consequences of increased atmospheric carbon dioxide on coral reefs. Science 284:118–120

Kleypas JA, Feely RA, Fabry VJ, Langdon C, Sabine CL, Robins LL (2006) Impacts of ocean acidification on coral reefs and other marine calcifiers: a guide for future research. Report of a workshop, 2005. St. Petersburg, Florida. NSF, NOAA and US Geological Survey

Kock A, Gebhardt S, Bange HW (2008) Methane emissions from the upwelling area off Mauritania (NW Africa). Biogeosciences 5:1119–1125

Kock A, Schafstall J, Dengler M, Brandt P, Bange HW (2012) Sea-to-air and diapycnal nitrous oxide fluxes in the eastern tropical North Atlantic Ocean. Biogeosciences 9:957–964

Koné YJM, Abril G, Kouadio KN, Delille B, Borges AV (2009) Seasonal variability of carbon dioxide in the rivers and lagoons of Ivory Coast (West Africa). Estuar Coasts 32:246–260

Kreuzwieser J, Buchholz J, Rennenberg H (2003) Emission of methane and nitrous oxide by Australian mangrove ecosystems. Plant Biol 5:423–431

Krey V, Canadell JG, Nakicenovic N, Abe Y, Andruleit H, Archer D, Grubler A, Hamilton NTM, Johnson A, Kostov V, Lamarque J-F, Langhorne N, Nisbet EG, O'Neill B, Riahi K, Riedel M, Wang W, Yakushev V (2009) Gas hydrates: entrance to a methane age or climate threat? Environ Res Lett 4, 034007

Kristensen E, Flindt MR, Borges AV, Bouillon S (2008) Emission of CO_2 and CH_4 to the atmosphere by sediments and open waters in two Tanzanian mangrove forests. Mar Ecol Prog Ser 370:53–67

Kroeze C, Dumont E, Seitzinger SP (2005) New estimates of global emissions of N_2O from rivers and estuaries. Environ Sci 2:159–165

Kvenvolden KA (1993) Gas hydrates – geological perspective and global change. Rev Geophys 31(2):173–187. doi:10.1029/93RG00268

Kvenvolden KA (1999) Potential effects of gas hydrate on human welfare. Proc Natl Acad Sci USA 96:3420–3426

Kvenvolden KA, Rogers BW (2005) Gaia's breath – global methane exhalations. Mar Pet Geol 22(4):579–590

Lam P, Jensen MM, Lavik G, van de Vossenberg J, Schmid M, Woebken D, Gutierrez D, Amann R, Jetten MSM, Kuypers MMM (2009) Revising the nitrogen cycle in the Peruvian oxygen minimum zone. Proc Natl Acad Sci USA 106(12):4752–4757

Lamarque J-F (2008) Estimating the potential for methane clathrate instability in the 1% CO_2 IPCC AR4 simulations. Geophys Res Lett 35, L19806. doi:10.1029/2008GL035291

Lammers S, Suess E, Hovland M (1995) A large methane plume east of Bear Island (Barents Sea): implications for the marine methane cycle. Geol Rundsch 84:59–66

Laruelle GG, Dürr HH, Slomp CP, Borges AV (2010) Evaluation of sinks and sources of CO_2 in the global coastal ocean using a spatially-explicit typology of estuaries and continental shelves. Geophys Res Lett 37, L15607. doi:10.1029/2010GL043691

Le Quéré C, Rödenbeck C, Buitenhuis ET, Conway TJ, Lagenfelds R, Gomez A, Labuschagne C, Ramonet M, Nakazawa T, Metzl N, Gillett N, Heimann M (2007) Saturation of the Southern Ocean CO_2 sink due to recent climate change. Science 316:1735–1738

Le Quéré C, Takahashi T, Buitenhuis ET, Rödenbeck C, Sutherland SC (2010) Impact of climate change and variability on the global oceanic sink of CO_2. Global Biogeochem Cycles 24, GB4007

Lee K, Sabine CL, Tanhua T, Kim T-W, Feely RA, Kim H-C (2011) Roles of marginal seas in absorbing and storing fossil fuel CO_2. Energy Environ Sci 4:1133

Lefèvre N, Watson AJ, Olsen A, Ríos AF, Pérez FF, Johannessen T (2004) A decrease in the sink for atmospheric CO_2 in the North Atlantic. Geophys Res Lett 31(7), L07306

Lefèvre N, Watson AJ, Watson AR (2005) A comparison of multiple regression and neural network techniques for mapping in situ pCO_2 data. Tellus 57B:375–384

Leifer I, Patro RK (2002) The bubble mechanism for methane transport from the shallow sea bed to the surface: a review and sensitivity study. Cont Shelf Res 22:2409–2428

Leip A (1999) Nitrous oxide (N_2O) emissions from a coastal catchment in the delta of the Po river: measurements and modeling of fluxes from a Mediterranean lagoon and agricultural soils. Ph.D. thesis, University of Bayreuth, Bayreuth

Lenton A, Cordon G, Bopp L, Metzl N, Cadule P, Tagliabue A, Le Sommer J (2009) Stratospheric ozone depletion reduces ocean carbon uptake and enhances ocean acidification. Geophys Res Lett 36, L12606. doi:10.1029/2009GL038227

Liss PS, Merlivat L (1986) Air-sea exchange rates: introduction and synthesis. In: Buat-Ménard P (ed) The role of air-sea exchange in geochemical cycling. D. Reidel Publishing, Dordrecht, pp 113–127

Liu X, Millero FJ (2002) The solubility of Fe(III) in seawater. Mar Chem 77:43–54

Liu KK, Atkinson L, Quiñones RA, Talahue-McManus L (2010) Biogeochemistry of continental margins in a global context. In: Liu KK, Atkinson L, Quiñones RA, Talahue-McManus L (eds) Carbon and nutrient fluxes in continental margins. Springer, Berlin etc., pp 3–24

Löscher CR, Kock A, Könneke, M, LaRoche J, Bange HW, Schmitz RA (2012) Production of oceanic nitrous oxide by ammonia-oxidizing archaea. Biogeosciences 9:2419–2429. doi:10.5194/bg-9-2419-2012

Lovenduski NS, Gruber N, Doney SC, Lima ID (2007) Enhanced CO_2 outgassing in the Southern Ocean from a positive phase of the Southern Annular Mode. Global Biogeochem Cycle 21, GB2026. doi:10.1029/2006GB002900

Lovenduski NS, Gruber N, Doney SC (2008) Toward a mechanistic understanding of the decadal trends in the Southern Ocean carbon sink. Global Biogeochem Cycle 22, GB3016. doi:10.1029/2007GB003139

Lüthi D, Le Floch M, Bereiter B, Blunier T, Barnola J-M, Siegenthaler U, Raynaud D, Jouzel J, Fischer H, Kawamura K, Stocker TF (2008) High-resolution carbon dioxide concentration record 650,000–800,000 years before present. Nature 453:379–382. doi:10.1038/nature06949

Mackenzie FT, Lerman A, Andersson AJ (2004) Past and present of sediment and carbon biogeochemical cycling models. Biogeosciences 1(1):11–32

Manning AC, Keeling RF (2006) Global oceanic and land biotic carbon sinks from the Scripps atmospheric oxygen flask sampling network. Tellus 58B:95–116. doi:10.1111/j.1600-0889.2006.00175.x

Martens CS, Klump JV (1980) Biogeochemical cycling in an organic-rich coastal marine basin – I. Methane sediment-water exchange processes. Geochim Cosmochim Acta 44:471–490

Martens-Habbena WPM, Berube PM, Urakawa H, De la Torre J, Stahl DA (2009) Ammonia oxidation kinetics determine niche separation of nitrifying Archaea and Bacteria. Nature 461(7266):976–979

Marty D, Nival P, Yoon WD (1997) Methanoarchaea associated with sinking particles and zooplankton collected in the Northeastern tropical Atlantic. Oceanol Acta 20:863–869

Matsumoto K, Sarmiento J, Brezeinski MA (2002) Silicic acid leakage from the Southern Ocean: a possible explanation for glacial atmospheric pCO_2. Global Biogeochem Cycle 16(3):5. doi:10.1029/2001GB001442

Matthews BJH (1999) The rate of air-sea CO_2 exchange: chemical enhancement and catalysis by marine microalgae. Ph.D. thesis, University of East Anglia, Norwich

Mau S, Valentine DL, Clark JF, Reed J, Camilli R, Washburn L (2007) Dissolved methane distributions and air-sea flux in the plume of a massive seep field, Coal Oil Point, California. Geophys Res Lett 34, L22603. doi:10.1029/2007GL031344

McKinley GA, Fay AR, Takahashi T, Metzl N (2011) Convergence of atmospheric and North Atlantic carbon dioxide trends on multidecadal timescales. Nat Geosci 4:606–609. doi:10.1038/NGEO1193

Metzl N (2009) Decadal increase of oceanic carbon dioxide in Southern Indian Ocean surface waters (1991–2007). Deep-Sea Res Part II 56:607–619

Michelsen HA, Irion FW, Manney GL, Toon GC, Gunson MR (2000) Features and trends in Atmospheric Trace Molecule Spectroscopy (ATMOS) version 3 stratospheric water vapor and methane measurements. J Geophys Res 105(D18):22713–22724

Middelburg JJ, Klaver G, Nieuwenhuize J, Wielemaker A, de Haas W, Van der Nat JFWA (1996) Organic matter mineralization in intertidal sediments along an estuarine gradient. Mar Ecol Prog Ser 132:157–168

Middelburg JJ, Nieuwenhuize J, Iversen N, Høgh N, De Wilde H, Helder W, Seifert R, Christof O (2002) Methane distribution in European tidal estuaries. Biogeochemistry 59:95–119

Mikaloff Fletcher SE, Gruber N, Jacobson AR, Doney SC, Dutkiewicz S, Gerber M, Gloor M, Follows M, Joos F, Lindsay K, Menemenlis D, Mouchet A, Müller SA, Sarmiento JL (2007) Inverse estimates of the oceanic sources and sinks of natural CO_2 and the implied oceanic transport. Global Biogeochem Cycle 21, GB1010. doi:10.1029/2006GB002751

Miller LA, Papakyriakou TN, Collins RE, Deming JW, Ehn JK, Macdonald RW, Mucci A, Owens O, Raudsepp M, Sutherland N (2011) Carbon dynamics in sea ice: a winter flux time series. J Geophys Res 116(C2), C02028. doi:10.1029/2009jc006058

Monaco A, Biscay P, Soyer J, Pocklington R, Heussner S (1990) Particle fluxes and ecosystem respons on a continental margin: the 1985–1988 Mediterranean ECOMARGE Experiment. Cont Shelf Res 10(9–11):809–839. doi:10.1016/0278-4343(90)90061-P

Monteiro PMS, Schuster U, Hood M, Lenton A, Metzl N, Olsen A, Rogers K, Sabine CL, Takahashi T, Tilbrook B, Yoder J, Wanninkhof R, Watson AJ (2010) Community white paper. A global sea surface carbon observing system: Assessment of changing sea surface CO_2 and air-sea CO_2 fluxes. In: Hall J, Harrison DE, Stammer D (eds) Proceedings of OceanObs'09: sustained ocean observations and information for society, vol 2, Venice, Italy, 21–25 Sept 2009, ESA publication WPP-306. doi:10.5270/OceanObs09.cwp.64

Montzka SA, Dlugokencky EJ, Butler JH (2011) Non-CO_2 greenhouse gases and climate change. Nature 476:43–50

Moran JJ, Beal EJ, Vrentas JM, Orphan VJ, Freeman KH, House CH (2008) Methyl sulphides as intermediates in the anaerobic oxidation of methane. Environ Microbiol 10:162–173

Morell JM, Capella J, Mercado A, Bauzá J, Corredor JE (2001) Nitrous oxide fluxes in Caribbean and tropical Atlantic waters: evidence for near surface production. Mar Chem 74:131–143

Mucci A (1983) The solubility of calcite and aragonite in seawater at various salinities, temperatures, and one atmosphere total pressure. Am J Sci 283:780–799

Mudelsee M (2001) The phase relations among atmospheric CO_2 content, temperature and global ice volume over the past 420 ka. Q Sci Rev 20:583–589

Naik H, Naqvi SWA, Suresh T, Narvekar PV (2008) Impact of a tropical cyclone on biogeochemistry of the central Arabian Sea. Global Biogeochem Cycle 22, GB3020. doi:10.1029/2007GB003028

Naqvi SWA (2008) The Indian Ocean. In: Capone DG, Carpenter EJ, Bronk DA (eds) Nitrogen in the marine environment, 2nd edn. Elsevier, Amsterdam, pp 631–681

Naqvi SWA, Jayakumar DA, Narvekar PV, Naik H, Sarma VVSS, D'Souza W, Joseph S, George MD (2000) Increased marine production of N_2O due to intensifying anoxia on the Indian continental shelf. Nature 408:346–349

Naqvi SWA, Bange HW, Gibb SW, Goyet C, Hatton AD, Upstill-Goddard RC (2005) Biogeochemical ocean–atmosphere transfers in the Arabian Sea. Prog Oceanogr 65:116–144

Naqvi SWA, Bange HW, Farías L, Monteiro PMS, Scranton MI, Zhang J (2010) Marine hypoxia/anoxia as a source of CH_4 and N_2O. Biogeosciences 7:2159–2190

Naudin JJ, Cauwet G, Chrétiennot-Dinet MJ, Deniaux B, Devenon JL, Pauc H (1997) River discharge and wind influence upon particulate transfer at the land-ocean interaction: case study of the Rhône river plume. Estuar Coast Shelf Sci 45:303–316. doi:10.1006/ecss.1996.0190

Nevison CD, Weiss RF, Erickson DJ III (1995) Global oceanic emissions of nitrous oxide. J Geophys Res 100:15809–15820

Nevison C, Lueker T, Weiss RF (2004) Quantifying the nitrous oxide source from coastal upwelling. Global Biogeochem Cycle 18, GB1018. doi:1010.1029/2003GB002110

Nightingale PD, Malin G, Law CS, Watson AJ, Liss PS, Liddicoat MI, Boutin J, Upstill-Goddard RC (2000) In-situ evaluation of air-sea gas exchange parameterisations using novel conservative and volatile tracers. Global Biogeochem Cycle 14(1):373–387

Nirmal Rajkumar A, Barnes J, Ramesh R, Purvaja R, Upstill-Goddard RC (2008) Methane and nitrous oxide fluxes in the polluted Adyar River and estuary. SE India Mar Pollut Bull 56:2043–2051

O'Connor FM, Boucher O, Gedney N, Jones CD, Folberth GA, Coppell R, Friedlingstein P, Collins WJ, Chappellaz J, Ridley J, Johnson CE (2010) Possible role of wetlands, permafrost, and methane hydrates in the methane cycle under future climate change: a review. Rev Geophys 48, RG4005. doi:10.1029/2010RG000326

Odum HT, Hoskin CM (1958) Comparative studies of the metabolism of Texas bays. Publ Inst Mar Sci Univ Tex 5:16–46

Odum HT, Wilson R (1962) Further studies on the reaeration and metabolism of Texas bays. Publ Inst Mar Sci Univ Tex 8:23–55

Ohde S, van Woesik R (1999) Carbon dioxide flux and metabolic processes of a coral reef, Okinawa. Bull Mar Sci 65:559–576

Olsen A, Brown KR, Chierici M, Johannessen T, Neill C (2008) Sea surface CO_2 fugacity in the subpolar North Atlantic. Biogeosciences 5:535–547, www.biogeosciences-5/535/2008/

Omar A, Johannessen T, Bellerby RGJ, Olsen A, Anderson LG, Kivimäe C, Omar A, Johannessen T, Bellerby RGJ, Olsen A, Anderson LG, Kivimäe C (2005) Sea-ice and brine formation in Storfjorden: implications for Arctic wintertime air-sea CO_2 flux. In: Drange H, Dokken T, Furevik T, Gerdes R, Berger W (eds) The Nordic seas: an integrated perspective, vol 158, American Geophysical Union Geophysical Monograph. American Geophysical Union, Washington, DC, pp 117–187

Oremland RS (1979) Methanogenic activity in plankton samples and fish intestines: a mechanism for in situ methanogenesis in ocean surface waters. Limnol Oceanogr 24:1136–1141

Orr JC, Fabry VJ, Aumont O, Bopp L, Doney SC, Feely RA, Gnanadesikan A, Gruber N, Ishida A, Joos F, Key RM, Lindsay K, Maier-Reimer E, Matear R, Monfray P, Mouchet A, Najjar RG, Plattner G-K, Rodgers KB, Sabine CL, Sarmiento JL, Schlitzer R, Slater RD, Totterdell IJ, Weirig M-F, Yamanaka Y, Yool A (2005) Anthropogenic ocean acidification over the twenty-first century and its impact on calcifying organisms. Nature 437:681–686

Ostrovsky I (2003) Methane bubbles in Lake Kinneret: quantification and temporal and spatial heterogeneity. Limnol Oceanogr 48:1030–1036

Oudot C, Jean-Baptiste P, Fourré E, Mormiche C, Gueve M, Ternon J-F, Le Corre P (2002) Transatlantic equatorial distribution of nitrous oxide and methane. Deep-Sea Res Part I 49(7):1175–1193

Paull CK, Brewer PG, Ussler W III, Peltzer ET, Rehder G, Clague D (2003) An experiment demonstrating that marine slumping is a mechanism to transfer methane from seafloor gas-hydrate deposits into the upper ocean and atmosphere. Geo-Mar Lett 22:198–203. doi:10.1007/s00367-002-0113-y

Paull CK, Ussler W, Holbrook S, Hill TM, Keaten R, Mienert J, Haflidaon H, Johnson JE, Winters WG, Lorenson TD (2008) Origin of pockmarks and chimney structures on the flanks of the Storegga slide, offshore Norway. Geo-Mar Lett 28:43–51. doi:10.1007/s00367-007-0088-9

Peters GP, Marland G, Le Quéré C, Boden T, Canadell JG, Raupach MR (2012) Rapid growth in CO_2 emissions after the 2008–2009 global financial crisis. Nat Clim Change 2:2–4. doi:10.1038/nclimate1332

Petit JR, Jouzel J, Raynaud D, Barkov NI, Barnola J-M, Basile I, Bender M, Chappellaz J, Davis M, Delaygue G, Delmotte M, Kotlyakov VM, Legrand M, Lipenkov VY, Lorius C, Pépin L, Ritz C, Saltzman E, Stievenard M (1999) Climate and atmospheric history of the past 420,000 years from the Vostok ice core, Antarctica. Nature 399:429–436. doi:10.1038/20859

Pfeil, B, Olsen, A, Bakker, DCE, Hankin S, Koyuk H, Kozyr A, Malczyk J, Manke A, Metzl N, Sabine CL, Akl J, Alin SR, Bates N, Bellerby RGJ, Borges A, Boutin J, Brown PJ, Cai W-J, Chavez FP, Chen A, Cosca C, Fassbender AJ, Feely RA, González-Dávila M, Goyet C, Hales B, Hardman-Mountford N, Heinze C, Hood M, Hoppema M, Hunt CW, Hydes D, Ishii M, Johannessen T, Jones SD, Key RM, Körtzinger A, Landschützer P, Lauvset SK, Lefèvre N, Lenton A, Lourantou A, Merlivat L, Midorikawa T, Mintrop L, Miyazaki C, Murata A, Nakadate A, Nakano Y, Nakaoka S, Nojiri Y, Omar AM, Padin XA, Park G-H, Paterson K, Perez FF, Pierrot D, Poisson A, Ríos AF, Salisbury J, Santana-Casiano JM, Sarma VVSS, Schlitzer R, Schneider B, Schuster U, Sieger R, Skjelvan I, Steinhoff T, Suzuki T, Takahashi T, Tedesco K, Telszewski M, Thomas H, Tilbrook B, Tjiputra J, Vandemark D, Veness T, Wanninkhof R, Watson AJ, Weiss R, Wong CS, Yoshikawa-Inoue H (2013) A uniform, quality controlled Surface Ocean CO2 Atlas (SOCAT). Earth Syst Sci Data 5:125–143. doi:10.5194/essd-5-125-2013

Philippot L (2002) Denitrifying genes in bacterial and Archaeal genomes. Biochim Biophys Acta Gene Struct Expr 1577 (3):355–376

Plattner G-K, Frenzel H, Gruber N, Leinweber A, McWilliams JC (2004) Changing winds and coastal carbon cycle: a case study for an upwelling region. The ocean in a high-CO_2 world. UNESCO, Paris

Plummer DH, Owens NJP, Herbert RA (1987) Bacteria-particle interactions in turbid estuarine environments. Cont Shelf Res 7:1429–1433. doi:10.1016/0278-4343(87)90050-1

Prytherch J, Yelland MJ, Pascal RW, Moat BI, Skjelvan I, Srokosz MA (2010) Open ocean gas transfer velocity derived from long-term direct measurements of the CO_2 flux. Geophys Res Lett 37, L23607. doi:10.1029/2010GL045597

Ramesh R, Purvaja R, Neetha V, Divia J, Barnes J, Upstill-Goddard RC (2007) CO_2 and CH_4 emissions from Indian mangroves and surrounding waters. In: Tateda Y, Upstill-Goddard RC, Goreau T, Alongi D, Nose A, Kristensen E, Wattayakorn G (eds) Greenhouse gas and carbon balances in mangrove coastal ecosytems. Gendai Tosho, Kanagawa, pp 153–164

Rangama Y, Boutin J, Etcheto J, Merlivat L, Takahashi T, Delille B, Frankignoulle M, Bakker DCE (2005) Variability of the net air-sea CO_2 flux inferred from shipboard and satellite measurements in the Southern Ocean south of Tasmania and New Zealand. J Geophys Res 110:1–17. C09005. doi: 10.1029/2004JC002619

Raven J, Caldeira K, Elderfield H, Hoegh-Guldberg O, Liss P, Riebesell U, Shepherd J, Turley C, Watson AJ (2005) Ocean acidification due to increasing atmospheric carbon dioxide, vol 12/05, Policy document. The Royal Society, London

Ravishankara AR, Daniel JS, Portmann RW (2009) Nitrous oxide (N_2O): the dominant ozone-depleting substance emitted in the 21st century. Science 326:123–125

Reagan MT, Moridis GJ (2009) Large-scale simulation of methane hydrate dissociation along the West Spitsbergen Margin. Geophys Res Lett 36, L23612. doi:10.1029/2009GL041332

Redfield AC, Ketchum BH, Richards FA (1963) The influence of organisms on the composition of seawater. In: Hill MN (ed) The sea, vol 2. Wiley Interscience, New York, pp 26–77

Reeburgh WS (2007) Oceanic methane biogeochemistry. Chem Rev 107(2):486–513

Rehder G, Keir RS, Suess E, Pohlmann T (1998) The multiple sources and patterns of methane in North Sea waters. Aquat Geochem 4:403–427

Rhee TS, Kettle AJ, Andreae MO (2009) Methane and nitrous oxide emissions from the ocean: a reassessment using basin-wide observations in the Atlantic. J Geophys Res 114, D12304. doi:10.1029/2008JD011662

Riebesell U, Schulz KG, Bellerby RGJ, Botros M, Fritsche P, Meyerhofer M, Neill C, Nondal G, Oschlies A, Wohlers J, Zollner E (2007) Enhanced biological carbon consumption in a high CO_2 ocean. Nature 450:545–548

Rigby M, Prinn RG, Fraser PJ, Simmonds PG, Langenfelds RL, Huang J, Cunnold DM, Steele LP, Krummel PB, Weiss RF, O'Doherty S, Salameh PK, Wang HJ, Harth CM, Mühle J, Porter LW (2008) Renewed growth of atmospheric methane. Geophys Res Lett 35, L22805. doi:10.1029/2008GL036037

Rixen T, Haake B, Ittekkot V, Guptha MVS, Nair RR, Schlüssel P (1996) Coupling between SW monsoon-related surface and deep ocean processes as discerned from continuous particle flux measurements and correlated satellite data. J Geophys Res 101:28569–28582

Robertson JE, Watson AJ (1992) Thermal skin effect of the surface ocean and its implications for CO_2 uptake. Nature 358:738–740

Romanovski NN, Hubberten H-W, Gavrilov AV, Eliseeva AA, Tipenkio GS (2005) Offshore permafrost and gas hydrate stability zone on the shelf of East Siberian Seas. Geo-Mar Lett 25(2–3):167–182. doi:10.1007/s00367-004-0198-6

Rost B, Riebesell U (2004) Coccolithophores and the biological pump: responses to environmental changes. In: Thierstein HR, Young JR (eds) Coccolithophores: from molecular processes to global impact. Springer, Berlin, pp 99–125

Roy T, Bopp L, Gehlen M, Schneider B, Cadule P, Fröhlicher TL, Segschneider J, Tjiputra J, Heinze C, Joos F (2011) Regional impacts of climate change and atmospheric CO_2 on future ocean carbon uptake: a multimodel linear feedback analysis. J Climate 24(9):2300–2318. doi:10.1175/2010JCLI3787.1

Rysgaard S, Bendtsen J, Delille B, Dieckmann GS, Glud R, Kennedy H, Mortensen J, Papadimitriou S, Thomas DN, Tison JL (2011) Sea ice contribution to the air–sea CO_2 exchange in the Arctic and Southern Oceans. Tellus 63B (5):1–8. doi:10.1111/j.1600-0889.2011.00571.x

Sabine CL, Feely RA, Gruber N, Key RM, Lee K, Bullister JL, Wanninkhof R, Wong CS, Wallace DWR, Tilbrook B, Millero FJ, Peng T-H, Kozyr A, Ono T, Ríos AF (2004) The oceanic sink for anthropogenic CO_2. Science 305:367–371

Sabine CL, Hankin S, Koyuk H, Bakker DCE, Pfeil B, Olsen A, Metzl N, Kozyr A, Fassbender A, Manke A, Malczyk J, Akl J, Alin SR, Bellerby RGJ, Borges A, Boutin J, Brown PJ, Cai W-J, Chavez FP, Chen A, Cosca C, Feely RA, González-Dávila M, Goyet C, Hardman-Mountford N, Heinze C, Hoppema M, Hunt CW, Hydes D, Ishii M, Johannessen T, Key RM, Körtzinger A, Landschützer P, Lauvset SK, Lefèvre N, Lenton A, Lourantou A, Merlivat L, Midorikawa T, Mintrop L, Miyazaki C, Murata A, Nakadate A, Nakano Y, Nakaoka S, Nojiri Y, Omar AM, Padin XA, Park G-H, Paterson K, Perez FF, Pierrot D, Poisson A, Ríos AF, Salisbury J, Santana-Casiano JM, Sarma VVSS, Schlitzer R, Schneider B, Schuster U, Sieger R, Skjelvan I, Steinhoff T, Suzuki T, Takahashi T, Tedesco K, Telszewski M, Thomas H, Tilbrook B, Vandemark D, Veness T, Watson AJ, Weiss R, Wong CS, Yoshikawa-Inoue H (2013) Gridding of the Surface Ocean CO_2 Atlas (SOCAT) Gridded data products. Earth Syst Sci Data 5:145–153. doi:10.5194/essd-5-145-2013

Santana-Casiano JM, González-Dávila M (2011) pH decrease and effects on the chemistry of seawater. In: Duarte P, Santana-Casiano JM (eds) Oceans and the atmospheric carbon content. Springer, Berlin, pp 95–114

Santana-Casiano JM, González-Davila M, Millero FJ (2006) The role of Fe(II) species on the oxidation of Fe(II) in natural waters in the presence of O_2 and H_2O_2. Mar Chem 99:70–82

Santoro AE, Buchwald C, McIlvin MR, Casciotti KL (2011) Isotopic signature of N_2O produced by marine ammonia-oxidizing archaea. Science 333(6047):1282–1285. doi:10.1126/science.1208239

Sarmiento JL, Gruber N (2002) Sinks for anthropogenic carbon. Phys Today 55:30–36

Sarmiento JL, Gruber N (2006) Ocean biogeochemical dynamics. Princeton University Press, Princeton

Sarmiento JL, Sundquist ET (1992) Revised budget for the oceanic uptake of anthropogenic carbon dioxide. Nature 356:589–593

Sarmiento JL, Orr JC, Siegenthaler U (1992) A perturbation simulation of CO_2 uptake in an ocean general circulation model. J Geophys Res 97(C3):3621–3646

Sarmiento JL, Dunne J, Gnanadesikan A, Key RM, Matsumoto K, Slater R (2002) A new estimate of the CaCO3 to organic carbon export ratio. Global Biogeochem Cycle 16(4):1107. doi:10.1029/2002GB001919

Sasakawa M, Tsunogai U, Kameyama S, Nakagawa F, Nojiri Y, Tsuda A (2008) Carbon isotopic characterization for the origin of excess methane in subsurface seawater. J Geophys Res 113, C03012. doi:10.1029/2007JC004217

Schlünz B, Schneider RR (2000) Transport of terrestrial organic carbon to the oceans by rivers: re-estimating flux and burial rates. Int J Earth Sci 88:599–606

Schmale O, Greinert J, Rehder G (2005) Methane emission from high intensity marine gas-seeps in the Black Sea into the atmosphere. Geophys Res Lett 32, L07609. doi:10.1029/2004GL021138

Schmidt GA, Shindell DT (2003) Atmospheric composition, radiative forcing, and climate change as a consequence of a massive methane release from gas hydrates. Paleoceanography 18(1):1004. doi:10.1029/2002PA000757

Schuster U, Watson AJ (2007) A variable and decreasing sink for atmospheric CO_2 in the North Atlantic. J Geophys Res 112(C11), C11006

Schuster U, Watson AJ, Bates NR, Corbière A, González-Dávila M, Metzl N, Pierrot D, Santana-Casiano M (2009) Trends in North Atlantic sea-surface fCO_2 from 1990 to 2006. Deep-Sea Res Part II 56(8–10):620–629

Scranton MI, McShane K (1991) Methane fluxes in the southern North Sea: the role of European rivers. Cont Shelf Res 11:37–52

Seitzinger SP, Kroeze C (1998) Global distribution of nitrous oxide production and N inputs in freshwater and coastal marine ecosystems. Global Biogeochem Cycle 12:93–113

Seitzinger SP, Kroeze C, Bouwman AE, Caraco N, Dentener F, Styles RV (2002) Global patterns of dissolved inorganic and particulate nitrogen inputs to coastal systems. Estuaries 25:640–655

Shakhova N, Semiletov I (2007) Methane release and coastal environment in the East Siberian Arctic shelf. J Mar Syst 66:227–243

Shakhova N, Semiletov I, Salyuk AN, Belcheva N, Kosmach D (2007) Methane anomalies in the near-water atmospheric layer above the shelf of East Siberian Arctic Shelf. Trans Russ Acad Sci 415:764–768

Shakhova N, Semiletov I, Salyuk A, Yusupov V, Kosmach D, Gustafsson O (2010) Extensive methane venting to the atmosphere from sediments of the East Siberian Arctic Shelf. Science 327:1246–1250. doi:10.1126/science.1182221

Silverman J, Lazar B, Cao L, Caldeira K, Erez J (2009) Coral reefs may start dissolving when atmospheric CO_2 doubles. Geophys Res Lett 36, L05606. doi:1029/2008GL036282

Sloan ED (2003) Fundamental principles and applications of natural gas hydrates. Nature 426:353–363. doi:10.1038/nature02135

Sloan ED, Koh CA (2008) Clathrate hydates of natural gases, 3rd edn. CRC Press, Boca Raton

Smith SV, Hollibaugh JT (1993) Coastal metabolism and the oceanic carbon balance. Rev Geophys 31:75–89

Smith SV, Mackenzie FT (1987) The ocean as a net heterotrophic system: implications from the carbon biogeochemical cycle. Global Biogeochem Cycles 1:187–198

Smith SV, Swaney DP, Talaue-McManus L, Bartley JD, Sandhei PT, McLaughlin CJ, Dupra VC, Crossland CJ, Buddemeier RW, Maxwell BA, Wulff F (2003) Humans, hydrology, and the distribution of inorganic nutrient loading to the ocean. Bioscience 53:235–245

Sowers TA, Alley R, Jubenville J (2003) Elemental and isotopic records of atmospheric nitrous oxide covering the last 106,000 years from the GISP II and Taylor Dome ice cores. Science 301:945–948

Spahni R, Chappellaz J, Stocker TF, Loulergue L, Hausammann G, Kawamura K, Flückiger J, Schwander J, Raynaud D, Masson-Delmotte V, Jouzel J (2005) Atmospheric methane and nitrous oxide of the late Pleistocene from Antarctic ice cores. Science 310(5752):1317–1321

Stramma L, Johnson GC, Sprintall J, Mohrholz V (2008) Expanding oxygen-minimum zones in the tropical oceans. Science 320:655–658

Stramma L, Schmidtko S, Levin A, Johnson GC (2010) Ocean oxygen minima expansions and their biological impacts. Deep-Sea Res Part I 57(4):587–595

Suntharalingam P, Sarmiento JL (2000) Factors governing the oceanic nitrous oxide distribution: simulations with an ocean general circulation model. Global Biogeochem Cycle 14:429–454

Suykens K, Delille B, Chou L, De Bodt C, Harlay J, Borges AV (2010) Dissolved inorganic carbon dynamics and air-sea carbon dioxide fluxes during coccolithophore blooms in the northwest European continental margin (northern Bay of Biscay). Global Biogeochem Cycle 24, GB3022. doi:10.2029/2009GB003730

Suzuki A, Kawahata K (2004) Reef water CO_2 system and carbon production of coral reefs: topographic control of system-level perfrormance. In: Shiyomi M, Kawahata H, Koizumi H, Tsuda A, Awaya Y (eds) Global environmental change in the ocean and on land. Terrapub, Tokyo, pp 229–248

Suzuki T, Ishii M, Aoyama M, Christian JR, Enyo K, Kawano T, Key RM, Kosugi N, Kozyr A, Miller LA, Murata A, Nakano T, Ono T, Saino T, Sasaki K, Sasano D, Takatani Y, Wakita M, Sabine CL (2013) PACIFICA Data Synthesis Project. ORNL/CDIAC-159, NDP-092. Carbon Dioxide Information Analysis Center, Oak Ridge National Laboratory, U.S. Department of Energy, Oak Ridge, Tennessee, USA. doi:10.3334/CDIAC/OTG.PACIFICA_NDP092

Sweeney C, Gloor E, Jacobson AR, Key RM, McKinley G, Sarmiento JL, Wanninkhof R (2007) Constraining global air-sea gas exchange for CO_2 with recent bomb ^{14}C measurements. Global Biogeochem Cycle 21, GB2015. doi:10.1029/2006GB002784

Takahashi T, Feely RA, Weiss RF, Wanninkhof RH, Chipman DW, Sutherland SC, Takahashi TT (1997) Global air-sea flux of CO_2: an estimate based on measurements of sea-air pCO_2 difference. Proc Natl Acad Sci USA 94:8292–8299

Takahashi T, Sutherland SC, Sweeney C, Poisson A, Metzl N, Tilbrook B, Bates N, Wanninkhof RH, Feely RA, Sabine CL, Olafsson J, Nojiri Y (2002) Global sea-air CO_2 flux based on climatological surface ocean pCO_2, and seasonal biological and temperature effects. Deep-Sea Res Part II 49:1601–1622

Takahashi T, Sutherland SC, Wanninkhof R, Sweeney C, Feely RA, Chipman DW, Hales B, Friederich G, Chavez F, Sabine C, Watson AJ, Bakker DCE, Schuster U, Metzl N, Inoue HY, Ishii M, Midorikawa T, Nojiri Y, Koertzinger A, Steinhoff T, Hoppema JMJ, Olafsson J, Arnarson TS, Tilbrook B, Johannessen T, Olsen A, Bellerby R, Wong CS, Delille B, Bates NR, de Baar HJW (2009) Climatological mean and decadal change in surface ocean pCO_2, and net sea-air CO_2 flux over the global oceans. Deep-Sea Res Part II 56:544–577. doi:10.1016/j.dsr2.2008.12.009

Takahashi T, Sutherland SC, Kozyr A (2011) Global ocean surface water partial pressure of CO_2 database: Measurements performed during 1957–2010 (Version 2010). ORNL/CDIAC-159, NDP-088(V2010). Carbon Dioxide Information Analysis Center, Oak Ridge Nat. Lab., US Department of Energy, Oak Ridge, Tenn, doi:10.3334/CDIAC/otg.ndp088 (V2010)

Tanhua T, van Heuven S, Key RM, Velo A, Olsen A, Schirnick C (2010) Quality control procedures and methods of the CARINA database. Earth Syst Sci Data 2:35–49. doi:10.5194/essd-2-35-2010

Telszewski M, Chazottes A, Schuster U, Watson AJ, Moulin C, Bakker DCE, González-Dávila M, Johannessen T, Körtzinger A, Lüger H, Olsen A, Omar A, Padin XA, Ríos A, Steinhoff T, Santana-Casiano M, Wallace DWR, Wanninkhof RH (2009) Estimating the monthly pCO_2 distribution in the North Atlantic using a self-organizing neural network. Biogeosciences 6:1405–1421, http://www.biogeosciences.net/6/1405/2009

Thomas H, Bozec Y, Elkalay K, de Baar HJW (2004) Enhanced open ocean storage of CO_2 from shelf sea pumping. Science 304(5673):1005–1008

Thomas H, Prowe F, van Heuven S, Bozec Y, de Baar HJW, Schiettecatte L-S, Suykens K, Koné M, Borges AV, Lima ID, Doney SC (2007) Rapid decline of the CO_2 buffering capacity in the North Sea and implications for the North Atlantic Ocean. Global Biogeochem Cycle 21, GB4001. doi:10.1029/2006GB002825

Thomas H, Prowe AEF, Lima I, Doney SC, Wanninkhof R, Greatbatch RJ, Schuster U, Corbière A (2008) Changes in the North Atlantic Oscillation influence CO_2 uptake in the North Atlantic over the past 2 decades. Global Biogeochem Cycle 22, GB4027. doi:10.1029/2007GB003167

Tréhua AM, Longb PE, Torresa ME, Bohrmannc G, Rackd FR, Collette TS, Goldbergf DS, Milkovg AV, Riedelh M, Schultheissi P, Bangsj NL, Barrk SR, Borowskil WS, Claypoolm GE, Delwichen ME, Dickenso GR, Graciap E, Guerinf G, Hollandq M, Johnsona JE, Leer Y-J, Lius C-S, Sut X, Teichertu B, Tomaruv H, Vannestew M, Watanabex M, Weinbergery JL (2004) Three-dimensional distribution of gas hydrate beneath southern Hydrate Ridge: constraints from ODP Leg 204. Earth Planet Sci Lett 222:845–862

Tsai W, Liu K-K (2003) An assessment of the effect of sea surface surfactant on global atmosphere–ocean CO_2 flux. J Geophys Res 108:3127. doi:10.1029/2000JC000740

Tsunogai S, Watanabe S, Sato T (1999) Is there a "continental shelf pump" for the absorption of atmospheric CO_2? Tellus 51B(3):701–712

Uncles RJ, Stephens JA (1993) The freshwater-saltwater interface and its relationship to the turbidity maximum in the Tamar estuary, United Kingdom. Estuaries 16:126–141. doi:10.2307/1352770

Upstill-Goddard RC (2006) Air-sea exchange in the coastal zone. Estuar Coast Shelf Sci 70:388–404

Upstill-Goddard RC (2011) The production of trace gases in the estuarine and coastal environment. In: Wolanski E, McLusky DS (eds) Treatise on estuarine and coastal science, vol 2, Geochemistry of estuaries and coasts. Elsevier, Amsterdam, pp 271–309

Upstill-Goddard RC, Owens NJP, Barnes J (1999) Nitrous oxide and methane during the 1994 SW monsoon in the Arabian Sea/northwestern Indian Ocean. J Geophys Res 104:30067–30084

Upstill-Goddard RC, Barnes J, Frost T, Punshon S, Owens NJP (2000) Methane in the southern North Sea: low-salinity inputs, estuarine removal, and atmospheric flux. Global Biogeochem Cycle 14:1205–1217

Van der Nat F-JWA, Middelburg JJ (1998) Seasonal variation in methane oxidation by the rhizosphere of *Phragmites australis* and *Scirpus lacustris*. Aquat Bot 61(2):95–110

Van der Nat F-JWA, Middleburg JJ (2000) Methane emission from tidal freshwater marshes. Biogeochemistry 49(2):103–121

Van der Nat F-JWA, Middelburg JJ, Van Meteren D, Wielemakers A (1998) Diel methane emissions patterns from *Scirpus lacustris* and *Phragmites australis*. Biogeochemistry 41:1–22

Van Scoy KA, Morris KP, Robertson JE, Watson AJ (1995) Thermal skin effect and the air-sea flux of carbon dioxide: a seasonal high-resolution estimate. Global Biogeochem Cycle 9(2):253–262

Volk T, Hoffert MI (1985) Ocean carbon pumps: analysis of relative strengths and efficiencies in ocean-driven atmospheric CO_2 changes. In: Sundquist E, Broecker WS (eds) The carbon cycle and atmospheric CO_2: natural variations Archean to present, vol 32, American Geophysical Union

Geophysical Monograph. American Geophysical Union, Washington, DC, pp 99–110

Wakelin SL, Holt JT, Blackford JC, Allen JI, Butenschön M, Artioli Y (2012) Modeling the carbon fluxes of the northwest European continental shelf: validation and budgets. J Geophys Res 117, C05020. doi:10.1029/2011JC007402

Walsh JJ (1988) On the nature of continental shelves. Academic Press, San Diego

Walter S, Bange HW, Breitenbach U, Wallace DWR (2006) Nitrous oxide in the North Atlantic Ocean. Biogeosciences 3:607–619

Wanninkhof RH (1992) Relationship between wind speed and gas exchange over the ocean. J Geophys Res 97(C5):7373–7382

Wanninkhof RH, McGillis WR (1999) A cubic relationship between air-sea CO_2 exchange and wind speed. Geophys Res Lett 26(13):1889–1892

Wanninkhof RH, Asher WE, Ho DT, Sweeney C, McGillis WR (2009) Advances in quantifying air-sea gas exchange and environmental forcing. Annu Rev Mar Sci 1:213–244

Watson AJ, Orr JC (2003) Carbon dioxide fluxes in the global ocean. In: Fasham MJR (ed) Ocean biogeochemistry: a JGOFS synthesis, Global change. IGBP series. Springer, Berlin, pp 123–143

Watson AJ, Schuster U, Bakker DCE, Bates N, Corbière A, González-Dávila M, Friedrich T, Hauck J, Heinze C, Johannessen T, Körtzinger A, Metzl N, Olaffson J, Oschlies A, Pfeil B, Olsen A, Oschlies A, Santano-Casiano JM, Steinhoff T, Telszewski M, Ríos A, Wallace DWR, Wanninkhof RH (2009) Tracking the variable North Atlantic sink for atmospheric CO_2. Science 326(5958):1391–1393

Wayne RP (2000) Chemistry of atmospheres, 3rd edn. Oxford University Press, Oxford, 775 pp

WDCGG (2012) World Meteorological Organization (WMO) Global Atmosphere Watch (GAW) Data. Greenhouse gases and other atmospheric gases. WMO WDCGG (World Data Centre for Greenhouse Gases) 36(4). Japan Meteorological Agency and the WMO, Tokyo, p. 100

Weiss RF (1974) Carbon dioxide in water and seawater: the solubility of a non-ideal gas. Mar Chem 2:203–205

Weiss RF, Van Woy FA, Salameh PK (1992) Surface water and atmospheric carbon dioxide and nitrous oxide observations by shipboard automated gas chromatography: Results from expeditions between 1977 and 1990. Scripps Institution of Oceanography reference 92–11, ORNL/CDIAC-59, NDP-044, Carbon Dioxide Information Analysis Center, Oak Ridge National Laboratory, US Department of Energy, Oak Ridge, Tennessee, USA

Westbrook GK, Thatcher KE, Rohling EJ, Piotrowski AM, Palike H, Osborne AH, Nisbet EG, Minshull TA, Lanoiselle M, James RH, Huhnerbach V, Green D, Fisher RE, Crocker AJ, Chabert A, Bolton C, Beszczynska-Moller A, Berndt C, Aquilina A (2009) Escape of methane gas from the seabed along the West Spitsbergen continental margin. Geophys Res Lett 36, L15608. doi:10.1029/2009GL039191

Wetzel P, Winguth A, Maier-Reimer E (2005) Sea-to-air fluxes CO_2 fluxes from 1948 to 2003: a model study. Global Biogeochem Cycle 19, GB2005. doi:10.1029/2004GB002339

Wever TF, Abegg F, Fiedler HM, Fechner G, Stender IH (1998) Shallow gas in the muddy sediments of Eckernförde Bay, Germany. Cont Shelf Res 18:1715–1739

Wittke F, Kock A, Bange HW (2010) Nitrous oxide emissions from the upwelling off Mauritania (NW Africa). Geophys Res Lett 37, L12601. doi:10.1029/2010GL042442

Wollast R (1998) Evaluation and comparison of the global carbon cycle in the coastal zone and in the open ocean. In: Brink KH, Robinson AR (eds) The global coastal ocean. Wiley, New York, pp 213–252

Wollast R, Chou L (2001) The carbon cycle at the ocean margin in the northern Gulf of Biscay. Deep-Sea Res Part II 48:3265–3293

Wong CS, Christian JR, Wong S-KE, Page J, Xie L, Johannessen S (2010) Carbon dioxide in surface sea water of the eastern North Pacific Ocean (Line P), 1973–2005. Deep-Sea Res Part I 57:687–695

Woodwell GM, Rich PH, Hall CAS (1973) Carbon in estuaries. In: Woodwell GM, Pecan EV (eds) Carbon and the biosphere. United States Atomic Energy Commission, Springfield, pp 221–240

Wuchter C, Abbas B, Coolen MJL, Herfort L, van Bleijswijk J, Timmers P, Strous M, Teira E, Herndl GJ, Middelburg JJ, Schouten S, Damste JSS (2006) Archaeal nitrification in the ocean. Proc Natl Acad Sci USA 103(33):12317–12322

Wuchter C, Abbas B, Coolen MJL, Herfort L, van Bleijswijk J, Timmers P, Strous M, Teira E, Herndl GJ, Middelburg JJ, Schouten S, Damste JSS (2007) Archaeal nitrification in the ocean (vol 103, pg 12317, 2006). Proc Natl Acad Sci USA 104(13):5704–5704

Yavitt JB, Fahey TJ (1991) Production of methane and nitrous oxide by organic soils within a northern hardwood forest ecosystem. In: Oremland RS (ed) Biogeochemistry of global change: radiatively active trace gases. Chapman and Hall, New York, pp 261–277

Yoshida O, Inoue HY, Watanabe S, Suzuki K, Noriki S (2011) Dissolved methane distribution in the South Pacific and the Southern Ocean in austral summer. J Geophys Res 116, C07008. doi:10.1029/2009JC006089

Zhang G-L, Zhang J, Liu SM, Ren J-L, Xu J, Zhang F (2008) Methane in the Changjiang (Yangtze River) Estuary and its adjacent marine area: riverine input, sediment release and atmospheric fluxes. Biogeochemistry 91:71–84

Zhang G-L, Zhang J, Liu S-M, Ren J-L, Zhao Y-C (2010) Nitrous oxide in the Changjiang (Yangtze River) estuary and its adjacent marine area: riverine input, sediment release and atmospheric fluxes. Biogeosciences 7:3505–3516

Zumft WG (1997) Cell biology and molecular basis of denitrification. Microbiol Mol Biol Rev 61:533–616